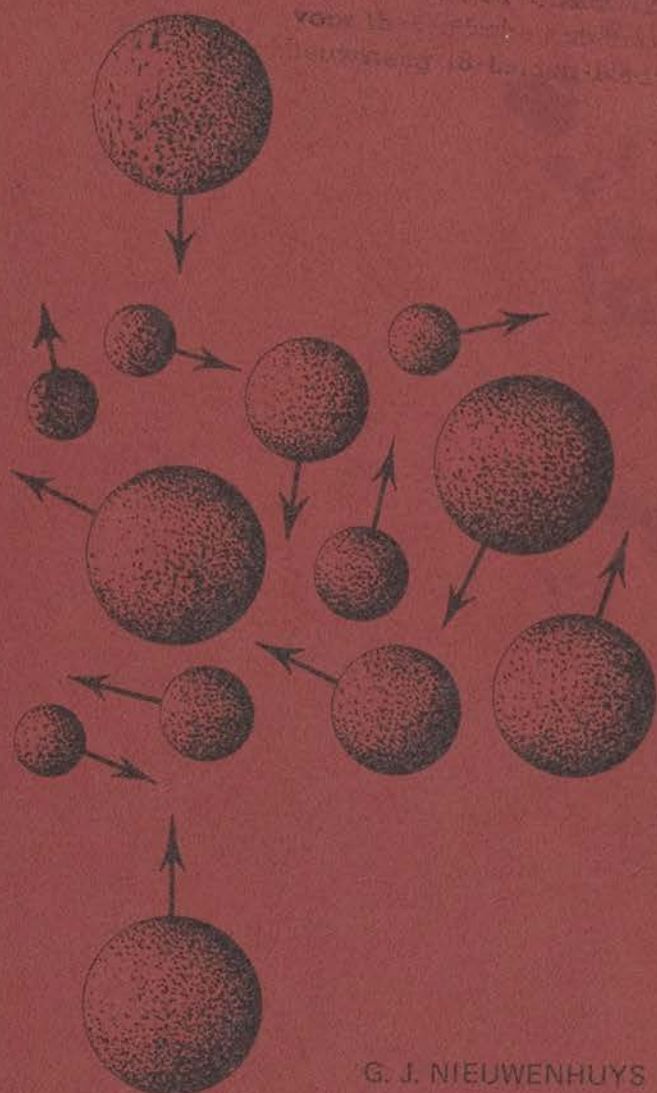


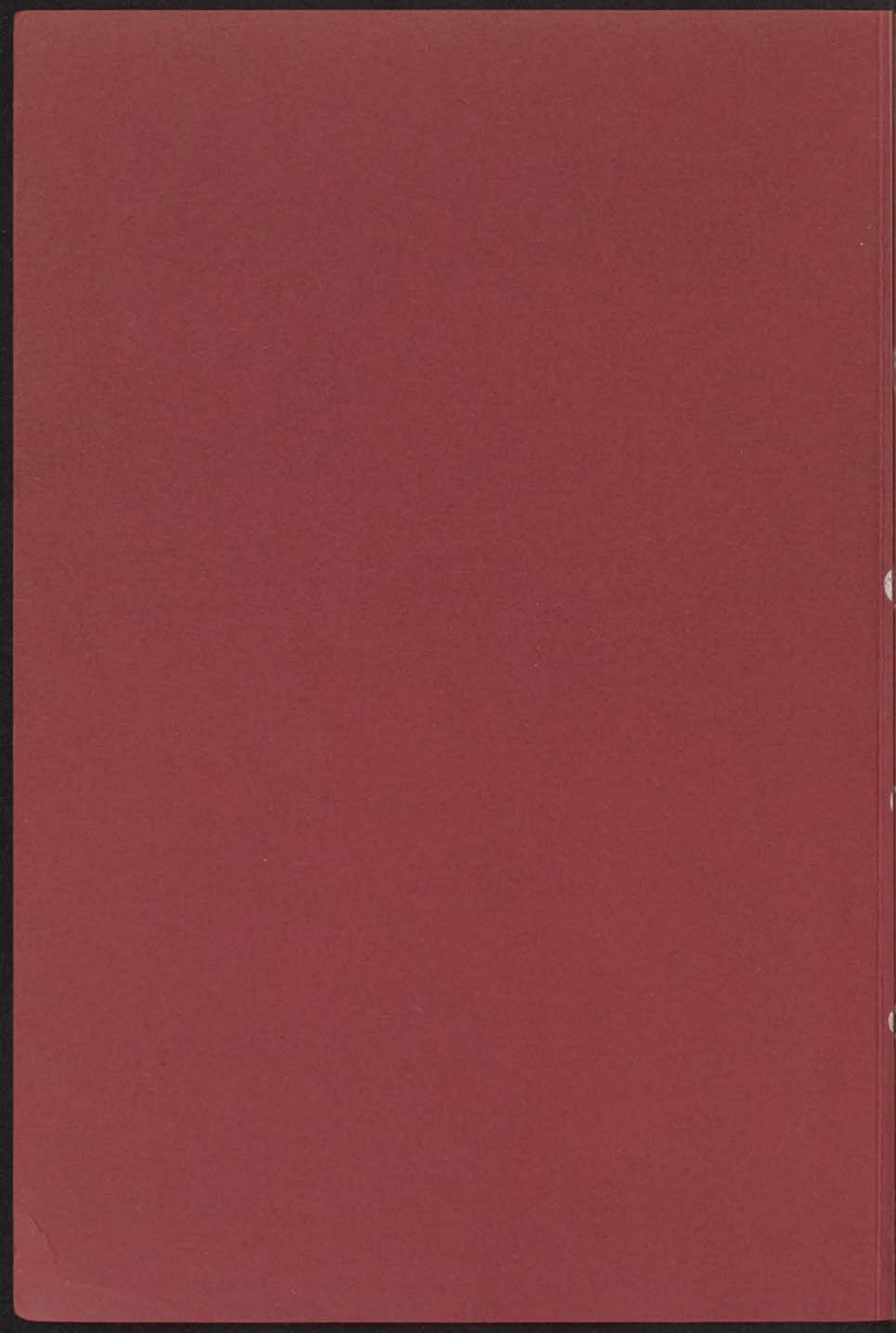
L. 10112

MAGNETIC BEHAVIOUR OF COBALT, IRON AND MANGANESE DISSOLVED IN PALLADIUM

INSTITUT-LORÉNTZ
voor theoretische natuurkunde
Leuvening 16-L. 10112-10113



G. J. NIEUWENHUIJS



13 JUNI 1974

MAGNETIC BEHAVIOUR OF
COBALT, IRON AND MANGANESE
DISSOLVED IN PALLADIUM

WETenschappelijk Instituut
voor de studie van de
magnetische eigenschappen
van de metalen en metalen
oplossingen in Leiden Nederland

DE VERVOLGING VAN DE GRADUS DOCTOR IN
DE WISSENSCHAPPEN IN NEDERLANDSCHE
KIEMERLEERDEETDE, OF HETZELFDE VAN DE
DOCTORAL DISSERTATION IN A.B. COHEN, WOOLEMAN
IN DE FACULTEIT DER LETTEREN, VOLGENS BESLUIT
VAN HET COLLEGE VAN DOCTOREN, DE VERVOLGING OP
DINAGEL 25 JUNI 1974 TE KLONEN 15.15 OER

227

Gerard Johannes Binnemans

geboren te Leiden in 1946

Erste Paper A. V. te Nijmegen

kast dissertaties

MAINTENANCE RECORDS
OF THE
UNITED STATES DEPARTMENT OF AGRICULTURE
OFFICE OF THE ASSISTANT SECRETARY FOR
GENERAL INVESTIGATIONS

**MAGNETIC BEHAVIOUR OF
COBALT, IRON AND MANGANESE
DISSOLVED IN PALLADIUM**

INSITUUT-LORENTZ
voor theoretische natuurkunde
Nieuwsteeg 18-Leiden-Nederland
PROEFSCHRIFT

TER VERKRIJGING VAN DE GRAAD VAN DOCTOR IN
DE WISKUNDE EN NATUURWETENSCHAPPEN AAN DE
RIJKSUNIVERSITEIT TE LEIDEN, OP GEZAG VAN DE
RECTOR MAGNIFICUS DR. A.E. COHEN, HOOGLEERAAR
IN DE FACULTEIT DER LETTEREN, VOLGENS BESLUIT
VAN HET COLLEGE VAN DEKANEN TE VERDEDIGEN OP
DINSDAG 25 JUNI 1974 TE KLOKKE 15.15 UUR

door

Gerard Johannes Nieuwenhuys

geboren te Leiden in 1946

Krips Repro B.V. te Meppel

Promotoren: Prof. Dr. C.J. Gorter

Dr. J. de Nobel

COBALT, IRON AND MANGANESE
DISSOLVED IN PALLADIUM

Co-referenten: Dr. G.J. van den Berg

Dr. P.F. de Chatel

This investigation is part of the research program of the "Stichting voor Fundamenteel Onderzoek der Materie (F.O.M.)", which is financially supported by the "Nederlandse Organisatie voor Zuiver-Wetenschappelijk Onderzoek (Z.W.O.)" and by the "Centrale Organisatie voor Toegepast-Natuurwetenschappelijk Onderzoek (T.N.O.)".

STELLINGEN

I

Caspers c.s. formuleren, gebruik makend van volledige stelsels diagonale operatoren, een criterium voor de ergodiciteit van operatoren van systemen met een niet-ontaard energiespectrum. Zij passen dit criterium toe op het c-cyclisch X-Y model. Het energiespectrum daarvan is echter wel ontaard. Hun redenering leidt evenwel niet tot onjuiste gevolgtrekkingen, omdat het seculaire gedeelte van de door hen beschouwde operator (de z-component van de magnetisatie) diagonaal is in de door hen gekozen representatie.

W.J. Caspers, H.P. van der Braak, P.W. Verbeek en J.C. Verstelle, Physica 53 (1971) 210.

II

In verband met de digitale verwerking van meetgegevens verdient het aanbeveling bij het bouwen van weerstandsbanken en ratiotransformatoren het tientallig stelsel te vervangen door het tweetallig stelsel.

III

Het verdient aanbeveling de soortelijke warmte van Kondo legeringen te meten als functie van de sterkte van een uitwendig magnetisch veld bij temperaturen boven en beneden de Kondo temperatuur.

T.A. Kitchens, W.A. Steyert en R.D. Taylor, Phys. Rev. 138 (1965) A 467.

IV

Bij het waarnemen van electron paramagnetische resonantie in verdunde magnetische legeringen verdient het gebruik van een modulatie van de temperatuur voorkeur boven het gebruik van een modulatie van de sterkte van het uitwendige magnetische veld.

G. Feher, R.A. Isaacson en J.D. McElroy, Rev. Sci. Instr. 40 (1969) 1640.

V

Bij de interpretatie van electron paramagnetische resonantie waarnemingen aan Mn in Pd mogen dynamische effecten (zoals beschreven door Hasegawa) niet worden verwaarloosd. Rekening houdend met deze effecten kan de interpretatie beter in overeenstemming worden gebracht met de resultaten van soortelijk warmte en magnetisatie metingen aan Pd-Mn legeringen.

- H. Hasegawa, Prog. Theor. Phys. 21 (1959) 483.
 D. Shaltiel, J.H. Wernick, H.J. Williams en M. Peter,
 Phys. Rev. 135 (1964) A 1346.
 D. Shaltiel en J.H. Wernick, Phys. Rev. 136 (1964) A 245.
 H. Cottet, proefschrift, Universiteit van Genève, 1971.

VI

Isaacs gaat bij het berekenen van de kristalveldbijdrage tot de extra soortelijke warmte van Pd-Dy legeringen uit van de veronderstelling, dat de Dy-atomen zich niet in een magnetisch veld bevinden. Het deel van de extra soortelijke warmte, dat overblijft na aftrek van de zo berekende kristalveldbijdrage, schrijft hij toe aan ferromagnetische clusters, hetgeen zijn eerste veronderstelling onjuist maakt.

- L.L. Isaacs, Phys. Rev. B 9 (1974) 2228.

VII

De door Hultgren c.s. getabelleerde waarden voor de exces vrije vormingsenthalpie van een aantal geordende legeringen zijn onjuist.

- R. Hultgren, P.D. Desai, D.T. Hawkins, M. Gleiser en K.K. Kelley,
 Selected Values of Thermodynamic Properties of Binary Alloys,
 American Society for Metals.

VIII

Bij de analyse van hun Knight-shift metingen aan AuGa₂ hebben Weaver c.s. onvoldoende rekening gehouden met effecten ten gevolge van thermische uitzetting. Indien met deze effecten wel rekening wordt gehouden kan, in tegenstelling tot de conclusie van Weaver c.s., geen overeenstemming tussen de resultaten van de modelberekening en die van de experimenten worden verkregen.

- H.T. Weaver, J.E. Schirber en A. Narath, Phys. Rev. B 8 (1973) 5443
 L.R. Testardi, Phys. Rev. B 1 (1970) 4851.
 J.E. Schirber, Phys. Rev. Letters 28 (1972) 1127.
 W.W. Warren Jr., R.W. Shaw Jr., A. Menth, F.J. DiSalvo,
 A.R. Storm en J.H. Wernick, Phys. Rev. B 7 (1973) 1247.
 J.E. Schirber en A.C. Switendick, Solid State Comm. 8 (1970) 1383.

IX

De Brillouin funktie wordt ten gevolge van zijn flexibiliteit in verscheidene gevallen op inconsistente wijze gebruikt voor het interpreteren van experimentele resultaten.

Dit proefschrift, blz. 103.

X

Er bestaat op historische gronden een aanzienlijk verschil tussen de subsidieregeling voor het buurt- en klubhuiswerk en die voor het jeugdwerk uitgevoerd door vrijwilligers. Dit verschil kan niet meer worden verdedigd.

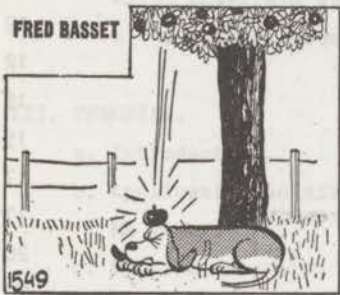
XI

In de subsidieregeling voor het openbaar vervoer wordt de rol van de taxi onderschat.

G.J. Nieuwenhuys

Leiden, 25 juni 1974.

FRED BASSET



1549



Gek toch... het lijkt wel, of de dingen worden aange-trokken door de aarde!



Interessante theorie... zou daar al eens iemand aan gedacht hebben?

Remarkable.... it seems	Interesting theory....
like things are	I wonder if somebody
attracted by the earth.	else has thought
	about that.

From "Leidsch Dagblad".

CONTENTS.

I. INTRODUCTION AND SUMMARY.	9
a. Introduction.	9
b. Summary.	10
II. EXPERIMENTAL INFORMATION.	12
a. Introduction.	12
b. Pure palladium.	12
c. Experimental methods.	15
c.1. Specific heat.	15
c.2. Electrical resistivity.	17
c.3. Magnetization and susceptibility measurements.	17
c.4. Electron paramagnetic resonance.	20
c.5. Mössbauer effect.	20
c.6. Determination of the transition temperature, T_C .	22
c.6.a. T_C from the specific heat in zero external field.	22
c.6.b. T_C from magnetization measurements.	23
c.6.c. T_C from the electrical resistivity.	23
c.6.d. T_C from the Mössbauer effect.	23
c.6.e. T_C from susceptibility measurements.	24
c.6.f. Discussion.	24
d. General results.	25
d.1. Pd-Co and Pd-Fe alloys.	26
d.2. Pd-Mn alloys.	28
d.3. The concentration dependence of the transition temperature.	29
d.4. Investigations of the ferromagnetic phase.	30
d.5. Two remarks.	31
d.6. Table.	31
e. Detailed results.	38
e.1. Specific heat of Pd-Co.	38
e.2. Electrical resistivity of Pd-Co.	41
e.3. Measurements of the Mössbauer effect in Pd-Co.	43
e.4. Magnetization measurements on Pd-Co.	44
e.5. Magnetic susceptibility of Pd-Co.	46

e.6. Specific heat of Pd-Fe.	47
e.7. Electrical resistivity of Pd-Fe.	53
e.8. Measurements of the Mössbauer effect in Pd-Fe.	56
e.9. Magnetization of Pd-Fe.	58
e.10. Specific heat of Pd-Mn.	58
e.11. Electrical resistivity of Pd-Mn.	60
e.12. Electron paramagnetic resonance of Mn in Pd.	66
e.13. Low-field susceptibility of Pd-Mn.	66
e.14. Magnetic susceptibility and magnetization of Pd-Mn.	68
 III. THEORIES.	 70
a. Introduction.	70
b. Application to dilute Pd-based alloys with Co, Fe or Mn impurities.	70
c. Spatial extension of the induced moment.	71
d. Interaction between the moments (origin of ferromagnetism).	72
d.1. The itinerant picture.	73
d.2. The localized picture.	73
d.3. Choice between the two pictures.	73
d.4. The model of Takahashi and Shimizu.	76
d.5. Calculation of the specific heat.	79
d.6. Incorporation of the statistical spatial distribution of the magnetic moments.	80
d.6.a. The zero temperature case.	81
d.6.b. The non-zero temperature case.	84
 IV. MODEL CALCULATIONS.	 88
a. Introduction.	88
b. Calculation of the specific heat of a ferromagnet using the Weiss molecular-field model.	88
c. Variant involving a distribution of molecular-field coefficients.	91
d. Variant involving a <i>macro</i> distribution of <i>g</i> -values.	93
e. Variant involving a <i>micro</i> distribution of <i>g</i> -values.	95
f. Variant involving a <i>micro</i> distribution of <i>g</i> -values as well as a distribution of molecular-field coefficients.	98
g. Calculation of the electrical resistivity using the W.M.F. model.	400

V.	INTERPRETATIONS.	102
a.	Magnetic quantum number.	102
b.	Paramagnetic behaviour.	105
b.1.	Paramagnetic behaviour of Pd-Mn.	105
b.2.	Paramagnetic behaviour of Pd-Co and Pd-Fe.	105
c.	Ferromagnetism.	115
c.1.	Transition temperature.	115
c.2.	Character of the transition.	117
d.	Ferromagnetism, spin glass and transition temperature.	122
e.	Note added in proof.	124
VI.	INFLUENCE OF THE ADDITION OF RH AND AG ON THE BEHAVIOUR OF DILUTE PD-BASED ALLOYS WITH CO, FE OR MN IMPURITIES.	126
a.	Introduction.	126
b.	Results.	127
c.	Discussion.	132
	APPENDICES.	134
1.	Apparatus for the measurement of low-field susceptibility.	134
2.	The a.c. system for heat-capacity measurements.	136
3.	Experimental set-up for the measurements of the electrical resistivity.	147
4.	Preparation of the specimens.	151
	BIBLIOGRAPHY.	161
	SAMENVATTING.	168

CHAPTER I
INTRODUCTION AND SUMMARY.

I.a. Introduction.

Elements situated in the first long period of transition metals in the periodic system show a number of remarkable effects, when dissolved in palladium. Obviously this should be ascribed to the peculiarly large paramagnetic susceptibility of this host; to some extent Pd may be called a nearly ferromagnetic metal. Dilute alloys of Cr in Pd exhibit the so-called Kondo effect. For concentrations below 2 at.% Pd-Ni alloys typically reflect the influence of local spin fluctuations.

The elements Co, Fe and Mn maintain more or less their magnetic properties when dissolved in Pd, namely permanent magnetic moments are associated with them. However, measurements of the magnetization of this kind of alloys have demonstrated that the moment of dissolved magnetic atom is quite large, about $10 \mu_B$ per Co- or Fe-atom and $7.5 \mu_B$ per Mn-atom (μ_B is the Bohr magneton). The last result has been established only recently. Theory strongly indicates that atoms dissolved in a non-magnetic matrix should obey Hund's rule. This rule, however, does not allow the building up of such large moments as has been found. Hence, it should be assumed that part of these moments is due to the polarized d-band of Pd-metal. Diffuse neutron scattering experiments succour this assumption and show that the magnetic moments associated with Co- and Fe-atoms are spatially extended over more than 200 Pd-atoms. Unfortunately, no neutron scattering experiments on Pd-Mn have been published yet. Because of their largeness the moments mentioned above are called "giant moments".

Inevitably, the question arises how large the multiplicity (or the magnetic quantum number J) of these moments is. When the value of J has been determined, we should wonder whether, when the saturation value of the moment is written as $\mu_{\text{sat}} = g_{\text{eff}} J \mu_B$, the magnetization and the specific heat in an external magnetic field behave in accordance with a Brillouin function involving these values of J and g_{eff} . Theory, although able to account for the existence, the magnitude and the spatial extension of the giant moment, returns no answers to these questions.

In general interpretations of magnetic measurements, assuming a behaviour according to a Brillouin function, result in a large value of J

and a small one of g_{eff} . Calculations of the magnetic entropy based on specific-heat investigations are in contrast with this result. This contradiction was the main reason for our investigation.

Obviously due to the large spatial extension of the moments ferromagnetic ordering at low temperatures occurs in this alloy system down to rather low concentrations ($c < 0.1$ at.%). The value of the transition temperature T_C and the character of the magnetic ordering have been the subject of a large number of investigations (experiments on more than 100 Pd-based alloys with Co, Fe or Mn have been carried out). To give a rough sketch we might say that T_C is proportional to c^2 for small amounts of Co or Fe in Pd and linear in c for large concentrations. The onset of ferromagnetism does not occur at a sharply defined temperature, but rather more in a wide temperature range of order of $0.5 T_C$ (dependent on concentration). This temperature range is larger in the case of Co and in the case of Fe. On the other hand, recent specific-heat measurements on Pd-Mn alloys ($c < 2.5$ at.%) reveal a remarkable sharp transition to ferromagnetism at decreasing temperature. For this alloy system T_C seems to be proportional to c . The question whether the behaviour of Pd-Mn is really exceptional will be one of the subjects of this thesis.

The magnetic moments being associated with impurity atoms, the localized model for ferromagnetism seems to be appropriate for the alloy systems mentioned. However, since a large part of the moment originates from the Pd d-band, one can imagine that the presence of the impurity atoms drives Pd to be a band ferromagnet. Theories and arguments based on one of these models or on a mixing of them can be found in the literature. In the case of dilute alloys a choice between the theories will be made in this thesis.

I.b. Summary.

A summary of the main results of the present and of directly related investigations will be presented here in telegraphese.

- The giant moment should be accounted for by "normal" values of the magnetic quantum number ($3/2$ for Co, 2 for Fe and $5/2$ for Mn) and a large value of g_{eff} .
- Paramagnetic alloys of Mn in Pd do, but alloys of Co or Fe in Pd do not behave according to Brillouin functions. Hence, a number of interpretations of magnetic measurements should be considered as incorrect.

- The localized model for ferromagnetism can well account for the magnetic ordering of dilute Pd-based alloys (certainly if $c < 1$ at.%).

A straightforward generalization of the Weiss molecular-field model may be applied.

- The transition temperature of Pd-Mn alloys is not proportional to the concentration, but after scaling the behaviour is similar to what has been found for Pd-Co and Pd-Fe alloys. The concentration dependence can be explained from a calculation of the strength of the interaction between two impurity atoms as a function of the distance.

- Comparison between alloys with equal concentration shows that the magnetic ordering in Pd-Mn is not at all exceptional, but analogous to that in Pd-Co and in Pd-Fe. It should be mentioned, however, that Pd-Mn at $c > 3$ at.% is a so-called spin glass.

- Addition of Ag or Rh to Pd-alloys with Co, Fe or Mn has important influences on their properties. Unfortunately the effects are not completely understood.

CHAPTER II

EXPERIMENTAL INFORMATION

II.a. Introduction.

If one wants to review the experimental information known up to the present about dilute alloys of Co, Fe or Mn in Pd, one is confronted with a large number of papers containing experimental methods, analyses, results and interpretations amounting to what may be called now "the puzzling world" of dilute Pd-based alloys (1). In this chapter an attempt is made at giving a guide into this world.

The experiments, carried out in the course of our investigation cannot be described as a closed series of measurements of a special property of dilute Pd-based alloy systems, but should be considered as a supplement to the experimental data reported up till now. This supplement was necessary in order to obtain a more consistent picture of Pd-based alloys with Co, Fe or Mn. Therefore, the presentation of our experimental results has been incorporated in the review of the literature on experimental work.

Generally speaking, an experimental investigation consists of the following steps: 1^o measurement; 2^o analysis of the data leading to interpretable results; 3^o interpretation of the results by comparing them with theory or models. Therefore, the presentation of the results in this thesis has been organized as follows: in section II.b some general facts about Pd will be given; in section II.c the experimental methods used will be outlined together, when necessary, with the method for analysis of the data. In section II.d general results on dilute alloys are presented, partly in the form of a table, while section II.e contains the detailed results of those experiments which are of special interest in connection with the model calculations of chapter IV. When appropriate, reference will be made for the experimental technique to the appendices or to the literature. The interpretation of the results and their comparison with theory or with model calculations will be presented in chapter V.

II.b. Pure palladium.

The special interest, which dilute Pd alloys with Co, Fe and Mn impurities have received, is due to peculiar properties of pure Pd. A brief description of these properties is therefore necessary.

A detailed account concerning pure Pd can be found in ref.2 and in the references quoted therein.

Palladium, with atomic number 46, has ten electrons outside a krypton-like core. The ground state configuration is (krypton) $(4d)^{10}$, but the $(4d)^9(5s)^1$ configuration lies only $6.56402 \cdot 10^3 \text{ cm}^{-1}$ above this state (3) ($6.56402 \cdot 10^3 \text{ cm}^{-1} = 0.813551 \text{ eV} = 0.0598483 \text{ Ry} = 1.30322 \cdot 10^{-12} \text{ erg}$). In metallic palladium, due to the changed boundary conditions (4), the 5s-state is lowered relative to the 4d-state, and the broad conduction band arising from 5s and from 5d-states overlaps the narrow 4d-band. This is schematic shown in fig.II.1. Consequently, as ten band states per atom are filled up below the Fermi energy, there are 0.36 unoccupied d-states (holes).

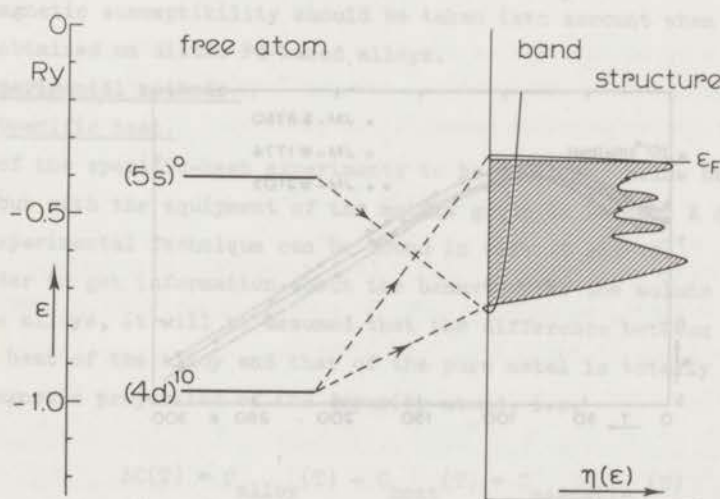


Fig. II.1. Change of the energy levels due to the transition from atomic Pd to metallic Pd.

The following distinction should be noticed. The expression "itinerant electrons" means the electrons contained in the d-band as well as in the s-band. The words "band electrons" will be used for electrons in the d-band only, the electrons in the s-band will be called "conduction electrons" since these electrons carry the electrical current for the main part.

Due to the narrowness of the d-band the density of states of the itinerant electrons at the Fermi energy, $\eta(\epsilon_F)$, is much larger than for most other metals. The quantity $\eta(\epsilon)$ is defined as the number of states per unit of energy (usually eV) per spin direction per atom at the energy ϵ . Band structure calculations by Mueller and by Anderson (5-7) result in a value of order of 1.4 for $\eta(\epsilon_F)$. The large density of states is also reflected by the large contribution of the itinerant electrons to the specific heat and by the large paramagnetic susceptibility. The latter quantity of itinerant electrons, assuming no interaction between them, is given by the Pauli susceptibility

$$\chi_P = 2 \mu_B^2 \eta(\epsilon_F). \quad (II.1)$$

This means that even the Pauli susceptibility is much larger than for other metals, and should be $0.8 \cdot 10^{-4}$ emu/mol according to band structure calculations.

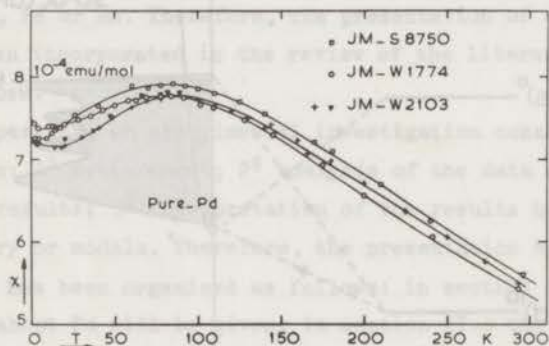


Fig. II.2. Susceptibility versus temperature for three "pure" Pd samples. Data marked (∇) were taken on 16-5-'68, while those designated (+) were obtained on 21-1-'70 (after Van Dam (2)).

In fig.II.2 the magnetic susceptibility as measured by Van Dam (2) on three "pure" Pd samples of different lot number is shown as a function of temperature. As is evident from this figure the susceptibility of Pd is much larger than the calculated value. Thus from experiments the conclusion can be drawn that the magnetic susceptibility is enhanced

with respect to Pauli's value. It is generally accepted that this enhancement is caused by exchange interactions between band electrons. Within Stoner's theory (8) the susceptibility in such a case is given by

$$\chi = \frac{\chi_P}{1 - I \eta(\epsilon_F)}, \quad (\text{II.2})$$

wherein I is a measure for the exchange interactions and the factor $\{1 - I\eta(\epsilon_F)\}^{-1}$ is called the Stoner enhancement factor.

Another experimental fact seen in fig.II.2 is the peculiar temperature dependence of the susceptibility, which is quite unexpected for Pauli paramagnetism. Van Dam (2) discussed this temperature dependence in detail. In connection with the present work the temperature dependence of the magnetic susceptibility should be taken into account when analysing results obtained on dilute Pd-based alloys.

II.c. Experimental methods.

II.c.1. Specific heat.

Most of the specific-heat experiments to be described below have been carried out with the equipment of the metals group in Leiden. A description of the experimental technique can be found in refs. 9 and 10.

In order to get information about the behaviour of the solute atoms in dilute alloys, it will be assumed that the difference between the specific heat of the alloy and that of the pure metal is totally due to the magnetic properties of the impurity atoms, i.e.

$$\Delta C(T) = C_{\text{alloy}}(T) - C_{\text{host}}(T) = C_{\text{magnetic}}(T) \quad (\text{II.4})$$

When investigating the specific heat of more concentrated alloys or of alloys where the masses of the impurity atoms and those of the host atoms differ much, one should take into account the change of the lattice specific heat. In such cases measurements on comparable nonmagnetic impurities are necessary (11). Apart from the influence of the impurities on the lattice specific heat the electron-phonon interaction might be effected by the decreased mean free path. However, since the electron-phonon interaction is accounting only for less than 20% of the observed enhancement of the electronic specific heat of Pd (12), the effect of the mean free path is not likely to be important. For dilute alloys of

Pd with Mn, Fe or Co eq.II.4 may assumed to be correct.

Once ΔC is known as a function of temperature, the magnetic entropy can be calculated from the data via

$$S_m = \lim_{T \rightarrow \infty} \int_0^T \frac{\Delta C}{T'} dT' \quad (II.5)$$

In order to evaluate this integral ΔC has to be extrapolated at the low temperature side to $T=0$ and at the high temperature side to $T=\infty$.

In most cases a sufficiently accurate extrapolation to $T=0$ is possible. For the high temperature side the assumption is made that ΔC varies as T^{-2} , as has been found for many magnetic systems. Then $S_m(T)$ also varies as T^{-2} , making an extrapolation in a graph of $S_m(T)$ versus T^{-2} possible (13).

Since the entropy involved is due to a magnetic ordering process (in zero or finite external field) it follows from statistical thermodynamics that the entropy per magnetic moment S'_m is given by

$$S'_m = k_B \ln(2J + 1), \quad (II.6)$$

where k_B is Boltzmann's constant and J is the magnetic quantum number. Assuming all magnetic moments to have the same magnetic quantum number, the entropy per mol of alloy can be written as

$$S_m = cR \ln(2J + 1), \quad (II.7)$$

where R is the gasconstant and c the concentration of magnetic impurities.

When the excess specific heat has been determined from measurements in external magnetic fields, it may be possible to deduce the magnitude of the magnetic moment involved in the ordering process. For that purpose use has to be made of models describing the magnetic properties of the alloys. Comparison between the results of the specific-heat investigations and those of model calculations results in a value for g_{eff} (defined as $g_{\text{eff}} = \mu/(J\mu_B)$), together with the value of J from the entropy μ can be evaluated.

One of the experimental difficulties in the determination of the magnetic contribution to the specific heat is that the specific heat of the host, which has to be subtracted, is so large. Heat-capacity

measurements can generally be carried out with an accuracy of 0.5%, while the maximum contribution of the magnetic impurities is less than 5% in some cases. Therefore, when in the course of our investigation the excess specific heat of very dilute alloys had to be determined as a function of an external magnetic field, a different method only giving relative values has been used. This method has been called a.c. method and will be described in appendix 2. We will refer to the method as e.g. used by Boerstoeel et al. (10) as to the d.c. or adiabatic method.

II.c.2. Electrical resistivity.

What has been written about the problems of additivity of the specific heat holds for the electrical resistivity as well. The contribution due to the impurities, denoted by $\Delta\rho(T)$, is assumed to be given by

$$\Delta\rho(T) = \rho_{\text{alloy}}(T) - \rho_{\text{host}}(T), \quad (\text{II.8})$$

which is Matthiessen's rule. This rule implies that no changes occur in the phonon-electron interaction on alloying and that multiple (phonon + impurity) scattering is negligible. For most metal alloys Matthiessen's rule is not fulfilled; many workers have examined deviations from it (14). Nevertheless, in the context of the present work Matthiessen's rule will be assumed to be obeyed. Reference will be made to this somewhat doubtful assumption, when it is appropriate.

The resistivity measurements have been carried out by means of the usual four-probe technique using the equipment of the metals group as described by Star et al. (15). The character of the resistivity versus temperature curve of the alloys under investigation made it necessary to take many data points in a small temperature range. Therefore, the equipment has been partly automatized (see appendix 3).

II.c.3. Magnetization and susceptibility measurements.

The essential part of a measurement of the magnetization M and of the susceptibility χ is the determination of the magnitude of the bulk magnetic moment of a specimen as a function of temperature and of magnetic field strength. This can be done either by measuring the voltage induced by a moving sample in a pair of solenoids (see Foner et al. (16)) or by measuring the force on the sample exerted by an inhomogeneous magnetic field (Faraday method, see e.g. ref.17). As the magnetization

does not vary with time during the measurement, these methods may be called d.c. methods.

The vibrating sample method is particularly useful for the determination of M as a function of temperature and of magnetic field, while the Faraday method is commonly applied for the measurement of χ , defined as

$$\lim_{H_{\text{ex}} \rightarrow 0} M/H_{\text{ex}}, \quad H_{\text{ex}} \text{ being the external field.}$$

The assumption of additivity, made in connection with the specific heat and with the electrical resistivity, is generally accepted to pertain in the cases of the magnetization and of the susceptibility as well. In order to obtain the value for the contribution of the impurities to the susceptibility $\Delta\chi$ one has to measure χ_{host} of a sample of the pure metal in a separate experiment. In the case of the magnetization the assumption is made that

$$M_{\text{alloy}} = M_{\text{imp}} + \chi_{\text{HF}} H_{\text{ex}}, \quad (\text{II.9})$$

χ_{HF} being defined as dM/dH_{ex} for values of H_{ex} large enough to saturate M_{imp} . Although for most dilute alloys χ_{HF} equals χ_{host} , the advantage of the magnetization measurement is that a comparison between these quantities forms a test for the additivity (assuming χ_{host} to be independent on the external field).

The magnetic quantum number can only be determined from the results of the magnetization measurements by fitting the experimental data to a Brillouin function, which implies the assumption that all magnetic moments have the same magnetic quantum number and that all magnetic moments have the same effective g -value.

It is also possible to deduce J from the saturation magnetization combined with the result of the susceptibility measurements. If $\Delta\chi$ obeys the Curie-Weiss law, the Curie constant C_C is given by

$$C_C = \frac{c N g_{\text{eff}}^2 J(J+1) \mu_B^2}{3 k_B} \quad (\text{II.10})$$

Combined with the value for $M_{\text{imp,sat}}$, given by $c N g_{\text{eff}} J \mu_B$, a value for J can be derived, hardly dependent on the assumption of equal values for g_{eff} (18).

At temperatures in the vicinity of the ferromagnetic transition temperature the measured value of dM/dH_{ex} has a large field dependence. On the other hand it has also a large absolute value. In order to determine χ in these cases an a.c. method (see appendix 1) using an external magnetic field down to 0.04 Oe has been applied.

Another difficulty shows up when analyzing $\Delta\chi$ of dilute Pd-based alloys as a function of temperature. This kind of alloys, having a localized magnetic moment associated with the magnetic impurities, is expected to obey the Curie-Weiss law:

$$\Delta\chi = \frac{c N p_{eff}^2}{3k_B(T-\theta)} \quad (II.11)$$

where p_{eff} is the effective magnetic moment and θ is the Curie-Weiss temperature. However, from experiments, it was evident that eq.II.11 did not fit the data, unless the temperature dependence of the host susceptibility was taken into account by assuming p_{eff} to be temperature dependent. Denoting χ_{host} and p_{eff} at a fixed temperature $T^{(r)}$ by $\chi_{host}^{(r)}$ and $p_{eff}^{(r)}$, respectively, this can be done by writing the effective moment as

$$p_{eff}^{(T)} = p_{eff}^{(r)} \frac{\chi_{host}^{(T)}}{\chi_{host}^{(r)}} \quad (II.12)$$

The value of $p_{eff}^{(r)}$ has to be determined from a fit to the experimental data. Another way of incorporating the temperature dependence of the susceptibility of the host is to assume

$$p_{eff}^{(T)} = p_{eff}^{(0)} \{1 + \alpha \chi_{host}^{(T)}\} \quad (II.13)$$

where $p_{eff}^{(0)}$ is the bare effective moment of the magnetic impurity (without the moment of the polarized d-band) and α is a parameter to be deduced from the experimental results. As will be outlined in chapter III these equations do not add an extra parameter, but have a physical background.

II.c.4. Electron paramagnetic resonance.

The analysis of the results of electron paramagnetic resonance experiments on dilute alloys is quite complicated. The analysis of the data and their interpretation in the light of the existing theories are more or less intertwined. Nevertheless, because some E.P.R. measurements have been carried out on these alloys, results of which are important in connection with the models used in this thesis, some aspects of these investigations have to be elucidated.

In a dilute binary alloy of a non-magnetic metal with magnetic impurities there are two spin systems capable of responding to the high-frequency field applied in E.P.R.; the impurity system (denoted by S_I) and that of the itinerant electrons (denoted by S_{ie}). Since the magnetic susceptibility of S_I is larger in most cases (see however Monod et al.(21)), the response will be determined by this system. For a description of the alloy the following simple model will be used (see fig.II.3): The system S_I is energetically coupled to the lattice via a relaxation mechanism characterized by a relaxation time T_{IL} . The relaxation to the S_{ie} -system and vice versa are characterized by T_{Iie} and T_{ieI} , respectively. The strength of the interaction of the S_{ie} -system with the lattice is reflected by T_{ieL} . When the impurity atom is in the S-state its g-value will be nearly 2, the same value as that of the itinerant electrons. The resonance of non S-state impurities is rather difficult to observe. If the g-values are nearly the same and if $T_{ieL} \gg T_{Iie}$ there will occur a large cross relaxation between the two spin systems. The effective relaxation time deduced from the width of the resonance line will then be determined for the main part by T_{ieL} . This is the so-called bottleneck effect (19). In this case it is trivial that the polarization of the itinerant electrons is no able to cause a shift $\Delta\omega$ of the resonance frequency of the S_I -system. In fig.II.4 curves are shown for $1/T_{eff}$ and $\Delta\omega$ as a function of $x=T_{Iie}/T_{ieL}$.

Dynamic effects like the bottleneck effect mentioned above must be taken into account at drawing conclusions from E.P.R. investigations on dilute alloys.

II.c.5. Mössbauer effect.

The Mössbauer effect or the recoilless gamma emission has proved to be a very effective tool for studying magnetism in solids. When an excited nucleus is bound to a crystal lattice, there is a large probability

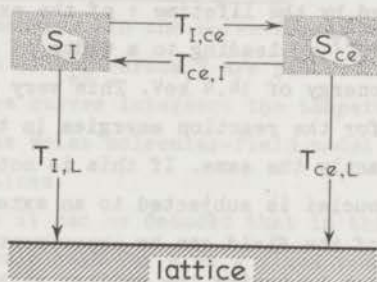


Fig. II.3. Sketch of the spin systems and interactions in dilute alloys.

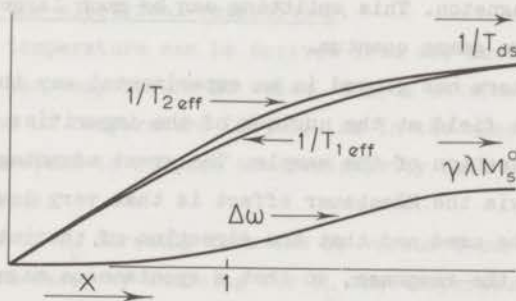


Fig. II.4. The inverse of the relaxation times and the frequency shift as a function of the ratio of the relaxation time T_{Iie} and T_{ieL} . (after Hasegawa (19)). Note that Hasegawa used T_{sd} for T_{Iie} and T_{sL} for T_{ieL} .

for recoilless emission of a gamma photon. The energy of the gamma photon is equal to the reaction energy involved in the decay process. Therefore, this gamma photon can excite another nucleus. The natural width of the gamma photon is mainly determined by the lifetime τ of the excited state. For instance for ^{57}Fe $\tau = 10^{-7}$ s, leading to a width of $4.6 \cdot 10^{-9}$ eV, while the gamma quantum has an energy of 14.4 keV. This very small relative width makes it necessary for the reaction energies in the emitting and absorbing nuclei to be exactly the same. If this is not the case, because for instance, one of the nuclei is subjected to an external field, the spectrum in the presence of the field can be experimentally measured utilising the Doppler effect by moving the emitter with respect to the absorber or vice versa.

The Mössbauer effect thus offers the possibility to determine internal magnetic fields acting on the nucleus in a solid. If, to take a simple example, the excited state of the nucleus has a nuclear spin I , a nuclear gyromagnetic ratio g_N and the ground state has no spin and if it is placed in an external magnetic field H , the energy levels of the decay will be split up into $2I+1$ levels with a spacing of $\mu_N g_N H$, where μ_N is the nuclear Bohr magneton. This splitting can be much larger than the natural width of the gamma quantum.

A number of workers has proved in an experimental way that e.g. for Pd-based alloys the field at the nucleus of the impurities is proportional to the bulk magnetization of the sample. The great advantage of measuring the magnetization via the Mössbauer effect is that very low concentrations of impurities can be used and that the direction of the internal field does not influence the response, so that a spontaneous magnetization can easily be determined.

II.c.6. Determination of the transition temperature T_C .

The transition temperature of a ferromagnetic material can be determined in several ways. Due to the presence of "tails" of the spontaneous magnetization and due to the width of the transition, particularly in alloys, the results obtained can differ by an amount of 30% or more.

II.c.6.a. T_C from the specific heat in zero external field.

There are two methods for determining T_C from specific heat data measured as a function of temperature. The simplest way is to identify T_C with the temperature at which ΔC attains its maximum value as a function of T . Another way is to compare the specific-heat results with model

calculations. In a model ΔC is calculated as a function of T/T_C so that T_C can be found from a fit to the experimental data.

II.c.6.b. T_C from magnetization measurements.

Here are also two methods. In the Weiss-Forrer method (22) curves at constant magnetization of H_{ex} versus T are plotted. The limit of the values of T where these curves intersect the temperature axis is identified as T_C . According to the Weiss molecular-field model such curves should approximate straight lines.

From thermodynamics it can be deduced that in the vicinity of T_C the following relation should hold for M at a fixed temperature:

$$\alpha' M + \beta' M^3 = H_{ex}, \quad \alpha' = 0 \text{ at } T = T_C \quad (\text{II.14})$$

By plotting M^2 versus H_{ex}/M (the so-called Arrott-plot (23)) values for α' can be found for each temperature. The transition temperature can then be determined from a plot of α' versus T at the intersection with the temperature axis.

II.c.6.c. T_C from the electrical resistivity.

The transition temperature can be derived from the resistivity by identifying it as the temperature at which $d\Delta\rho/dT$ attains its maximum value as a function of temperature (24,25). As in the case of the specific heat it is also possible to compare the resistivity data with the results of model calculations.

A determination of T_C directly from the $\Delta\rho$ versus T curve has been carried out on most cases by choosing for T_C the temperature at which a knee appears in the $\Delta\rho$ versus T plot. Of course the result of this method and the result from the maximum of $d\Delta\rho/dT$ only coincide when the knee is infinitely sharp (a discontinuity in $d\Delta\rho/dT$). In the case of broad transitions a number of authors has defined T_C as that temperature where the $\Delta\rho$ versus T curve starts to deviate from a straight line with increasing temperature. This method results in nearly the same value as derived from the maximum of $d\Delta\rho/dT$.

II.c.6.d. T_C from the Mössbauer effect.

At temperatures above T_C (and without an external magnetic field) there is no hyperfine field acting on the nucleus (it has been proved in an experimental way that the hyperfine field is proportional to the

magnetization, see section II.d.). The Mössbauer spectrum will therefore be a single line. Below T_C the spontaneous magnetization causes a hyperfine field, so that the spectrum will now be splitted in a number of lines (six in the case of ^{57}Fe). The transition temperature is now defined as that temperature at which the single line starts to broaden with decreasing temperature.

II.c.6.e. T_C from susceptibility measurements.

Deriving T_C from susceptibility measurements is done by fitting the data to the Curie-Weiss law or to the modified one (see section II.c.3) and identifying θ as T_C . It should be noticed that θ equals T_C only in the Weiss molecular-field approximation.

II.c.6.f. Discussion.

In view of the experimental results (see e.g. table II.I) it can roughly be said that the values of T_C are in the following order from low to high values: maximum of $d\Delta\rho/dT$, maximum of ΔC , model calculations of $d\Delta\rho/dT$, model calculations of ΔC , Mössbauer effect, magnetization Arrott-plot, magnetization Weiss-Forrer and at last susceptibility. Results from model calculations concerning random dilute ferromagnetic alloys (see chapter III and IV) are more or less in agreement with this experimentally found order of T_C -values.

It is difficult to make a choice between the values of T_C , which is rigidly based on theory. Nevertheless, based on the agreement between the results of various experiments and based on the experience with model calculations it may be said that the values for T_C obtained from the maximum of ΔC , from model calculations of $d\Delta\rho/dT$, from model calculations of ΔC and from the Mössbauer effect are the most reliable values.

It should be noted that the use of H_{ex} in the equations given above is not exactly correct. A value of the magnetic field H_1 , as defined $H_1 = H_{\text{ex}} - D'M$ should be used, wherein D' is the demagnetization factor. However, since M of dilute alloys is small this correction can be neglected in most cases.

II.d. General results.

Experimental evidence for the existence of the magnetic moments associated with Co, Fe or Mn impurities in Pd can be obtained from susceptibility measurements. It appeared that the susceptibility obeys the Curie-Weiss law or the modified one and that the Curie constant C_c is proportional to the amount of impurities present in the alloy.

From theory (e.g. the Anderson model) it is known that the local magnetic moment associated with the impurity should be ascribed to an extra density of states for spin up electrons located below the Fermi level and an extra density of states for spin down electrons located above the Fermi energy. Due to the hybridization of the band states with the localized states of the impurity atom, these extra densities of states have a width Δ on the energy scale. This width is sometimes interpreted in terms of the lifetime of the magnetic moment; Δ being of order of electronvolts, this lifetime should be very short ($\sim 10^{-14}$ s). Nevertheless, it has proved possible to observe the electron paramagnetic resonance for a number of alloy systems (20). Therefore, the interpretation of Δ in terms of a lifetime is not correct. Indeed, it can be shown (26) on theoretical grounds that such an interpretation is untenable, in particular, it is not consistent with the Pauli principle.

Realizing these arguments, we may say that the magnetic moments associated with Co, Fe or Mn in Pd are rather well defined. Important properties of these moments therefore are the magnetic quantum number J (or the multiplicity), the magnitude of the moment μ and the effective g -value, being defined as $\mu/(J \mu_B)$. Whether the magnetization as a function of temperature and external field strength can be described by a Brillouin function involving these values of J and g_{eff} is one of the main questions experiment has to answer.

The strength of the interaction between the magnetic moments in the alloy, causing ferromagnetism in the systems under investigation, is characterized by the value of the transition temperature. These values as a function of the concentration of the impurities contain therefore information about the strength of the interaction as a function of the distance of the impurities.

A table containing the results from experiments for the quantities mentioned above will be submitted with this section (see II.d.6).

II.d.1. Pd-Co and Pd-Fe alloys.

Regarding Co and Fe impurities in Pd there are two striking features of the experimental data: ferromagnetism exists in these alloys down to very low concentrations, 0.01 at.% for Fe (27,28) and 0.1 at.% for Co impurities (29); the magnitude of the magnetic moment associated with the impurity atom is very large, about $10\mu_B$ per Co- or Fe-atom (27-32). The magnitude of the moments decreases with increasing concentration of the impurities.

The observed $10\mu_B$ is much larger than the maximum moment for a Co- or Fe-atom according to the Pauli principle. Obviously, part of the observed moment must be due to a polarization of the host metal. If this is correct, the "giant moment" must be extended over a large number of Pd-atoms, since the moment per Pd-atom is limited by the low number of d-holes (0.36) per atom and probably to a much lower value by energy considerations. The crucial evidence for the existence of the polarization cloud came from diffuse neutron scattering experiments carried out by Cable et al. (33) and by Phillips (34) on Pd-Fe alloys and by Low and Holden (35-37) on Pd-Fe and on Pd-Co alloys. Low et al. used a special technique of diffuse scattering of long wave length neutrons ($\lambda=5 \text{ \AA}$), which enables an examination of the spatial distribution of the magnetic moment in the vicinity of the impurity atom. The results of the experiments on Pd-Fe 0.25 at.% and on Pd-Co 0.3 at.% are shown in fig.II.5, where the moment density is plotted versus the distance from the impurity. The long range nature of the polarization is clear from the graph.

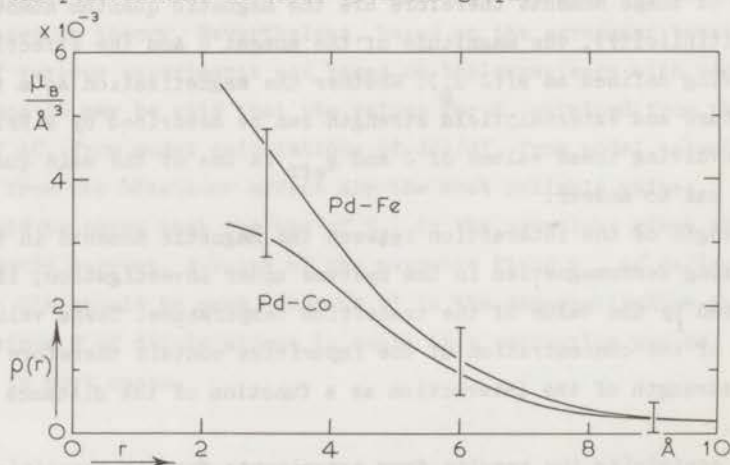


Fig. II.5. Magnetic-moment density as a function of the distance from the solute site in dilute Pd-Fe and Pd-Co alloys (after Low and Holden (36)).

A possible anisotropy of the moment distribution has been investigated by Hichs et al. (37) on a Pd-Fe 0.25 at.% single crystal. No anisotropy has been detected.

In view of this long range the occurrence of ferromagnetism down to very low concentrations becomes somewhat comprehensible, for even at these very low concentrations of solute atoms a considerable overlap of the polarization clouds will occur, causing an interaction between the moments.

From measurements of the Mössbauer effect two important facts have become evident: 1⁰ the giant moment exists not only in the ferromagnetic state but also in the paramagnetic one down to a fairly small amount of Fe, about 30 ppm; 2⁰ spontaneous magnetization exists in zero external magnetic field.

The concept of ferromagnetism in Pd-based alloys was mainly due to magnetization experiments. Values of the spontaneous magnetization are obtained from these experiments by extrapolation of the data obtained in an external field. In the case of dilute alloys of Co or Fe in Pd, the result of such an extrapolation looks similar to the magnetization versus temperature curve of a paramagnet in a constant external field. Besides, the extrapolation procedure might be considered as doubtful at establishing spontaneous magnetization (38). The results from the Mössbauer effect measurements must therefore be considered as a necessary supplement to the magnetization investigations.

Spontaneous magnetization in Pd-Co alloys has been investigated by Dunlap and Dash (39) and that in Pd-Fe alloys by Trousdale et al. (40). It should be noticed that the Co-nucleus is not a good Mössbauer probe. Measurements on Pd-Co alloys have been carried out by using small amounts of ⁵⁷Fe (see section II.e.3).

A general feature of the magnetic ordering process in dilute alloys of Co and Fe in Pd is the width of the transition, particularly at very low concentrations. The spontaneous magnetization has a very long tail at $T > T_C$; the ΔC versus temperature curve has a broad wedge-shaped maximum and the electrical resistivity decreases more gradually with decreasing temperature than should be expected in the case of a uniform ferromagnet [†])

[†]) Uniform ferromagnet means a ferromagnet with a sharp transition, such as has been observed in Ni or Fe.

This spread in the transition is revealed in table II.I by the large discrepancy in the values for T_C derived from different experiments. A more detailed discussion will be found in section II.e and in chapter V.

Concerning the results for the magnetic quantum number, there exists a large discrepancy between the values deduced from measurements of the magnetization and of the Mössbauer effect in an external magnetic field on one hand and the results obtained from specific-heat experiments on the other. It should be noticed that, as already mentioned in section II.c, if the magnetic quantum number is derived from magnetization and related experiments, this is done by fitting the data to a Brillouin function (incorporating a molecular field if necessary), while the value of J can be derived from the specific heat data via thermodynamic relations, which are only based on the assumption of equal values of J for all magnetic moments.

The specific heat of Pd-Co and Pd-Fe dilute alloys has also been determined in external magnetic fields. From these experiments it could be learnt that these alloys did not show normal behaviour (i.e. Schottky behaviour), not even in the case of extreme dilution investigated in the strongest external field available. This implies that it is not possible to describe the specific heat in an external field by the temperature derivative of the Brillouin function involving the values of J and g_{eff} as obtained from the entropy content and magnetization measurements, respectively. As mentioned above the magnetization as a function of temperature and external field strength could only be described by a Brillouin function with a value of J larger than that obtained from entropy calculations. The impossibility of describing it with the correct value for J is in agreement with the results of the specific-heat investigations. These consistent observations formed the first ground for the modifications of the Weiss molecular-field model used in chapter V to interpret the experimental results.

II.d.2. Pd-Mn alloys.

In contrast to the Pd-alloys containing Co and Fe the Pd-Mn system has not received much attention until recently. Resistance measurements by Sarachik and Shaltiel (41) and by Williams and Loram (42) indicate that ferromagnetism occurs in the Pd-Mn system at low temperatures, although the transition temperatures were much lower than for alloys with the same concentration of Co or Fe.

Boerstoeel et al.(13) have investigated the specific heat of a number of Pd-Mn alloys with concentrations ranging from 0.08 at.% up to 2.45 at.%. The most striking feature of the results obtained in zero external field was the sharp cusp in the ΔC versus T curve, indicative of a rather sharp transition to ferromagnetism. As known up till now such a sharp transition has not been found in any other disordered dilute alloy system.

Boerstoeel et al.(13) has also measured the excess specific heat in external magnetic fields. It appeared that for very dilute alloys the specific-heat results obtained in strong magnetic fields could be described by the Weiss molecular-field model. In order to make the molecular-field coefficient consistent with the zero field data a rather large value (of about 3) of the effective g-value had to be assumed.

This rather peculiar behaviour of Pd-Mn alloys attracted the attention of a number of other workers. Star et al.(18) measured the magnetization of a number of dilute Pd-Mn alloys and found that the saturation moment is about $7.8 \mu_B$, which value is consistent with the value of g_{eff} and the value of the magnetic quantum number as derived before from specific-heat experiments. Star et al. (18) has also shown that the magnetic isotherms as a function of H_{ex} could be accounted for by the Weiss molecular-field model in agreement with the analyses by Boerstoeel et al. (13).

It should be emphasized that very dilute alloys of Pd-Mn do behave according to a Brillouin function involving J as obtained from the entropy and g_{eff} as obtained from the magnetization, contrary to very dilute alloys of Pd-Co and (as will be shown in the next section) of Pd-Fe.

II.d.3. The concentration dependence of the transition temperature.

Collecting the data on T_C for Pd-Co and Pd-Fe alloys, it appeared that T_C is not proportional to the concentration, but varies as shown in fig. II.6. Until recently T_C of the Pd-Mn system seemed to be proportional to the concentration.

The comparison between Pd-Co, Pd-Fe and Pd-Mn alloys was unfortunately somewhat confusing, because of the larger concentrations of Mn that were needed to have the transition temperature in the range of liquid-He temperatures. Within the context of our investigation a number of resistance measurements have been carried out on very dilute alloys down to a temperature of 50 mK. The results of these experiments

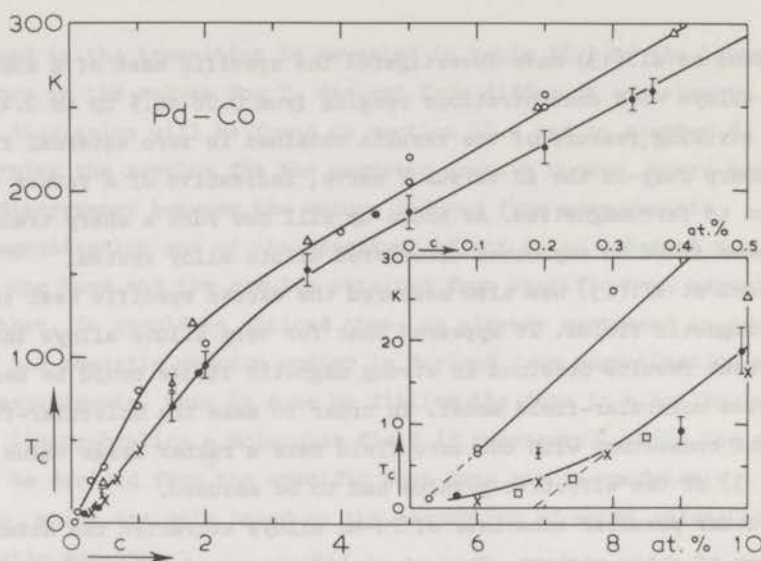


Fig. II.6. Transition temperature of Pd-Co alloys as a function of Co concentration (after Boerstael (9)).

demonstrated that the transition becomes broader with decreasing concentration as well as that T_C as a function of c behaves in a way similar to that of Pd-Co and of Pd-Fe.

An explanation of this behaviour for alloys with a concentration smaller than 1 at.% will be given in chapter III.

II.d.4. Investigations of the ferromagnetic phase.

Extensive investigations of the ferromagnetic phase of dilute Pd-based alloys with Co, Fe and Mn impurities have been carried out by Williams, Colp, Loram and Swallow (43-47).

In crystallographically ordered ferromagnetic systems the first possible excitations of the ordered state with increasing temperature are spin waves. If the ferromagnet is an electrical conductor (e.g. Fe) these spin waves give rise to an increase of the electrical resistivity proportional to T^2 for $T < T_C$. In alloy systems, where the magnetic moments are distributed at random over the lattice sites, the behaviour of the spin waves is different due to lack of translational invariance of the spinsystem.

Calculations via a modification of the conventional spin wave theory by Cole and Turner (48) and by Long and Turner (49) as well as calculations

by Doniach and Wohlfarth (50) indicate that the T^2 dependence has to be replaced by a $T^{3/2}$ one. This latter temperature dependence has been found to be in agreement with the experimental results. Nevertheless, resistance measurements on more concentrated alloys have revealed a T^2 dependence for $\Delta\rho$ at low temperatures.

The dependence of the acoustic spin wave stiffness constant (D , defined as the ratio between the energy of the spin wave and its wave vector squared) on the concentration and on the external field strength is somewhat vague from a theoretical point of view. At any rate, in all cases D showed up to be proportional to T_C (18,45).

Conclusions from the comparison between spin wave theory and the experimental results should be drawn with some care, because theory does not incorporate a variation in the strength of the interaction between the magnetic moments due to their random distribution over the lattice sites. Also a possible distribution in the magnitudes of the magnetic moments, to be discussed in chapter V, may play a role in the low temperature behaviour of these systems.

II.d.5. Two remarks.

A general remark about the magnetization measurements has to be made. For the three alloy systems mentioned, it is difficult to saturate the magnetization of the localized moments; fields up to 200 kOe are necessary. No clear-cut explanation is available for this effect.

Bearing in mind that the properties of dilute Pd-based alloys are due to the extremely large magnetic susceptibility of the host metal, an investigation of the influence of the addition of Ag or Rh seems inevitable. Addition of Ag to Pd decreases the susceptibility, while addition of Rh increases it. Experiments on these alloys have been carried out within the context of our investigation, but for reasons of clarity the discussion of these experiments and their results will be postponed to chapter VI.

II.d.6. Table.

Data reported in the literature and data obtained from the present investigation for in the transition temperature T_C , the saturation moment μ , the magnetic quantum number J and effective g -value g_{eff} (defined as $\mu/(J\mu_B)$) have been tabulated in table II.I for Pd-Co, Pd-Fe and Pd-Mn alloys. The first column contains the concentration of the alloy in at.%, the second column an abbreviation of the experimental method.

The meaning of the abbreviations are: Mössb.: Mössbauer effect; s.h.: specific heat; res.: electrical resistivity; $d\rho/dT$: temperature derivative of the electrical resistivity; magn.: magnetization measurement; susc.: susceptibility measurement; F.M.R.: ferromagnetic resonance; Arrott: T_C determined by means of an Arrott plot; W.F.: T_C determined applying the Weiss-Forrer method; model: T_C determined using model calculations; infl.: T_C determined as that temperature at which $\Delta\rho$ starts to deviate from a straight line as a function of T with increasing temperature; max.: T_C defined as that temperature at which ΔC -or $d\rho/dT$ attains its maximum value; knee: T_C defined as that temperature where a knee can be found in the resistivity versus temperature curve; W.M.F.: T_C determined from W.M.F. model calculations.

In the third column the number of the reference is given, p.w. stands here for "present work". The fourth, fifth, sixth and seventh column contains the values reported for the transition temperature in K, for the saturation moment μ in μ_B , for the magnetic quantum number J and for the effective g-value g_{eff} , respectively.

TABLE II.I

Main properties of Pd-Co alloys.

conc. (at.%)	exp. method.	ref.	transition temperature (K)	saturation moment (μ_B)	magn. quantum number	eff. g-value
0.07	Mössb	39	1.55			
0.075	s.h.	51			1.2	
0.098	res. (infl)	58	0.8			
0.1	magn. (Arrott)	29	7	10.8		
0.16	s.h. (model)	51	1.84		1.35	5.3
0.19	Mössb.	39	6.5			
0.2	d $\Delta\rho$ /dT (model)	51	3.5			
0.2	res. (infl)	58	2.95			
0.24	s.h. (model)	51	4.16		1.44	6.7
0.3	res. (infl)	58	6.45			
0.35	s.h. (max.)	51	8.8		1.35	
0.49	Mössb.	39	18.8			
0.5	magn. (Arrott)	29	25	9		
0.5	res. (infl)	58	16.2			
0.7	res. (infl)	58	27.5			
1.0	res. (infl)	58	44.0			
1	magn. (Arrott)	29	90	8.9		
1	susc.	52	253	3.3		
1.91	Mössb.	39	90			
3	susc.	52	305	3.5		
4.5	Mössb.	39	186			
5	susc.	52	323	3.5		
5	magn.	29		6.2		
7	susc.	52	353	3.4		
8	magn.	29		5.3		
10	magn. (W.F.)	53	300			
13	magn.	29		4.7		
16	magn. (W.F.)	53	400			
20	magn	29		3.7		

conc. (at.%)	exp. method.	ref.	transition temperature (K)	saturation moment (μ_B)	magn. quantum number	eff. g-value
30	magn. (W.F.)	53	650			
40	magn.	29		2.8		
40	magn. (W.F.)	53	800			
50	magn. (W.F.)	53	920			
60	magn.	29		2.2		
60	magn. (W.F.)	53	1100			
70	magn. (W.F.)	53	1180			
80	magn. (W.F.)	53	1260			
80	magn.	29		1.9		
90	magn. (W.F.)	53	1350			
100	magn. (W.F.)	53	1400			
100	magn.	29		1.7		

Main properties of Pd-Fe alloys.

conc. (at.%)	exp. method.	ref.	transition temperature (K)	saturation moment (μ_B)	magn. quantum number	eff. g-value
0.005	susc.	54	0.016			
0.007	susc.	54	0.036			
0.009	susc.	54	0.054			
0.01	magn. (Arrott)	27	0.44	4.5	16	2
0.01	susc.	54	0.059			
0.01	magn. (W.M.F.)	28	0.22			
0.01	Mössb.	30		12.6	6.5	2.4
0.013	susc.	54	0.097			
0.018	susc.	54	0.16			
0.02	susc.	54	0.2			
0.02	magn. (Arrott)	54	0.055			
0.03	susc.	54	0.39			
0.03	magn. (Arrott)	54	0.115			

conc. (at.%)	exp. method.	ref.	transition temperature (K)	saturation moment (μ_B)	magn. quantum number	eff. g-value
0.035	magn. (Arrott)	54	0.13			
0.043	magn. (Arrott)	54	0.2			
0.05	magn. (W.M.F.)	28	0.55			
0.05	magn. (Arrott)	27	0.6	6	8.5	2
0.06	magn. (Arrott)	54	0.41			
0.068	magn. (Arrott)	54	0.47			
0.07	magn. (Arrott)	27	0.78	7	8.5	2
0.07	magn. (W.M.F.)	28	0.67			
0.1	magn. (Arrott)	27	1.08	8.5	8.5	2
0.1	magn. (W.M.F.)	28	1.1			
0.1	Mössb.	31		11.1	3.76	2.95
0.1	$d\Delta\rho/dT$ (max.)	55	0.7			
0.15	magn. (Arrott)	56	4.3			
0.15	$d\Delta\rho/dT$ (max.)	57	2			
0.15	magn. (Arrott)	27	2.12	10	8.5	2
0.15	magn. (W.M.F.)	28	2.2			
0.16	s.h. (model)	51	2.2		1.6	6.3
0.16	res. (knee)	58	2.8			
0.19	s.h. (max.)	59	2			
0.22	Mössb.	40	3.5			
0.22	$d\Delta\rho/dT$ (model)	51	3			
0.23	s.h. (max.)	p.w.	3.7		2	
0.23	res. (knee)	58	5.4			
0.25	$d\Delta\rho/dT$ (max.)	55	4.2			
0.28	magn. (Arrott)	56	9.5			
0.29	$d\Delta\rho/dT$ (max.)	57	7.5			
0.35	s.h. (max.)	p.w.	6.7		2.1	
0.4	Mössb.	40	17			
0.41	res. (knee)	58	13.0			
0.5	F.M.R. (W.F.)	60	29			
0.5	$d\Delta\rho/dT$ (max.)	61	7			
0.53	$d\Delta\rho/dT$ (max.)	57	20			
0.53	magn. (Arrott)	56	23			

conc. (at.%)	exp. method.	ref.	transition temperature (K)	saturation moment (μ_B)	magn. quantum number	eff. g-value
0.54	res. (knee)	58	20.1			
0.78	res. (knee)	58	32.6			
1	$d\Delta\rho/dT$ (max.)	61	28			
1	susc.	32	55	11.3		
1	susc.	52	238	4.1		
1	magn. (Arrott)	32	39	9.7		
1	F.M.R. (W.F.)	60	60			
1.03	$d\Delta\rho/dT$ (max.)	57	40			
1.25	magn. (W.F.)	62	66			
1.26	Mössb.	63	90		1	
1.5	s.c. F.M.R. (W.F.)	60	69			
1.7	s.c. F.M.R. (W.F.)	60	112			
2.8	Mössb.	64	95			
3	$d\Delta\rho/dT$ (max.)	65	97			
3	susc.	52	253	4.4		
3.16	magn. (W.F.)	62	122			
4.0	Mössb.	64	106			
4	F.M.R. (W.F.)	60	140			
4	Mössb.	40	85			
5	susc.	52	273	4.4		
5.11	magn. (W.F.)	62	162			
5.8	Mössb.	64	146			
6	$d\Delta\rho/dT$ (max.)	65	162			
6.4	Mössb.	64	147			
7	susc.	52	288	4.3		
7.2	Mössb.	64	168			
7.5	Mössb.	40	170			
9.78	magn. (W.F.)	62	236			
9	$d\Delta\rho/dT$ (max.)	65	212			
9.5	Mössb.	64	220			
10.3	Mössb.	64	246			
12.3	Mössb.	64	282			
13	Mössb.	40	300			
15.75	magn. (W.F.)	62	377			

Main properties of Pd-Mn alloys.

conc. (at.%)	exp. method.	ref.	transition temperature (K)	saturation moment (μ_B)	magn. quantum number	eff. g-value
0.05	magn. susc.	18	0.18	7.4	1.5	3.15
0.054	magn. susc.	18	0.24	7.3	2.4	3.18
0.08	magn. susc.	18	0.39	7.8	2.4	3.18
0.08	s.h. (W.M.F.)	13			2.2	2.6
0.15	res. (knee)	p.w.	0.22			
0.19	s.h. (W.M.F.)	13			2.9	2.8
0.2	res. (knee)	p.w.	0.39			
0.23	magn. susc.	18	1.33	8.0	2.5	2.97
0.31	res. (knee)	p.w.	0.76			
0.4	res. (knee)	p.w.	1.03			
0.45	magn.	66	1.41			
0.49	magn. susc.	18	2.66	6.6	1.9	2.91
0.49	magn. (Arrott)	18	1.55			
0.5	res. (knee)	41	1.6			
0.5	res. (knee)	p.w.	1.44			
0.54	s.h.	13	1.98		2.31	3.0
0.7	res. (knee)	p.w.	2.48			
0.96	magn. susc.	18	4.56	6.9	2.4	2.84
0.96	magn. (Arrott)	18	3.45			
1	res. (knee)	41	3.6			
1	res. (knee)	67	3.41			
1.05	res. (knee)	42	3.9			
1.2	magn.	66	4.95			
1.33	magn. susc.	18	7.48	6.8	2.1	2.86
1.33	magn. (Arrott)	18	4.54			
1.35	s.h.	13	4.48		2.37	3.2
1.8	magn.	66	7.5			
2.4	res. (knee)	42	7.35			
2.45	s.h.	13	5.78		2.33	
2.45	magn. susc.	18	7.12	5.7	2.2	2.65
2.45	magn. (Arrott)	18	6.14			
2.7	s.h. (max.)	69	4.75			

conc. (at.%)	exp. method.	ref.	transition temperature (K)	saturation moment (μ_B)	magn. quantum number	eff. g-value
2.91	res. (knee)	42	7.71			
3	susc.	52	60	2		
3.0	s.h. (max.)	69	4.5			20.0
3.3	s.h. (max.)	69	4.8			20.0
3.78	magn.	66	6			20.0
4.0	s.h. (max.)	69	7.5			20.0
4.95	magn.	66	3.9			21.0
5	susc.	52	63	2.1		21.0
5.5	s.h. (max.)	69	10.4			21.0
6.75	magn.	66	1.17			25.0
9.5	s.h. (max.)	69	16.2			25.0
10	magn.	66	2			24.0
15	magn.	66	6.5			24.0
25	magn.	66	25			24.0

II.e. Detailed results.

II.e.1. Specific heat of Pd-Co.

The magnetic contribution to the specific heat of dilute Pd-Co alloys has been the subject of investigations of the metals group in Leiden for a number of years. The measurements of the specific heat in zero as well as in finite external magnetic fields by Boerstael and coworkers (9,51) have provided the starting point of our investigation. In fig.II.7 the excess specific heat of four Pd-Co alloys are shown as a function of temperature and external field. From the entropy content Boerstael deduced a magnetic quantum number of 1.4, so that a value 3/2 has to be adopted.

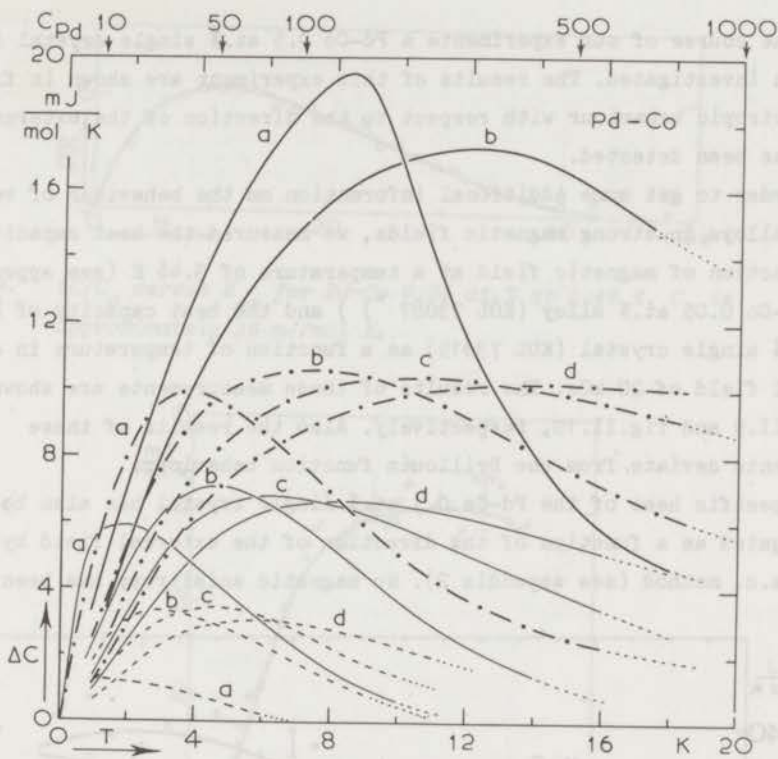


Fig. II.7; ΔC versus T for Pd-Co alloys containing 0.075 at.% Co (---), 0.16 at.% Co (—), 0.24 at.% Co (-·-·-) and 0.35 at.% Co (—). a, b, c and d refer to measurements at $H_{ex} = 0, 9, 18$ and 27 kOe, respectively. Figures at the top of the graph indicate the specific heat of pure Pd in mJ/mol K at the marked temperatures.

As mentioned in section II.d.1 the specific heat of very dilute alloys measured at the largest external field strength available did not show a behaviour according to a Brillouin function with $J=3/2$. The experimentally obtained curves are broader and have a smaller maximum value. Since such a broadened "Schottky" specific heat can possibly be caused by an anisotropic g -value, measurements on single crystals had to be carried out. Also an examination of the specific heat as a function of external field seems worthwhile.

In the course of our experiments a Pd-Co 0.5 at.% single crystal (70) has been investigated. The results of this experiment are shown in fig.II.8. No anisotropic behaviour with respect to the direction of the external field has been detected.

In order to get some additional information on the behaviour of very dilute alloys in strong magnetic fields, we measured the heat capacity as a function of magnetic field at a temperature of 3.46 K (see appendix 2) of a Pd-Co 0.05 at.% alloy (KOL 73087⁺) and the heat capacity of Pd-Co 0.1 at.% single crystal (KOL 73015) as a function of temperature in an external field of 20 kOe. The results of these measurements are shown in fig.II.9 and fig.II.10, respectively. Also the results of these experiments deviate from the Brillouin function behaviour.

The specific heat of the Pd-Co 0.1 at.% single crystal has also been investigated as a function of the direction of the external field by means of the a.c. method (see appendix 2). No magnetic anisotropy has been found.

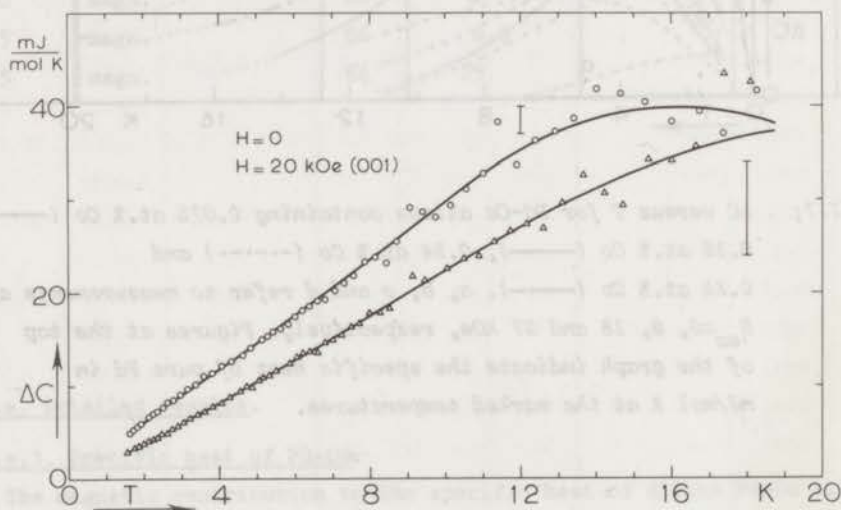


Fig. II.8. ΔC versus T for Pd-Co 0.5 at.% s.c. Data points for the other directions of the magnetic field have been omitted, since they coincide with the data drawn for the (001) direction.

⁺) These numbers refer to numbering of the specimens by the metallurgical department of the Kamerlingh Onnes Laboratory. The same numbers will be used in table A.4.I.

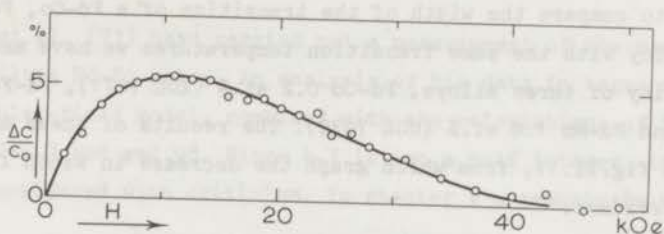


Fig. II.9. $\Delta C/C_0$ versus H_{ex} for Pd-Co 0.05 at.% at 3.46 K. C_0 is approximately 36 mJ/mol K.

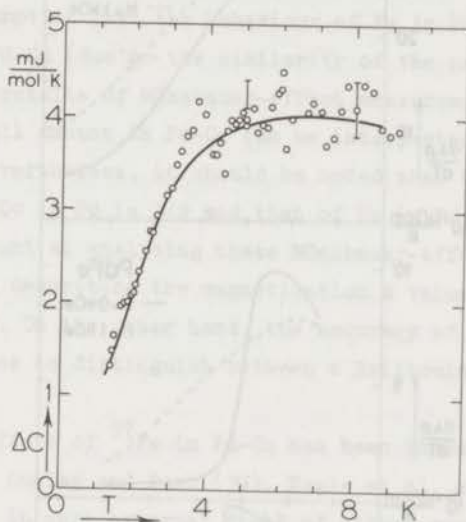


Fig. II.10. ΔC versus T for Pd-Co 0.1 at.% s.e.

II.e.2. Electrical resistivity of Pd-Co.

Measurements of the electrical resistance of Pd-Co alloys have been carried out by Williams (68). He found that the transition to ferromagnetism occurred in a much wider temperature range than in the cases of Pd-Fe and of Pd-Mn. Therefore, he used for T_C that temperature at which the resistivity versus temperature curve starts to deviate from a straight line with increasing temperature. This criterion is similar to that of the maximum of $d\rho/dT$. In view of this difficulty of the determination of T_C the results of Williams are in fair agreement with those of Boerstael (9,51) obtained from the maximum of the excess specific heat.

In order to compare the width of the transition of a Pd-Co, Pd-Fe and Pd-Mn alloy with the same transition temperatures we have measured the resistivity of three alloys, Pd-Co 0.2 at.% (KOL 7071), Pd-Fe 0.22 at.% (KOL 7070) and Pd-Mn 1.0 at.% (KOL 7035). The results of these measurements are shown in fig.II.11, from which graph the decrease in width from Pd-Co to Pd-Mn is evident.

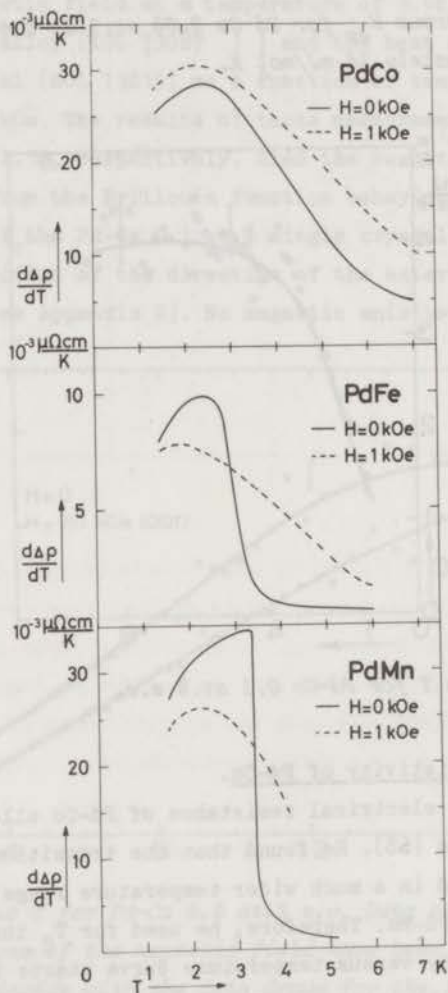


Fig. II.11. $d\rho/dT$ versus T of Pd-Co 0.2 at.% (upper graph), Pd-Fe 0.22 at.% (middle graph) and Pd-Mn 1.0 at.% (Lower graph). Data obtained at zero external field are represented by a solid line, results obtained in a magnetic field of 1 kOe are shown by dashed lines.

Grassie et al. (71) have carried out a measurement of the magnetoresistance of a very dilute Pd-Co alloy. An analysis of his data in terms of the Weiss molecular-field model, combined with the calculations of Yosida (72), results in $J=4.7$ and $g=2.98$. Since 4.7 is not a half integer, this analysis should be considered with criticism. In chapter V a reanalysis will be given.

II.e.3. Measurements of the Mössbauer effect in Pd-Co.

Because the Co-nucleus is not a good Mössbauer probe, measurements as reported on Pd-Fe alloys are impossible in the case of Pd-Co. However, accepting the assumption that the behaviour of Fe in Pd-Co is the same as that of Co in Pd-Co (due to the similarity of the properties of Pd-Co and Pd-Fe), results of Mössbauer-effect measurements on ^{57}Fe contained to a small amount in Pd-Co can be interpreted as measurements on Co in Pd-Co. Nevertheless, it should be noted that the magnetic quantum number of Co in Pd is $3/2$ and that of Fe in Pd is 2. This should be taken into account at analysing these Mössbauer-effect data. In the Brillouin function describing the magnetization a value of 2 for J should be involved. On the other hand, the accuracy of the experiment is probably too poor to distinguish between a Brillouin function with 2 and one with $3/2$.

The Mössbauer effect of ^{57}Fe in Pd-Co has been investigated by Nagle et al. (73) and by Dunlap and Dash (39). Nagle et al. studied the Mössbauer spectrum in zero external field of alloys containing 3 at.% up to almost 100 at.% Co. At temperatures between $0.7 T_C$ and T_C they found an anomalous spectrum, obviously a convolution of resolved and unresolved six-line patterns. At temperatures below $0.5 T_C$ a resolved six-line spectrum was found. These measurements show the existence of long-range magnetic order in Pd-Co alloys and indicate the onset of this ordering at T_C characteristic for random alloys.

In order to investigate the onset of magnetic order more extensively, Dunlap and Dash (39) carried out zero external field experiments on a number of alloys with Co contents ranging from 0.07 at.% to 4.5 at.% by means of a thermal scan technique. They analysed their data in terms of the Weiss molecular-field model incorporating a gaussian distribution of molecular-field coefficients (see also chapter IV). With respect to the experimental accuracy (the authors could not decide between a magnetic quantum number of 1 or 6.5) they obtained a fair agreement.

The values for T_C obtained from these experiments have been quoted in table II.I and are in agreement with the results of BoerstoeI (9,51).

From the interpretation of their data Dunlap and Dash found that the width of the transition to ferromagnetism is proportional to $c^{1/2}$ within the experimental error. From their model they also derived such a concentration dependence, but unfortunately this derivation is based on a simple error in the calculations. Consequently, no attention should be paid to this result.

II.e.4. Magnetization measurements on Pd-Co.

For many years magnetization measurements on Pd-Co alloys have been reported. These measurements were important in establishing the magnitude of the magnetic moment per Co-atom, and gave a fair evidence for the existence of the ferromagnetic ordering down to very low concentrations.

For the interpretation of the present experimental results, for the test of the models used and in view of the specific heat results on very dilute alloys in strong external magnetic fields, some special magnetization measurements seemed expedient. Star [†]) determined the magnetization of a Pd-Co 0.24 at.% alloy, a part of the specimen BoerstoeI (9,51) used, in external fields in which also the specific heat has been investigated. He also measured the magnetization of a Pd-Co 0.1 at.% alloy (the sample was kindly supplied by Narath, Stanford, U.S.A.) in order to investigate the paramagnetic (see also chapter V) behaviour of Co in Pd. The results of these experiments are shown in fig. II.12 and fig. II.13, respectively.

The peculiar behaviour of the weak field magnetization should be noted. These curves as a function of temperature differ much from similar curves for a uniform ferromagnet (e.g. Ni). Obviously, this kind of curve is caused by the width of the transition. During the measurements on this Pd-Co sample a hysteresis of the magnetization was observed, a hysteresis loop with a width of about hundred Oe could be detected. This observation is in agreement with our measurements of the low field susceptibility, see section II.e.13. Remarkably, even at a temperature of 20 K a small hysteresis loop was found.

[†]) Thanks are due to Dr. W.M. Star for carrying out these measurements during his stay at the Francis Bitter Nat. Magnet Laboratory, M.I.T., Cambridge, U.S.A.

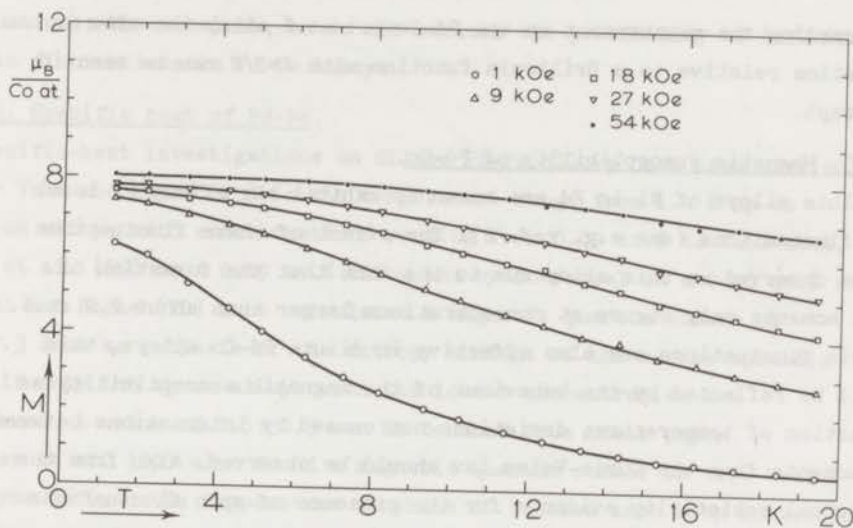


Fig. II.12. Magnetization of Pd-Co 0.24 at.% as a function of temperature.

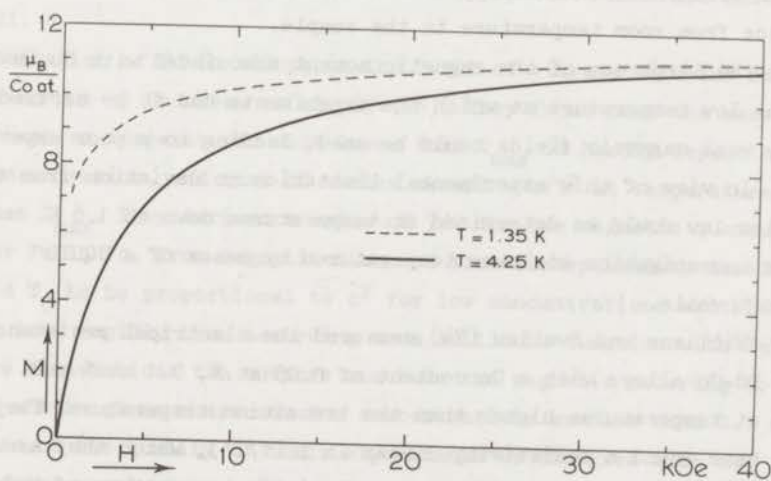


Fig. II.13. Excess magnetization of Pd-Co 0.1 at.% at $T=1.35$ K and $T=4.25$ K as a function of temperature. The susceptibility of Pd has been assumed to be $7.42 \cdot 10^{-4}$ emu/mol. No saturation of M_{imp} has been achieved, since dM_{tot}/dH_{ex} is $8.2 \cdot 10^{-4}$ emu/mol at 50 kOe and 1.35 K.

Regarding the measurement on the Pd-Co 0.1 at.% alloy the slow saturation relative to a Brillouin function with $J=3/2$ can be seen in the graph.

II.e.5. Magnetic susceptibility of Pd-Co.

Dilute alloys of Ni in Pd are known to exhibit the effect of local spin fluctuations (see e.g. ref. 2). The effect of these fluctuations can be observed in this alloy due to the fact that the formation of local moments only occurs at concentrations larger than about 2.2 at.%. If spin fluctuations are also effective in dilute Pd-Co alloys, this should be reflected by the behaviour of the magnetic susceptibility as a function of temperature; deviations not caused by interactions between the moments from the Curie-Weiss law should be observed. Also from the electrical resistivity evidence for the presence of spin fluctuations might be obtained.

In the course of our investigation the magnetic susceptibility of two alloys containing 50 ppm and 250 ppm have been measured using the equipment described by Van Dam et al. (17). However, we used a glass suspension wire instead of a copper one, in order to diminish the thermal conductance from room temperature to the sample.

Due to the largeness of the magnetic moment associated with Co in Pd and to the low temperature at which the experiments had to be carried out, only weak magnetic fields could be used, leading to a poor experimental accuracy. In view of this experimental limitation no deviation from the Curie-Weiss law could be determined at temperatures down to 1.8 K. A further investigation at lower temperatures by means of a SQUID may be worthwhile.

Loram, Williams and Swallow (74) measured the electrical resistance of three Pd-Co alloys with a Co content of 0.05 at.%, 0.1 at.% and 0.2 at.% at temperatures higher than the transition temperature. They claim to have found a resistivity linear in $\ln(T/T')$, which they ascribe to spin fluctuation effects with a characteristic temperature of order of T' . Such a kind of temperature dependence at temperatures higher than T_C has also been found in our experiments. However, in view of the poor quality of the fits of Loram et al. (74) and bearing in mind that a decreasing resistivity with decreasing temperature ($T > T_C$) may also be caused by short range order of the magnetic moments, we consider this resistance measurements as an insufficient evidence for the presence of spin

fluctuations. Nevertheless, we do not exclude the possibility of influences of spin fluctuations in Pd-Co alloys.

II.e.6. Specific heat of Pd-Fe.

Specific-heat investigations on dilute Pd-Fe alloys have been carried out by Veal and Rayne (75) in the temperature range from 1.4 K up to 100 K on alloys with concentrations ranging from 0.09 at.% to 1.52 at.%, by Coles et al. (59) on a 0.19 at.% alloy and by Boerstael on a 0.16 at.% alloy (9).

Veal and Rayne (75) have calculated a magnetic quantum number of 1.1 ± 0.3 from an estimate of the entropy content of the excess specific heat. If only the three alloys with the lowest concentration are considered, a value of 1.5 ± 0.3 can be deduced from their paper.

Coles et al. (59) also found a magnetic quantum number of 1.5. Veal and Rayne defined the temperature at which ΔC becomes zero with increasing temperature as T_C . This definition is not at all accurate. Moreover, it is not sustained by any theory.

Boerstael (9) has investigated Pd-Fe 0.16 at.% in zero external field as well as in external magnetic fields up to 27 kOe. He deduced a value of 1.6 ± 0.2 for J . His results for the excess specific heat are shown in fig. II.14.

An examination of Pd-Fe alloys in the limit of extreme dilution has been carried out by Chouteau et al. (54,76). They found that the excess specific heat at temperatures much lower than T_{max} is hardly depending on the concentration, and that ΔC varies as $a/T - b/T^2$ at temperatures higher than T_{max} . They derived a value of $7/2$ for the magnetic quantum number for Fe in Pd. From magnetization and from susceptibility measurements they found T_C to be proportional to c^2 for low concentrations and also M to vary less rapidly than according to a Brillouin function with $J=5$. From these observations the authors conclude the magnetic ordering to become of a spin glass character for concentrations smaller than 0.1 at.%.

In spite of the quality of their experiments we disagree with the drawing of the conclusions, since :

- A nearly concentration independent specific heat at the lowest temperatures may also be due to an increase of the width of the distribution in the strength of the interaction between the local moments, even when the interaction is ferromagnetic. According to statistical theory this increase in the width can simply be ascribed to the concentration

dependence of the spatial distribution of the impurities and the distance dependence of the interaction strength (see chapter III).

- A deviation of M from a Brillouin function is not unexpected since to our opinion it is not possible to describe the magnetization of Pd-Fe alloys in a consistent way with this function (see chapter V). According to the results for the saturation magnetization and for the Curie constant deduced from the same measurement by Chouteau et al. (54) the magnetic quantum number should be 1.5 instead of 5 (18).
- The c^2 dependence of the transition temperature can also be ascribed to a ferromagnetic interaction with a dependence on the distance as r^{-6} (see chapter V).
- In order to obtain agreement between their specific-heat data and calculations based on the R.K.K.Y. interaction, the authors assumed the magnetic quantum number to be 5 instead of $7/2$ which they obtained from the entropy content or 1.5 which could be deduced from their magnetization measurements.

Nevertheless, we do not exclude the possibility of a different magnetic ordering in the limit of extreme dilution.

In order to obtain more complete zero field results, alloys with a larger concentration than 0.16 at.% have been measured in the course of our investigation. In fig. II.15 the results are shown for Pd-Fe 0.23 at.% (KOL 7273), in fig II.16 those for Pd-Fe 0.35 at.% (KOL 73044). In order to obtain data for ΔC the specific heat of pure Pd as determined by Boerstoeel et al. (9,77) has been subtracted.

As was to be expected, the general behaviour of the excess specific heat as a function of temperature and external field strength is the same as has been found in the case of Pd-Co dilute alloys by Boerstoeel (9). However, a closer analysis shows that in the case of Pd-Fe the excess specific heat as a function of T decreases more rapidly for $T > T_{\max}$ than in the case of Pd-Co (T_{\max} is the temperature at which ΔC attains its maximum value as a function of T). Also the value of ΔC at the maximum is slightly larger than those of Pd-Co alloys with comparable concentration.

Entropy estimates with sufficient accuracy could be made in the cases of Pd-Fe 0.23 at.% for $H_{\text{ex}} = 0$ and $H_{\text{ex}} = 20$ kOe and in the case of Pd-Fe 0.35 at.% for $H_{\text{ex}} = 0$. The values for the magnetic quantum number deduced from the entropy were 1.9 ± 0.2 , 2.1 ± 0.2 and 2.1 ± 0.2 , respectively.

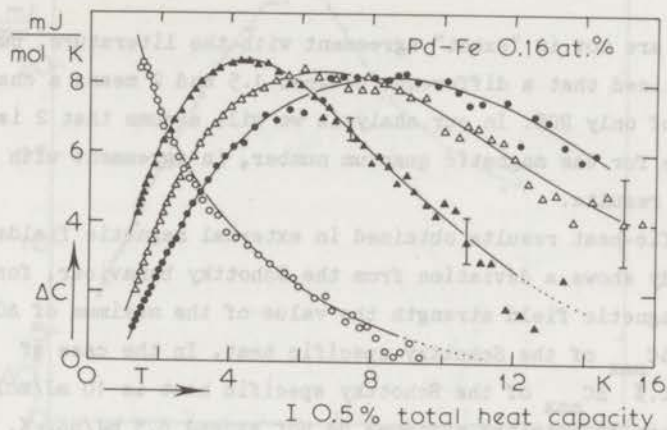


Fig. II.14. ΔC versus T for Pd-Fe 0.16 at.%. $\circ H_{ex}=0$, $\blacktriangle H_{ex}=9$ kOe, $\triangle H_{ex}=18$ kOe and $\bullet H_{ex}=27$ kOe (after Boerstel (9)).

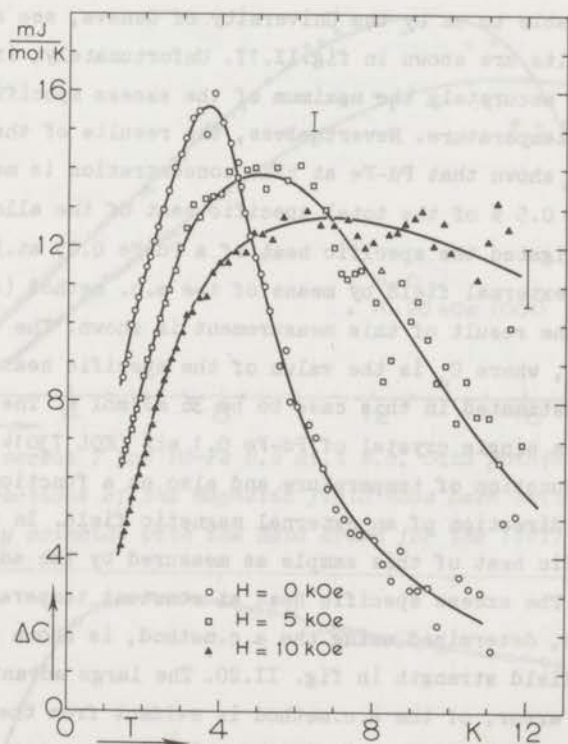


Fig. II.15. ΔC versus T for Pd-Fe 0.23 at.%. (2)

These values are not in "exact" agreement with the literature, but it should be noticed that a difference between 1.5 and 2 means a change in the entropy of only 20%. In our analysis we will assume that 2 is the correct value for the magnetic quantum number, in agreement with our experimental results.

The specific-heat results obtained in external magnetic fields on this alloys already shows a deviation from the Schottky behaviour, for at increasing magnetic field strength the value of the maximum of ΔC should approximate ΔC_{\max} of the Schottky specific heat. In the case of Pd-Fe 0.16 at.% ΔC_{\max} of the Schottky specific heat is 10 mJ/mol K, the experimentally obtained maximums do not exceed 8.5 mJ/mol K. Therefore, an investigation in external magnetic fields of alloys with very small concentration of Fe and an investigation on single crystals of Pd-Fe is expedient.

We have measured the heat capacity of a Pd-Fe 0.5 at.% single crystal (kindly put available to us by the University of Geneva, see also section II.e.1). The results are shown in fig.II.17. Unfortunately, it was not possible to trace accurately the maximum of the excess specific heat as a function of temperature. Nevertheless, the results of these measurements have shown that Pd-Fe at this concentration is magnetically isotropic (within 0.5 % of the total specific heat of the alloy).

We also investigated the specific heat of a Pd-Fe 0.05 at.% alloy as a function of external field by means of the a.c. method (see appendix 2).

In fig II.18 the result of this measurement is shown. The vertical scale gives $\Delta C/C_0$, where C_0 is the value of the specific heat at zero external field, estimated in this case to be 36 mJ/mol K. The excess specific heat of a single crystal of Pd-Fe 0.1 at% (KOL 73014) has been determined as a function of temperature and also as a function of the strength and the direction of an external magnetic field. In fig.II.19 the excess specific heat of this sample as measured by the adiabatic method is shown. The excess specific heat at constant temperature of the same specimen, determined using the a.c.method, is shown as a function of the external field strength in fig. II.20. The large advantage, being the small random error, of the a.c.method is evident from the graphs; the disadvantage cannot be seen, it is the quite large uncertainty in the absolute value (5 %).

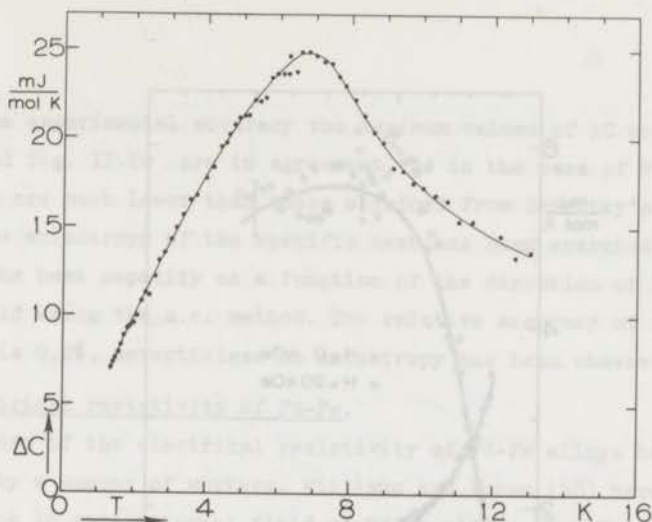


Fig. II.16. ΔC versus T for Pd-Fe 0.35 at.%. ΔC is in mJ/mol K.

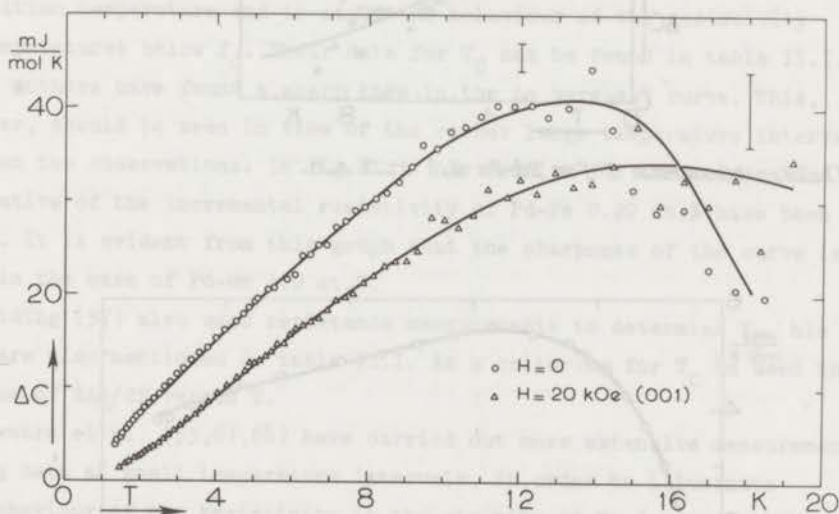


Fig. II.17. ΔC versus T for Pd-Fe 0.5 at.% s.c. Data points for the other directions of the magnetic field have been omitted, since they coincide with the data drawn for the (001) direction.

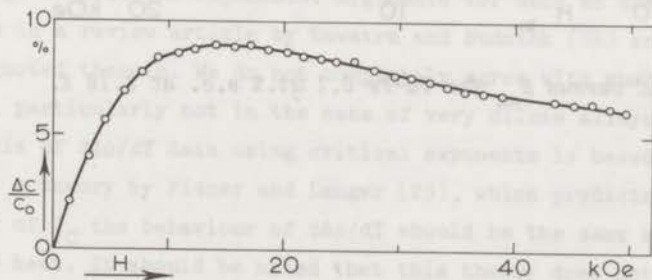


Fig. II.18. $\Delta C/C_0$ versus H_{ex} for Pd-Fe 0.05 at.% at $T=3.46$ K. C_0 is approximately 36 mJ/mol K.

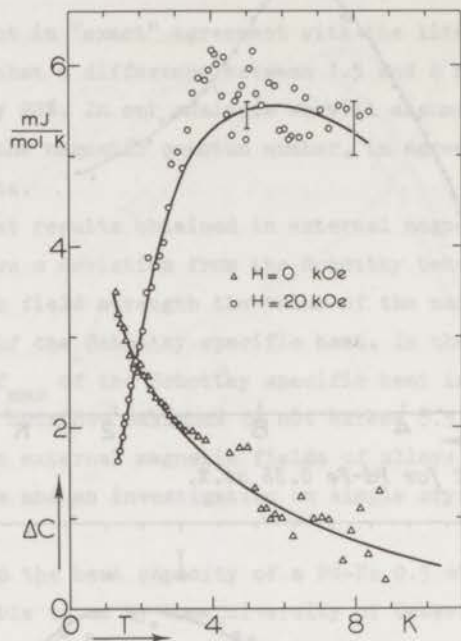


Fig. II.19. ΔC versus T for Pd-Fe 0.1 at.% s.c.

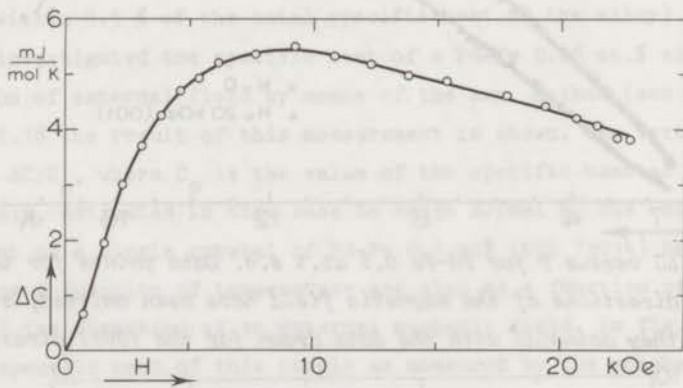


Fig. II.20. ΔC versus H_{ex} for Pd-Fe 0.1 at.% s.c. at 3.16 K.

Within the experimental accuracy the maximum values of ΔC as shown in fig. II.19 and fig. II.20 are in agreement. As in the case of Pd-Co alloys these values are much lower than those obtained from Schottky's calculations.

A possible anisotropy of the specific heat has been searched for by measuring the heat capacity as a function of the direction of the external field using the a.c. method. The relative accuracy of such a measurement is 0.2%, nevertheless no anisotropy has been observed.

II.e.7. Electrical resistivity of Pd-Fe.

Measurements of the electrical resistivity of Pd-Fe alloys have been carried out by a number of workers. Williams and Loram (58) have measured the resistance in zero external field of Pd-Fe alloys with Fe contents ranging from 0.1 at.% to 0.78 at.%. Their aim was to determine the transition temperature and to study the behaviour of the resistivity at temperatures below T_C . Their data for T_C can be found in table II.I. These authors have found a sharp knee in the $\Delta\rho$ versus T curve. This, however, should be seen in view of the rather large temperature intervals between the observations. In fig. II.11 our results for the temperature derivative of the incremental resistivity of Pd-Fe 0.22 at.% have been shown. It is evident from this graph that the sharpness of the curve is less than in the case of Pd-Mn 1.0 at.%.

Wilding (57) also used resistance measurements to determine T_C , his data are also mentioned in table II.I. As a criterium for T_C he used the maximum of $d\Delta\rho/dT$ versus T .

Kawatra et al. (55,61,64) have carried out more extensive measurements, taking data at small temperature intervals, in order to illuminate the behaviour of the resistivity in the vicinity of T_C in a plot of $d\Delta\rho/dT$ versus T . The aim of their research was to examine the critical behaviour of the resistivity in the light of the modern theories (78), expressed e.g. in critical exponents. Arguments for such an analysis can be found in a review article by Kawatra and Budnick (24) and in references quoted therein. We do not completely agree with such a method of analysis, particularly not in the case of very dilute alloys.

An analysis of $d\Delta\rho/dT$ data using critical exponents is based for the main part on a theory by Fisher and Langer (25), which predicts that in the vicinity of T_C the behaviour of $d\Delta\rho/dT$ should be the same as that of the specific heat. It should be noted that this theory does not take

into account the potential scattering of the conduction electrons. Therefore, the application to alloys should be done with care. In order to be able to test the validity of the theory of Fisher and Langer, we measured the electrical resistance of the Pd-Fe 0.23 at.% alloy of which the specific heat has been shown in fig. II.15. The result of this measurement together with the zero-field specific-heat curve is shown in fig. II.21. From this figure it is clear that the behaviour of $d\Delta\rho/dT$ and that of ΔC are different and that the assumption that T_{\max} of the excess specific heat equals the temperature at which $d\Delta\rho/dT$ attains its maximum value is not correct. We also found that at $T < T_{\max}$ (of $d\Delta\rho/dT$) the behaviour of $d\Delta\rho/dT$ depends on the thermal history of the sample.

Nevertheless, the results of the measurements by Kawatra et al. (55,61,64) reflect clearly the width of the transition. Therefore, we summarized their results in fig. II.22, where $d\Delta\rho/dT$ is plotted versus $(T-T_C)/T_C$, wherein T_C has been chosen to be the temperature at which $d\Delta\rho/dT$ attains its maximum value. As is evident from the graph the (relative) width of the transition decreases with increasing concentration.

Magnetoresistance measurements carried out in the ferromagnetic phase of Pd-Fe alloys have already mentioned in section II.d.5. Grassie et al. (71) have carried out measurements of the magnetoresistance of Pd-Fe 0.1 at.% in the paramagnetic phase. Adopting the model of Long and Turner (49) for the resistivity as a function of temperature and external magnetic field, (see also chapter IV), a value for the magnetic quantum number and for g_{eff} can be determined from such an experiment. In the case of Pd-Fe Grassie et al. (71) found $J = 4.5$ and $g_{\text{eff}} = 2.9$.

Koon et al. (79) also performed magnetoresistance measurements on Pd-Fe alloys with 0.15 at.% and 0.23 at.%. They analyzed their experimental data in view of model calculations incorporating a distribution in molecular field coefficients. From this analysis they obtained $J = 5$ and $g_{\text{eff}} = 3.3$ in the case of the 0.15 at.% alloy and $J = 5$ and $g_{\text{eff}} = 3.6$ in that of the 0.23 at.% alloy. Of course this result for J is in disagreement with our results from specific-heat investigations. Moreover, the product J times g_{eff} exceeds the value of the magnetic moment expressed in units of μ_B . Therefore, we consider the result of Koon et al. unreliable.

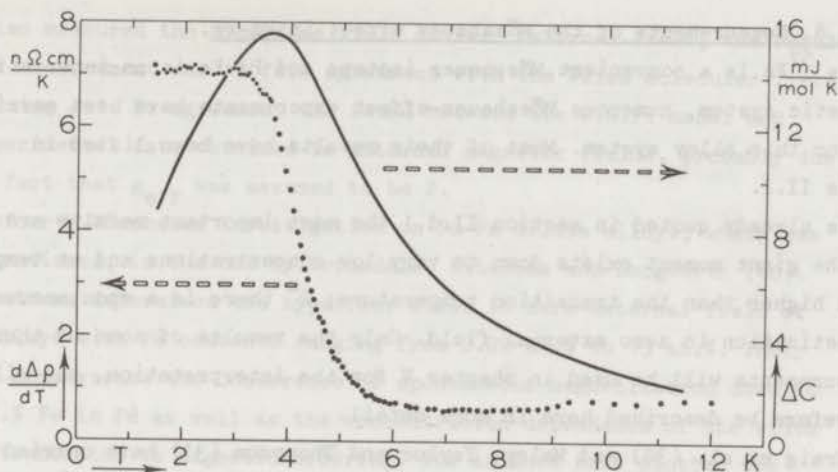


Fig. II.21. $d\Delta\rho/dT$ and ΔC as functions of temperature for Pd-Fe 0.23 at.%.

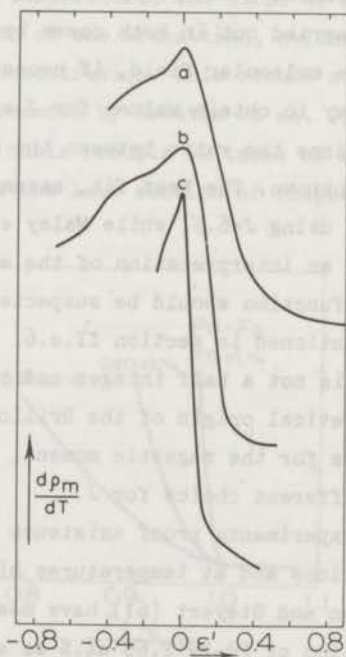


Fig. II.22. $d\Delta\rho/dT$ as a function of $\epsilon=(T - T_C)/T_C$. Curve a refers to Pd-Fe 0.25 at.%, b to Pd-Fe 0.5 at.% and c to Pd-Fe 3 at.%. Data sources: refs 55,61 and 65.

II.e.8. Measurements of the Mössbauer effect in Pd-Fe.

As ^{57}Fe is a convenient Mössbauer isotope and Pd-Fe is an interesting magnetic system, numerous Mössbauer-effect experiments have been carried out on this alloy system. Most of their results have been listed in table II.I.

As already quoted in section II.d.1 the most important results are: 1^o the giant moment exists down to very low concentrations and at temperatures much higher than the transition temperature; 2^o there is a spontaneous magnetization in zero external field. Only the results of some of these measurements will be used in chapter V for the interpretation, and will therefore be described here in more detail.

Craig et al. (30) and Maley, Taylor and Thompson (31) have carried out measurements on very dilute alloys ($c < 0.1$ at.%). From the measurements of Craig et al. the conclusion can be drawn that Fe has a giant moment of about $12.6 \mu_B$ in an alloy containing ± 30 ppm Fe. Maley et al. (31) have extended the measurements to higher external fields using an alloy with 0.1 at.% Fe; they deduced a saturation moment of $11.1 \mu_B$. The analysis of the experiments was carried out in both cases by fitting a Brillouin function (incorporating a molecular field, if necessary) to the experimental data. This is the only way to obtain values for J and μ from the Mössbauer-effect data, since the ratio between the magnetization and the hyperfine field is unknown. The best fit, assuming $g_{\text{eff}}=2$, was obtained by Craig et al. using $J=6.5$, while Maley et al. found $J=3.8$ and $g_{\text{eff}}=2.9$. Of course, an interpretation of the experimental data in terms of a Brillouin function should be suspected in view of the specific-heat results mentioned in section II.e.6. Moreover, the obtained value for J , being 3.8, is not a half integer and therefore not in agreement with the theoretical origin of the Brillouin function. The difference in the results for the magnetic moment, 12.6 and 11.1, can be explained from the different choice for J .

Nevertheless, these experiments proof existence of the giant moment at low concentrations and at temperatures higher than T_C .

Craig, Perisho, Segnan and Steyert (61) have measured the hyperfine field and the magnetization of Pd-Fe 2.65 at.% as a function of temperature and magnetic field strength. They proved that within the experimental error the hyperfine field is proportional to the bulk magnetization.

They also measured the hyperfine field at zero external field; the result of this measurement was in fair agreement with the Weiss molecular-field model using $J=1$. No agreement was found between the W.M.F. model and the experimental data obtained in external magnetic fields, probably due to the fact that g_{eff} was assumed to be 2.

The fourth Mössbauer investigation on Pd-Fe dilute alloys, which has to be mentioned, is the one by Trousdale, Kitchens and Longworth (40). These authors determined the hyperfine field in zero external field of Pd-Fe alloys with Fe contents ranging from 0.22 at.% to 13 at.%. Their results demonstrate the occurrence of spontaneous magnetization down to 0.22 at.% Fe in Pd as well as the concentration dependence of the width of the transition to magnetic ordering. The authors have plotted the relative spectrumwidth at half maximum as a function of T/T_C for three alloys containing 0.22 at.%, 0.4 at.% and 7.5 at.%. This plot is shown in fig.II.23. As can be seen from this graph, the onset of the spontaneous magnetization, exhibited by the broadening of the spectrum, occurs at a relatively well defined temperature. The slope of Δ versus T/T_C curve is indicative for the width of the transition, evidently this width depends strongly on the concentration. This result supports our conclusions from the resistance measurements by Kawatra et al. (55,61,64). Trousdale et al. (40) have analysed their results in terms of a model similar to the one to be presented in the last section of chapter III.

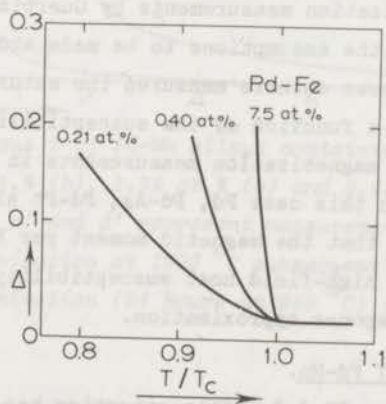


Fig. II.23. The broadening of the Mössbauer absorption spectrum at temperatures near T_C for three Pd-Fe alloys (after Trousdale et al. (40)).

Results of Mössbauer-effect experiments by Woodhams et al. (80) are in fair agreement with those of Trousdale et al. (40). Woodhams et al. carried out measurements on Pd-Fe alloys with 0.5 at.% Fe up to 4.7 at.% Fe. They were able to describe the zero external field data for the hyperfine field with the Weiss molecular-field model, assuming J to be 2 ± 1 . This value is not contradicted by our specific-heat results.

Remarkably, results for the spontaneous magnetization can be described by the W.M.F. model using a low value for J , while a fit to the data obtained as a function of an external field requires a large value for J .

II.e.9. Magnetization of Pd-Fe.

Magnetization measurements have been carried out on Pd-Fe alloys for a long time. As a matter of fact these were the first measurements from which the assumption of the giant moment has been established. The most important results of the magnetization experiments have been tabulated in table II.I.

Special attention should be paid to the measurements by McDougald and Manuel (27,28), because of their extensive research on very dilute alloys. From an analysis of the data in terms of the Weiss molecular-field model these authors have deduced rather large values (between 5 and 10) for the magnetic quantum number. These results disagree with our values for J obtained from the entropy. However, McDougald and Manuel used inconsistent values for g_{eff} , as in a number of other cases the produkt J times g_{eff} exceeds the observed value for the magnetic moment.

Results of the magnetization measurements by Guertin and Foner (81) are important in view of the assumptions to be made about the giant moment in chapter III. These authors measured the saturation moment of alloys with 1 at.% Fe as a function of the susceptibility of the host metal, obtained from the magnetization measurements in strong fields. The host "metals" were in this case Pd, Pd-Ag, Pd-Pt alloys. From the results it can be learnt that the magnetic moment per Fe impurity is not proportional to the bulk high-field host susceptibility as it should be according to a linear response approximation.

II.e.10. Specific heat of Pd-Mn.

As mentioned in section II.d.2 little attention has been paid to the Pd-Mn system until recently. Particularly, specific-heat measurements have been carried out so far only by Boerstael et al. (9,13) on alloys with a Mn content up to 2.45 at.% and by Zweers (69) for alloys with

concentrations ranging from 3 to 9 at.%.

The excess specific heat in zero external field of alloys with less than 3 at.% showed a remarkable sharp cusp when plotted as a function of temperature. Typical examples of these curves as obtained by Boerstael et al. (9,13) are shown in fig. II.24. The temperature at which the cusp occurs agrees with the T_C values as deduced by Sarachik and Shaltiel (41) and by Williams and Loram (42) from resistance measurements. It is generally accepted that this sharp cusp indicates a more uniform (or Ni-like) onset to ferromagnetism than found in Pd-Co and in Pd-Fe alloys. Probably, this effect is due to the larger concentration of Mn impurities involved.

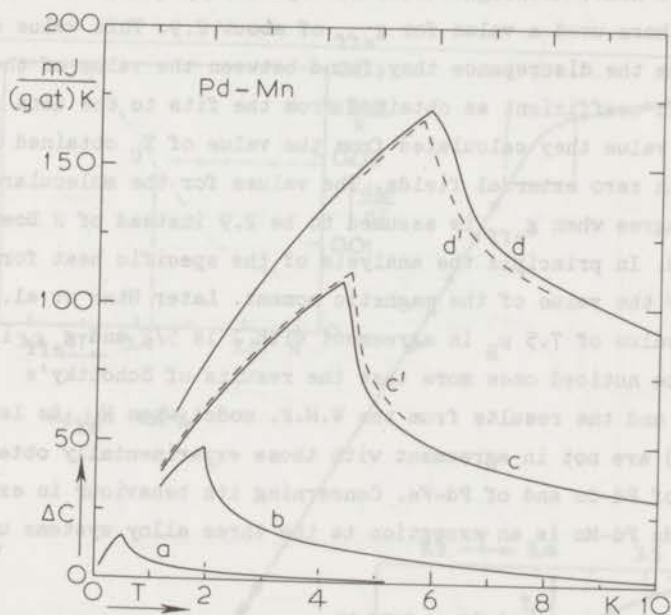


Fig. II.24. ΔC versus T of Pd-Mn alloys containing 0.19 at.% (a), 0.54 at.% (b), 1.35 at.% (c) and 2.45 at.% (d) at $H_{ex} = 0$. Curves c' and d' represent measurements after 220 hours homogenization at 1000°C subsequent to the usual homogenization (24 hours at 950°C) (after Boerstael et al. (13)).

In the case of concentrations ranging from 3 to 9 at.% the sharpness of the curve disappears caused by the presence of the (spin glass like) coexistence of ferromagnetic and antiferromagnetic ordering (82). This assumption is supported by magnetization measurements by Rault and Burger (66)

and by Star et al. (18) and by specific-heat and resistivity investigations by Zweers (69). In the course of our investigation we will restrict ourselves to the dilute Pd-Mn alloys.

Boerstoeel and coworkers (9,13) also measured the heat capacity in external magnetic fields. It was possible to fit the data for the most dilute alloys to a Weiss molecular-field calculation. It is not possible to describe the zero field results by means of this rather simple model. The value for the magnetic quantum number Boerstoeel et al. used was $5/2$, near to the average value of 2.3 they deduced from the entropy content of the specific heat. Although it is not explicitly quoted in their paper, the authors used a value for g_{eff} of about 2.9. This value can be deduced from the discrepancy they found between the value of the molecular-field coefficient as obtained from the fits to the data in external field and the value they calculated from the value of T_C obtained from measurements in zero external fields. The values for the molecular-field coefficients agree when g_{eff} is assumed to be 2.9 instead of 2 Boerstoeel et al. assumed. In principle the analysis of the specific heat forms a prediction for the value of the magnetic moment. Later Star et al. (18) determined a value of $7.5 \mu_B$ in agreement with J is $5/2$ and g_{eff} is 2.9.

It should be noticed once more that the results of Schottky's calculations and the results from the W.M.F. model when H_{ex} is larger than $H_{\text{mol}}(T=0)$ are not in agreement with those experimentally obtained in the cases of Pd-Co and of Pd-Fe. Concerning its behaviour in external magnetic fields Pd-Mn is an exception to the three alloy systems under investigation.

II.e.11. Electrical resistivity of Pd-Mn.

Sarachik and Shaltiel (41) and Williams and Loram (42) have reported results of measurements of the electrical resistance of Pd-Mn alloys. A great similarity, except for the value of the transition temperature, between Pd-Mn and Pd-Fe alloys was established from these measurements. As mentioned above our results on Pd-Fe alloys indicate that the transition in Pd-Mn is much sharper than in Pd-Fe alloys with the same T_C .

In order to investigate the sharpness of the transition in Pd-Mn the resistance of an alloy containing 1.0 at.% Mn (KOL 7035) has been measured, taking data at temperature intervals of 1.2 mK in the vicinity of T_C (67). An analysis of the results was made by comparison of the

experimental data with values calculated assuming an infinitely sharp knee in the resistivity versus temperature at T_C for an ideally homogeneous alloy and incorporating a gaussian of T_C values to account for the inhomogeneity of the real alloy. The relative width of the distribution necessary for the agreement with the experimental results was about 2%, this value is in agreement with the analyses of the specific heat by Boerstoel et al. (13). The result of our analysis is shown in fig. II.25. From this analysis T_C appeared to be 3,414 K and $\Delta\rho(T_C) - \Delta\rho(0)$ to be 0.0919 $\mu\Omega$ cm. in agreement with values quoted in literature.

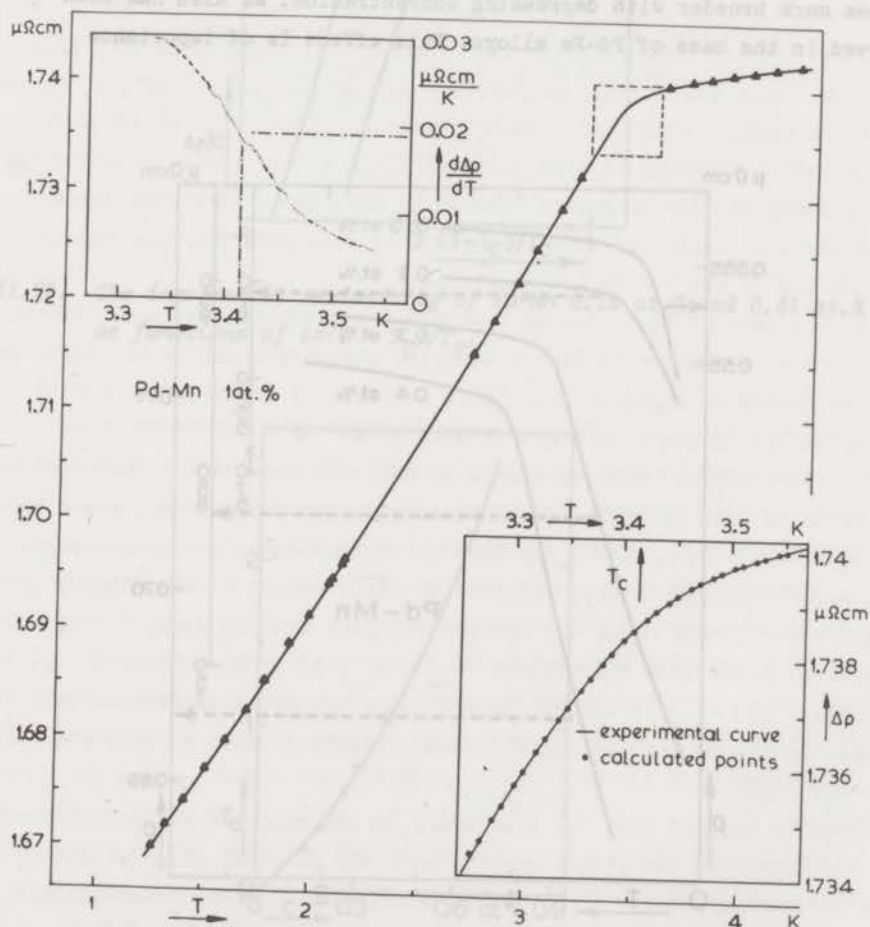


Fig. II.25. The incremental resistivity of Pd-Mn 1.0 at.% versus T .
The meaning of the inserts have been explained in the text.

Previous investigations of the transition to ferromagnetism in Pd-Mn alloys have been carried out mainly on alloys containing more than 0.5 at.% Mn, so that the transition temperature is within the liquid-He range. To extend this investigation, we have carried out resistance measurements on alloys containing 0.15 at.% up to 0.4 at.% Mn (KOL 7182, KOL 7228, KOL 7229 and KOL 7230) down to temperatures of 50 mK, obtained by means of an adiabatic demagnetization equipment (83). Results of these measurements are shown in fig.II.26 and fig.II.27. Values for $\Delta\rho$ were obtained by subtracting the resistivity of pure Pd as determined by Star et al. (84).

As is clear from the graphs, particularly from fig.II.27, the transition becomes much broader with decreasing concentration, as also has been observed in the case of Pd-Fe alloys. This effect is of importance

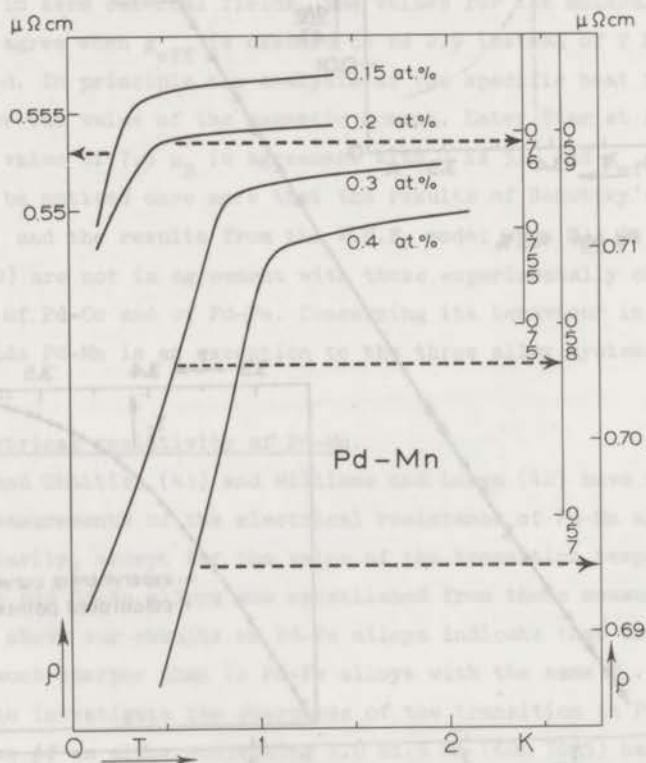


Fig. II.26. The incremental resistivity of Pd-Mn 0.15 at.%, 0.2 at.%, 0.31 at.% and 0.4 at.% as functions of temperature.

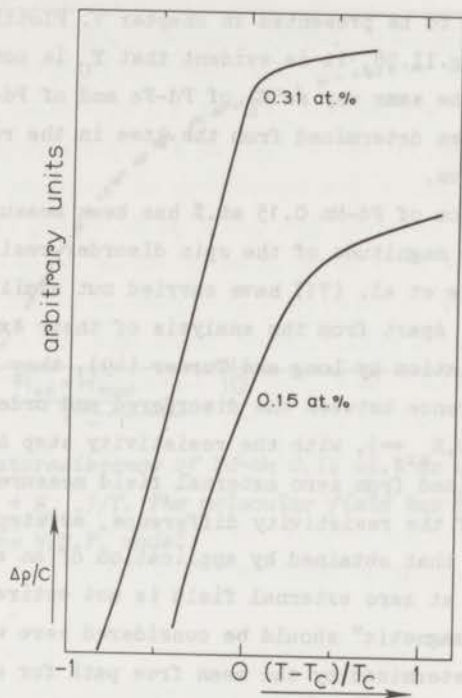


Fig. II.27. The incremental resistivity of Pd-Mn 0.15 at.% and 0.31 at.% as functions of $\epsilon = (T - T_C)/T_C$.

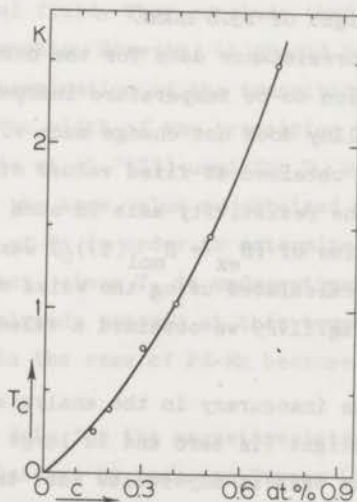


Fig. II.28. The transition temperature of Pd-Mn as a function of the Mn concentration.

for the interpretation to be presented in chapter V. Plotting T_C versus c as has been done in fig.II.28, it is evident that T_C is not proportional to c , but behaves in the same way as T_C of Pd-Fe and of Pd-Co alloys. The value of T_C has been determined from the knee in the resistivity versus temperature curve.

The magnetoresistance of Pd-Mn 0.15 at.% has been measured too in order to determine the magnitude of the spin disorder resistivity. As mentioned above Grassie et al. (71) have carried out similar experiments on Pd-Fe and on Pd-Co. Apart from the analysis of their experimental data in terms of the calculation by Long and Turner (49), they have compared the resistivity difference between the disordered and ordered state, $\Delta\rho(T \rightarrow \infty, H_{ex} = 0) - \Delta\rho(T \rightarrow 0, H_{ex} \rightarrow \infty)$, with the resistivity step $\Delta\rho(T = T_C, H_{ex} = 0) - \Delta\rho(T \rightarrow 0, H_{ex} = 0)$ as obtained from zero external field measurements. These authors assume that if the resistivity difference, or stepheight, in zero field is smaller than that obtained by application of an external field, the magnetic ordering at zero external field is not entirely ferromagnetic. The expression "ferromagnetic" should be considered here with respect to a distance scale determined by the mean free path for spin dependent scattering of the conduction electrons.

In the case of Pd-Mn 1.0 at.% we found a stepheight in zero external field of 91.9 n Ω cm which means, assuming the stepheight to be proportional to the number of magnetic impurities per unit of volume, that a 0.15 at.% alloy should have a stepheight of 13.8 n Ω cm.

We corrected our magnetoresistance data for the normal magnetoresistance by assuming this contribution to be temperature independent, since the total resistivity of the alloy does not change much with temperature. The magnetoresistance data obtained at fixed values of the external field were shifted along the resistivity axis in such a way that a universal curve as a function of $\{H_{ex} + H_{mol}(T)\}/T$ was obtained. The value for $H_{mol}(T)$ was calculated using the Weiss molecular-field model. As can be seen in fig.II.29 we obtained a value for the stepheight of 12.8 n Ω cm.

Bearing in mind that the inaccuracy in the analysis of the concentration is involved, the two stepheight (in zero and in large external fields) are in fair agreement. From this it may follow that the ordering in Pd-Mn dilute alloys is of a long-range ferromagnetic character.

In the cases of Pd-Fe and of Pd-Co Grassie et al. (71) found that the zero field stepheights were much smaller (30 - 50 %) than those

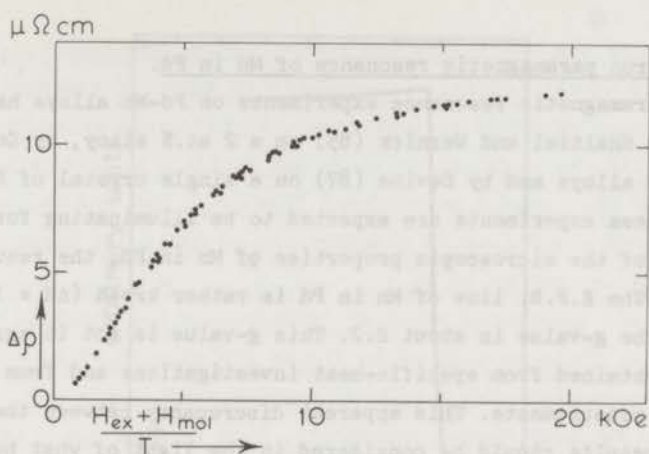


Fig. II. 29. Magnetoconductance of Pd-Mn 0.15 at.% as a function of $(H_{ex} + H_{mol})/T$. The molecular field has been determined by means of the W.M.F. model.

obtained in an external field. They conclude that the ordering in these alloys is not ferromagnetic. However, it should be noticed that, as mentioned above, a determination of the transition temperature is rather difficult because of the width of the transition present in these alloys. The temperature Grassie et al. (71) used for T_C was that of the point of inflection (almost the same value as obtained from the maximum of $d\Delta\rho/dT$). Probably, this choice of T_C in order to determine spin disorder resistivity is incorrect, since T_C is underestimated and part of the magnetic ordering is already present at this temperature. This difficulty does not play a role in the case of Pd-Mn because of the sharpness of the transition.

An analysis of the data for the magnetoconductance of Pd-Mn 0.15 at.% in terms of the calculations by Long and Turner (49, and also chapter IV) using the W.M.F. model shows a fair agreement between the experimental and calculated results when $J=5/2$ and $g_{eff}=3$ are chosen as parameters.

II.e.12. Electron paramagnetic resonance of Mn in Pd.

Electron paramagnetic resonance experiments on Pd-Mn alloys have been carried out by Shaltiel and Wernick (85) on a 2 at.% alloy, by Cottet (86) on more dilute alloys and by Devine (87) on a single crystal of Pd-Mn.

Although these experiments are expected to be illuminating for the understanding of the microscopic properties of Mn in Pd, the results are not striking. The E.P.R. line of Mn in Pd is rather broad ($\Delta H \approx 1500$ Gauss at 20 K) and the g-value is about 2.2. This g-value is not in agreement with g_{eff} as obtained from specific-heat investigations and from magnetization measurements. This apparent discrepancy between the two experimental results should be considered in the light of what has been written in section II.c.4 about the interpretation of E.P.R. experiments on dilute alloys. Probably dynamic effects play a role in Pd-Mn.

The experiments by Devine (87) on the Pd-Mn single crystal did not show anisotropy in the g-value or in the linewidth within experimental error.

II.e.13. Low-field susceptibility of Pd-Mn.

We have measured the susceptibility χ at temperatures in the vicinity of T_C of an alloy with 1.0 at.% Mn (KOL 7035) applying weak magnetic fields by means of the a.c. method (described in appendix 1). Magnetic fields down to 0.04 Oe have been used. The result of this measurement is shown in fig. II.30. At temperatures very near to T_C it was necessary to extrapolate χ obtained at various values of the magnetic field to a zero field value, because even below 0.25 Oe a considerable field dependence was observed.

We note that the values presented in fig. II.30 have not been corrected for the demagnetization factor. The measured value of χ is related to what may be called the internal one as

$$\chi_{\text{int}} = \frac{\chi_{\text{meas}}}{1 - D' \chi_{\text{meas}}}, \quad (\text{II.15})$$

where D' is the demagnetization factor of the specimen. In our experiment the samples were thin slabs with the surface parallel to the magnetic field, so D' will be small. Therefore, we did not take into account this correction.

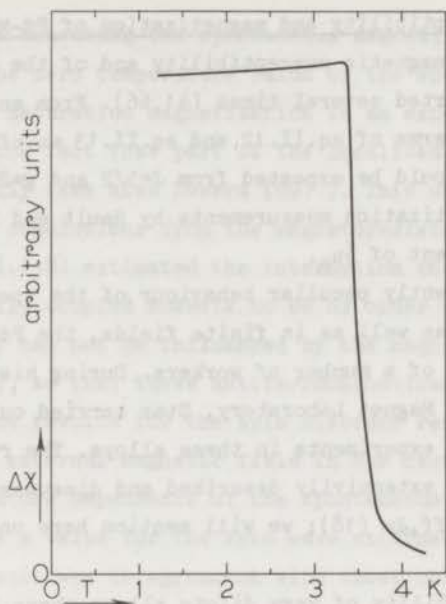


Fig.II.30. The low-field magnetic susceptibility of Pd-Mn 1.0 at.% as a function of temperature.

Another difficulty in this kind of measurements is the possible occurrence of magnetic hysteresis. If that is the case the a.c. method does not probe the initial susceptibility (dM/dH_{ex} at $H_{ex}=0$) but a mean value of dM/dH_{ex} over small hysteresis loops (88). (The latter quantity is of technical importance in the case of transformer-core material.) By application of a weak d.c. magnetic field we could detect whether hysteresis was present or not. If hysteresis is present the maximum of the measured value of dM/dH_{ex} is not obtained at zero external field but at a finite value for a field (a positive as well as a negative one). No hysteresis has been detected in the case of Pd-Mn. However, a sample of Pd-Co 0.2 at.% showed a hysteresis loop with a width of about 150 Oe. Therefore, we have not reported on low field susceptibility measurements of these alloys.

The result shown in fig. II.30 for Pd-Mn 1.0 at.% is characteristic for a uniform ferromagnet (89).

II.e.14. Magnetic susceptibility and magnetization of Pd-Mn.

Measurements of the magnetic susceptibility and of the magnetization of Pd-Mn have been reported several times (41,66). From an analysis of the susceptibility in terms of eq.II.12 and eq.II.13 an effective moment slightly larger than should be expected from $J=5/2$ and $g=2$ has been found. On the other hand magnetization measurements by Rault and Burger (66) reveal a saturation moment of $5\mu_B$.

Because of the apparently peculiar behaviour of the specific heat in zero external field as well as in finite fields, the Pd-Mn system attracted the attention of a number of workers. During his stay at the Francis Bitter National Magnet Laboratory, Star carried out a large number of magnetization experiments in these alloys. The results of this investigation have been extensively described and discussed in a paper by Star, Foner and McNiff, Jr (18); we will mention here only the most important facts.

- The magnetic susceptibility of very dilute alloys obeys the Curie-Weiss law in the temperature range where the susceptibility of pure Pd may be assumed to be temperature independent within the experimental error.

The values for the Curie temperature Θ are positive and in fair agreement with the T_C values obtained from our resistance measurements.

- The saturation moment is about $7.5 \mu_B$ per Mn impurity, thus larger than the free atom value and in agreement with the analysis of the specific-heat results.

- When the value of the Curie constant C_c and the value for the bulk saturation magnetization M_{sat} , given by

$$C_c = cN g_{eff}^2 \mu_B^2 J(J+1) \quad \text{and} \quad (II.16)$$

$$M_{sat} = cN g_{eff} J \mu_B, \quad \text{respectively,} \quad (II.17)$$

are combined it appears that $J=2.5$ and $g_{eff}=3.2$.

- The dependence of the magnetization of very dilute alloys on temperature and external magnetic field is in agreement with the calculations based on the Weiss molecular-field model. Parameters used for this comparison were $J=5/2$ and $g_{eff}=3.2$ obtained from eq.II.16 and eq.II.17 and $H_{mol}(T=0) = 3k_B\Theta / (J+1)g_{eff}\mu_B$, where Θ was obtained from the Curie-Weiss fit to the susceptibility.

- Star succeeded in measuring the spontaneous magnetization of a number of Pd-Mn alloys. The zero temperature value of the spontaneous magnetization was lower than the saturation magnetization in an external field, presumably due to the fact that part of the localized moments are coupled antiferromagnetically (see also Zweers (69)). This observation is not in agreement with our conclusions from the magnetoresistance measurements. However, Star et al. (18) estimated the interaction energy between these antiferromagnetically coupled moments to be of order of 50 K in units of k_B . Such a large energy can not be influenced by the magnetic fields we used (27 kOe at maximum), so that these antiferromagnetically coupled moments do not influence the results for the spin disorder resistivity obtained without or with an external magnetic field in our case.

From the temperature dependence of the spontaneous magnetization at the lowest temperatures a value for the spin wave stiffness constant could be deduced. The result was in agreement with those obtained from resistivity measurements.

A review of the literature on experiments and a presentation of our experimental investigation has been given in this chapter. However, it should be emphasized that the reviewing part should not be considered to be complete. Only the results important for a consistent interpretation of the behaviour of Co, Fe and Mn in Pd (to be presented in chapter V) have been mentioned in detail.

CHAPTER III

THEORIES

III.a. Introduction.

A theoretical treatment of the properties of a dilute alloy requires essentially doing atomic physics in a metallic environment (90). The virtual bound state put forth by Friedel (91) has provided a sound basis for understanding the various properties of dilute alloys. Anderson (92), Wolff (93) and Clogston et al. (32) have embodied this picture into simple tractable mathematical models.

A consistent review of the theory of dilute alloys should start with a treatment of these models. However, since the fifth volume of Magnetism (94,95) contains such excellent reviews, we feel exempted from the duty to describe the models here again. Nevertheless, a few words should be devoted to the Hirst model (26,96). The calculations of Anderson, Wolff and Clogston tend to overemphasize the itinerant character of the localized moments. As a matter of fact, they do not give the correct limit (the ionic picture) when the hybridization of the localized levels with the band state is neglected (26). In the Hirst model the ionic many-electron states are zero order ingredients. These states are thought to be perturbed but not wiped out by the hybridization with the conduction-electron states. Therefore, the central feature of the model is the integral occupation of the magnetic shell as a consequence of intraatomic correlations.

Since, following Hirst, Co, Fe and Mn are known to be magnetic when dissolved in Pd, the spin quantum number should be $3/2$, 2 and $5/2$, respectively. Whether the orbital angular momentum contributes to the total angular momentum of the localized moment depends on the symmetry of the crystalline electric field in the host metal. Unfortunately, calculations of the crystalline electric field in metallic hosts are almost prohibitively complicated.

III.b. Application to dilute Pd-based alloys with Co, Fe or Mn impurities.

The giant magnetic moments of Co, Fe and Mn in Pd are certainly related to the large susceptibility of the host metal. This large susceptibility in turn is caused by the intraatomic exchange interaction in Pd. Therefore, in order to get an appropriate description of these dilute alloys, this interaction should be incorporated in the Anderson model, the Wolff-Clogston model or in the Hirst model. The first two

models have been treated by Moriya (97), the Hirst model unfortunately has not been extended to exchange-enhanced hosts.

As a result of his calculations, Moriya found that the sign and the magnitude of the extra magnetic moment induced on the Pd matrix is determined by the competition between two large contributions. The first one, due to the shift of the energy of the ionic levels, gives an antiparallel polarization; the second one, caused by the admixture between the ionic levels and the band states, gives a positive polarization. The result does not depend on the choice of the model.

From his calculations Moriya was able to account for the giant moments associated with Co and Fe in Pd, observed at that time. Concerning the moment associated with Mn in Pd he could predict a small but positive polarization of the band, which turned out to be in agreement with the experimental results described in the preceding chapter. Similar calculations have been performed by Campbell (98).

The results of the calculation by Moriya are rather complicated; when interpreting experimental results in chapter V a rather more phenomenological expression (based on the linear response approximation) will be used.

III.c. Spatial extension of the induced moment.

It has been shown by Moriya (97) that when the exchange enhancement of the susceptibility of the band is large (as it is in Pd) the spatial extension of the induced polarization hardly depends on the original one (without exchange interactions between the bare moment and the band), but is determined for the main part by the spatial dependence of the zero frequency generalized susceptibility of the host metal.

Following Schrieffer (99) the susceptibility of exchange enhanced metal can be written within the random-phase approximation as

$$\chi(q, \omega) = \frac{\chi^{(0)}(q, \omega)}{1 - \gamma \chi^{(0)}(q, \omega)} \quad (\text{III.1})$$

where $\chi^{(0)}(q, \omega)$ is the magnetic susceptibility without exchange enhancement and γ is a measure for the intraatomic interactions, the quantity $S = \{1 - \gamma \chi^{(0)}(0, 0)\}^{-1}$ is the Stoner enhancement factor. For a parabolic band the generalized susceptibility $\chi^{(0)}(q, \omega)$ is given

by $\chi_P u(q, \omega)$ wherein $u(q, \omega)$ is the Lindhard function (100) with $u(0, 0) = 1$, so that $\chi^{(0)}(0, 0) = \chi_P$.

For values of q smaller than $2k_F$ (k_F is the Fermi wave vector) $u(q, 0)$ can be approximated by

$$u(q, 0) = \frac{1}{1 + \frac{1}{3} \left(\frac{q}{2k_F}\right)^2}, \quad (\text{III.2})$$

so that for these values of q , which are important in our case since we are interested in the long range nature of the susceptibility, $\chi(q, 0)$ can be written as

$$\chi(q, 0) = \frac{\chi_P}{1 - \gamma\chi_P + \frac{1}{3} \left(\frac{q}{2k_F}\right)^2} \quad (\text{III.3})$$

Taking the Fourier transform of eq. III.3, $\chi(r, 0)$ becomes

$$\chi(r, 0) = \chi_P \frac{3 k_F^2}{\pi r} e^{-\frac{r}{\sigma}} \quad (\text{III.4})$$

where σ equals $(S/3)^{1/2}/2k_F$.

If a spherical band model for Pd is accepted and S is assumed to be 10, the value of σ becomes 1 \AA ; in the tight binding model σ becomes 3 \AA (101). From diffuse neutron scattering experiments (35-37) σ was found to be 5 \AA in the case of Pd-Fe and of Pd-Co, thus the theoretical result is in fair agreement with those of experiments.

III.d. Interaction between the moments (origin of ferromagnetism).

In the preceding sections of this chapter the properties of a single impurity like Fe in an unchanged enhanced band has been described. The problem left now is to treat the case of many impurities in an exchanged enhanced band, a problem where one has to deal with the interaction between the moments of the impurities and with the possible extra enhancement of the band due to the presence of these moments. Obviously, since ferromagnetism has been observed down to fairly small concentrations the band plays an important role in the interaction.

In the theoretical treatment of ferromagnetic alloys, which has some specific difficulties, the same itinerant-localized duality (78) seems to pertain as in the theory of magnetism in pure transition metals.

III.d.1. The itinerant picture.

One approach has been made by Kim (102). He proposes that ferromagnetism in dilute Pd-based alloys is for the main part due to the ferromagnetism of the itinerant electrons of the host metal. The argument is that the Stoner enhancement factor for pure Pd is 10, so that Pd is a nearly ferromagnetic metal. Due to the presence of the magnetic moments there is an indirect interaction between the d-electrons of Pd via the magnetic moment. This additional interaction drives the alloy to ferromagnetism at non-zero temperatures, i.e. the additional interaction increases the factor γ . This argument implies that in principle the alloy may be ferromagnetic even when the localized moments are in the paramagnetic state. Of course the localized moments will also align due to their interaction with the band, which is now ferromagnetic.

III.d.2. The localized picture.

A different approach to the problem is to assume the bare magnetic moments to be localized within the impurity cell. Because of the polarization of the band there exists an indirect interaction between the magnetic moments. As far as the mechanism of the indirect interaction is concerned this is the same problem as found in alloys like Cu-Mn. In these alloys the interaction is of the R.K.K.Y. type (103-105).

Applying the same reasoning to Pd-based alloys the interaction strength between two bare magnetic moments will be determined by the magnitude of the moment density in the band caused by one impurity moment at the place of the other. The dependence of the interaction strength on the distance r' between the impurities is then simply given by $\chi(r',0)$ (see eq. III.4).

III.d.3. Choice between the two pictures.

The localized picture and the itinerant one give both an important aspect of the interesting problem of magnetic ordering in dilute Pd-based alloys. A problem where on the one hand the interaction between the impurities via the band and on the other hand the additional exchange enhancement of the susceptibility of the band due to the presence of the

magnetic moments plays an important role. A choice, rigidly based on theoretical arguments or on experimental results, between the two pictures is rather difficult to make. Nevertheless, we prefer the localized picture in the case of small amounts of Co, Fe or Mn in Pd since:

- No lowest value of the concentration for the occurrence of ferromagnetism has been found up to now in alloys with Co, Fe and Mn. Since $\gamma\chi_P$ is 0.9 for pure Pd, one should expect to find such a lowest value of the concentration for which $\gamma\chi_P$ becomes 1 at $T=0$ (in the case of Ni impurities such a critical concentration has been found).
- The entropy content of the specific heat is in agreement with the multiplicity of the bare magnetic moments according to Hirst (26).
- The magnetic field dependence of the specific heat indicates that large magnetic moments, not a large number of small moments, are involved.
- The high-field magnetic susceptibility of dilute alloys is the same as that of pure Pd within the experimental error.

However, we should be careful with the application of the localized model, since it is generally assumed in this case that only interaction between nearest neighbours has to be taken into account. Brout (105) has shown that such an assumption leads to some minimum concentration of magnetic moments for the occurrence of ferromagnetism in an alloy system. Only when long-range interactions are involved, is ferromagnetism down to the lowest concentrations possible. We have seen that, on theoretical grounds, one can expect the interactions in Pd-based alloys to have a very long range.

According to the localized picture the strength $J_{int}(r')$ of the interaction as a function of the distance r' between the magnetic moments is determined by

$$J_{int}(r') \propto \chi(r',0) \quad (III.5)$$

However, it may also be assumed (39,40,107) that not the moment density of the band at the impurity site is important, but the overlap between the moment densities caused by the two magnetic moments determines the interaction. Then $J_{int}(r')$ should be proportional to

$$\int_0^{\infty} \chi(\vec{r},0) \chi(\vec{r} - \vec{r}',0) d^3r \quad (III.6)$$

Unfortunately, no arguments in the case of Pd-based alloys for the application of either eq. III.5 or eq. III.6 have been given in the literature. Although we are not able to make a decisive choice, the following arguments should be considered:

- Using eq. III.5 for $J_{\text{int}}(r')$ implies that the magnitude of the interaction is determined by the moment density at the place of the second impurity times the volume of the impurity cell. This may lead to a rather small value.
- On the other hand we may urge against eq. III.6 that it implies that in the space between the magnetic moments the two polarization clouds tend to a parallel alignment. If we then figuratively take away the two bare magnetic moments, it should follow from the fact that the overlap integral (eq. III.6) gives an energy lowering for ferromagnetic alignment that Pd-metal itself is ferromagnetic, which is not the case. The application of eq. III.6 is therefore only correct if, following Kim (102), one can show that the exchange enhancement of the band is increased due to the presence of the magnetic moments.
- However, if because of the argument given above, eq. III.5 is preferred, it should be noted that then the effect of the interaction represented by eq. III.6 will counteract the one represented by eq. III.5.

A calculation of the energies involved, probably beyond the linear response approximation, might solve the problem.

Numerical calculations of eq. III.5 and of eq. III.6 have shown us, that the dependence of $J_{\text{int}}(r')$ on r' is nearly independent of the choice between the equations. Thus in order to carry out further calculations we are not obliged to make a choice, on the other hand we cannot expect to be able to distinguish between these equations on the bases of experimental results.

From now on we will assume that, without giving preference to one of the two equations, $J_{\text{int}}(r')$ is proportional to the result of eq. III.6. Knowing the distance dependence of the interaction, it should be possible to calculate "exactly" the ferromagnetic properties of the alloys. Nevertheless, in spite of several recent efforts utilizing sophisticated theoretical methods (108,109), one has to realize that the Weiss molecular-field model is the most workable model at the moment, mainly because it incorporates the assumption of infinitely long range interactions in a very simple way.

On the basis of this model we shall make an attempt at treating the magnetic properties and at incorporating the spatial randomness of the magnetic moments.

III.d.4. The model of Takahashi and Shimizu.

Takahashi and Shimizu (110) worked out a model for dilute Pd-based alloys on the basis of molecular-field theory. They made the following assumptions in order to simplify the calculations: 1° the rigid band model is a good approximation for the 4d-band; 2° the direct interaction between the dissolved magnetic atoms can be neglected; 3° the strength of the interaction among the 4d-electrons and the dissolved magnetic moments is independent of the concentration of the dissolved atoms and of the composition of the host metal; 4° the bare magnetic moments of the dissolved atoms are localized within their cells; 5° the polarization of the 4d-band is spatially uniform.

If the magnetic moment due to the polarization of the 4d-band is denoted by M_d , the total magnetic moment of the dissolved atoms by M_i , the molecular-field coefficient characterizing the interaction between the localized moments and the 4d-electrons by α and that of the 4d-4d interaction by γ , then the magnetic energy of the 4d-electron is given by

$$-\mu_B(\alpha M_i + \gamma M_d + H_{ex}) \quad (III.7)$$

The magnetic moments M_d and M_i are given by

$$N_d = \int_0^{\infty} \frac{\eta(\epsilon) d\epsilon}{\exp\{(\epsilon - E - \epsilon_F)/k_B T\} + 1} + \int_0^{\infty} \frac{\eta(\epsilon) d\epsilon}{\exp\{(\epsilon + E - \epsilon_F)/k_B T\} + 1}, \quad (III.8)$$

$$M_d = \mu_B \int_0^{\infty} \frac{\eta(\epsilon) d\epsilon}{\exp\{(\epsilon - E - \epsilon_F)/k_B T\} + 1} - \mu_B \int_0^{\infty} \frac{\eta(\epsilon) d\epsilon}{\exp\{(\epsilon + E - \epsilon_F)/k_B T\} + 1} \quad (III.9)$$

and

$$M_i = N_i g \mu_B J_B J \{g \mu_B J (\alpha M_d + H_{ex}) / k_B T\}, \quad (III.10)$$

wherein $E = \mu_B(\alpha M_i + \gamma M_d + H_{ex})$ and $\eta(\epsilon)$ is the density of states per spin direction of the 4d-electrons, N_d the number of 4d-electrons,

N_i the number of dissolved atoms, J the magnetic quantum number of the dissolved atoms and B_J the appropriate Brillouin function.

It is convenient to introduce the function $f(\epsilon_F)$ defined as

$$f(\epsilon_F) = \int_0^{\infty} \frac{\eta(\epsilon) d\epsilon}{\exp\{(\epsilon - \epsilon_F)/k_B T\} + 1} \quad \text{and} \quad f'(\epsilon_F) = \frac{df(\epsilon_F)}{d\epsilon_F} \quad (\text{III.11})$$

If no magnetic atoms are present and γ is zero, the susceptibility for $E < \epsilon_F$ is given by (for simplicity we will from now on replace H_{ex} by H in this section)

$$\chi = \lim_{H \rightarrow 0} \frac{M_d}{H} = \mu_B \{f'(\epsilon_F) E + f'(\epsilon_F) E\} = 2\mu_B f'(\epsilon_F) E \quad (\text{III.12})$$

and

$$N_d = 2f(\epsilon_F) .$$

If the temperature is much smaller than ϵ_F/k_B the function $f(\epsilon_F)$ becomes

$$f(\epsilon_F) = \int_0^{\epsilon_F} \eta(\epsilon) d\epsilon \quad \text{and} \quad f'(\epsilon_F) = \eta(\epsilon_F), \quad (\text{III.13})$$

leading to

$$\chi = \lim_{H \rightarrow 0} 2\mu_B f'(\epsilon_F) \frac{E}{H} = 2\mu_B^2 \eta(\epsilon_F) = \chi_P. \quad (\text{III.14})$$

If no magnetic atoms are present, but $\gamma \neq 0$ the susceptibility is given in the molecular-field approximation by

$$\chi = \lim_{H \rightarrow 0} \frac{M_d}{H} = \lim_{H \rightarrow 0} 2\mu_B^2 \eta(\epsilon_F) \left(\frac{H + \gamma M_d}{H} \right) \quad \text{or}$$

$$\chi = \frac{\chi_P}{1 - \gamma \chi_P} \quad (\text{III.15})$$

This enhanced susceptibility will be denoted by χ_0 . Note that χ_0 equals the $\chi^{(0)}(0,0)$ of section III.c. If $\gamma \neq 0$ and the magnetic atoms are

present in the Pd host the equation for the susceptibility reads

$$\begin{aligned} \chi &= \lim_{H \rightarrow 0} \frac{M_i + M_d}{H} = \lim_{H \rightarrow 0} \frac{C'}{TH} (\alpha M_d + H) + \frac{\chi_0}{H} (\alpha M_i + H) = \\ &= \lim_{H \rightarrow 0} \frac{C'}{T} + \frac{C' \alpha \chi_0}{T} + \frac{\chi_0 C' \alpha^2 M_i}{TH} + \chi_0 + \frac{\chi_0 C' \alpha^2 M_d}{TH} + \frac{C' \alpha \chi_0}{T}, \end{aligned} \quad (\text{III.16})$$

where

$$C' = N_i J(J+1) g^2 \mu_B^2 / 3k_B. \quad (\text{III.17})$$

Rearranging terms we find

$$\chi - \chi_0 = \frac{C'(1 + \alpha \chi_0)^2}{1 - \alpha^2 C' \chi_0}. \quad (\text{III.18})$$

When the denominator of this expression vanishes the total susceptibility diverges, indicating a transition to ferromagnetism. The transition temperature is given by

$$T_C = \alpha^2 C' \chi_0(T_C). \quad (\text{III.19})$$

If χ_0 may be assumed to be temperature independent

$$\Delta\chi = \chi - \chi_0 = \frac{N_i \mu_B^2 p_{\text{eff}}^2}{3k_B(T - T_C)} \quad (\text{III.20})$$

wherein

$$p_{\text{eff}} = g \mu_B \{J(J+1)\}^{1/2} (1 + \alpha \chi_0). \quad (\text{III.21})$$

Using the definition (eq. III.17) of C' we can express T_C in terms of the fundamental parameters of the model

$$T_C = N_i g^2 \mu_B^2 J(J+1) \alpha^2 \chi_0 / 3k_B. \quad (\text{III.21})$$

Expressions for T_C have also been derived by Kim (102) and by Long and Turner (49) based on the itinerant and localized picture, respectively.

However, these expressions are (as well as eq. III.21) such that T_C is proportional to the concentration of the magnetic atoms. This is not in agreement with experimental results on alloys with concentrations smaller than 0.5 at.%. We will come back to this point in chapter V.

According to the definition of p_{eff} in eq. III.20 the magnitude of the magnetic moment is given by

$$\mu = g \mu_B J (1 + \alpha \chi_0) \quad . \quad (\text{III.22})$$

Doniach and Wohlfarth (50) have derived the same equation using the linear response approximation. This approximation obviates the need for the assumptions of a uniform moment distribution in the band and of a rigid band model. Zuckermann (111) has also derived an equation like eq. III.22, but he did not only include the bulk susceptibility of the host metal but also a possible local enhancement of the susceptibility at the impurity site. His equation became

$$\mu = g \mu_B J \{1 + \alpha(\chi_0 + \chi_{\text{local}})\} \quad . \quad (\text{III.23})$$

In chapter V the equation $\mu = g_{\text{eff}} \mu_B J$ will be used, so that g_{eff} is given by $g(1 + \alpha\chi_0)$ i.e. according to eq. III.22.

III.d.5. Calculation of the specific heat.

In a second paper (112) Takahashi and Shimizu have calculated the specific heat of dilute alloys. When the concentration of the magnetic impurities is small, e.g. less than 1 at.%, the polarization of the 4d-band will be very small. Therefore, the density of states of the 4d-band can be assumed to be the same as without polarization and the 4d-levels can be considered to be degenerate. Then the equations III.8, III.9 and III.10 become (assuming the external field to be zero for simplicity)

$$M_d = \alpha \chi_0 M_i \quad \text{and} \quad (\text{III.24})$$

$$M_i = N_i g \mu_B J B_J(g \mu_B J \alpha M_d / k_B T) \quad . \quad (\text{III.25})$$

A combination of these equations leads to

$$M_i = N_i g \mu_B J B_J(g \mu_B J \alpha^2 M_i \chi_0 / k_B T) \quad . \quad (\text{III.26})$$

This expression gives the same result for the specific heat as the Weiss molecular-field model, thus for further calculations we can use this model, and we can make an attempt at incorporating in the calculations the obviously present statistical variation in the distances between the magnetic impurities.

III.d.6. Incorporation of the statistical spatial distribution of the magnetic moments.

In the Weiss model the molecular field can be thought to be a homogeneous magnetic field caused by the ordered magnetic moments (infinite range model). In this case the random position of the magnetic moments (as is the case in a dilute alloy) has no influence on the properties of the system. Another interpretation of the molecular field is via a Heisenberg-like model (108). In this case the hamiltonian of the magnetic system is given by

$$H = - \sum_{i>j} \vec{S}_i \cdot \vec{S}_j J_{\text{int}}(\vec{r}_i - \vec{r}_j) \cdot \quad (III.27)$$

In the W.M.F. model this becomes

$$H_j = - g_j \mu_B H_{\text{mol}} S_j^z \quad (III.28)$$

wherein

$$H_{\text{mol}} = \sum_i \frac{J_{\text{int}}(\vec{r}_i - \vec{r}_j) \langle S_i^z \rangle}{g_j \mu_B}$$

The g-value enters into these equations in order to give H_{mol} the dimension of a magnetic field. However, not too much importance should be given to the value of g since in most cases H_{mol} is not a real magnetic field. On the other hand, we replace g in the next chapters by g_{eff} which equals $g(1 + \alpha \chi_0(T))$. Then the notation used above is rather convenient because g_{eff} determines the interaction with the external field as well as the interaction between the magnetic moments via $\alpha \chi_0(T)$ i.e. the magnitude of the polarization cloud. We assume that the interaction is isotropic and not dependent on the place in the specimen, so that $J_{\text{int}}(\vec{r}_i - \vec{r}_j)$ becomes $J_{\text{int}}(r)$ where $r = |\vec{r}_i - \vec{r}_j|$ (for clarity of the equations we will use r instead of r' for the distance between the magnetic moments).

⁺We use S instead of J for the magnetic quantum number in order to avoid confusion with the interaction parameter.

As the interaction parameter is a function of the distance, the random distribution of the magnetic moments has to be taken into account.

This can be done by combining statistics with the function $J_{\text{int}}(r)$.

Such a kind of calculations has been carried out by Korenblitz and Shender (113) for Pd-Fe alloys and by Marshall, Klein and Brout (114-118) for Cu-Mn and diluted Ising systems. The calculations of Korenblitz and Shender are based on a statistical theory by Chandrasekhar (119), the authors used for the interaction parameter the form

$$J_{\text{int}}(r) = J_{\text{int}}^{(0)} \exp\left(-\frac{r}{\sigma}\right). \quad (\text{III.29})$$

Marshall, Klein and Brout applied a theory of Margenau (120) and in the case of Cu-Mn of course the R.K.K.Y. interaction. It should be noted that the statistical theories of Margenau and of Chandrasekhar are identical. We will use these theories and the dependence of the interaction strength on the distance as given by eq. III.6.

The procedure of the calculation is that H_{mol} is calculated for each possible spatial configuration of the magnetic moments. A probability function $P(H_{\text{mol}})$ is then calculated, which is defined in such a way that $P(H_{\text{mol}}) dH_{\text{mol}}$ equals the normalized sum of the probabilities of those spatial configurations giving rise to a molecular field between H_{mol} and $H_{\text{mol}} + dH_{\text{mol}}$.

III.d.6.a. The zero temperature case.

Let us first focus our attention to the zero temperature case, where, assuming ferromagnetic ordering, $\langle S_i^z \rangle = S_i$. We will assume that all magnetic moments are identical, so that we may drop the index i and $H_{\text{mol}}(r, T=0)$ depends only on $J(r)$ and on the coordinates of the magnetic moments ($H_{\text{mol}}(r, T=0)$ is the molecular field at the origin caused by a magnetic moment at a distance r). According to Chandrasekhar (119) the probability function can be calculated from

$$P(H_{\text{mol}}) = \frac{1}{2\pi} \int_{-\infty}^{\infty} \exp\{-i\rho H_{\text{mol}} - n D(\rho)\} d\rho, \quad (\text{III.30})$$

wherein n is the density of the magnetic moments and $D(\rho)$ is given by

$$D(\rho) = 4\pi \int_0^{\infty} r^2 \{1 - \exp(i\rho H_{\text{mol}}(r))\} dr, \quad (\text{III.31})$$

with $H_{\text{mol}}(r) = -J(r)S/\epsilon\mu_B$. The interaction function $J(r)$ is given by eq. III.6 for $r > \sigma$, while $J(r) = J(\sigma)$ for $r < \sigma$ (σ being the parameter in the equation for $\chi(r,0)$).

As the integral cannot be solved in closed form, $P(H_{\text{mol}})$ has to be calculated numerically. In order to get some idea about the behaviour of $P(H_{\text{mol}})$ it is interesting to examine eq. III.6. Numerical calculations have shown that for small values of r (i.e. large concentration) $J(r)$ can be approximated by ξ'/r^3 and that for large values of r it can be written in first approximation as ξ''/r^6 .

The low concentration limit gives the same type of interaction as the one Margenau (120) treated, so that his calculation can be adopted:

$$D(\rho) = 4\pi \int_0^{\infty} r^2 (1 - e^{i\rho\xi''/r^6}) dr. \quad (\text{III.32})$$

Introducing $x = 1/r^6$ one partial integration of eq. III.32 leads to

$$\begin{aligned} D(\rho) &= -\frac{4\pi}{3} (\xi''\rho)^{\frac{1}{2}} \int_{r=0}^{r=\infty} \left(\frac{\sin x}{\sqrt{x}} - \frac{i \cos x}{\sqrt{x}} \right) dx = \\ &= \frac{4\pi (2\pi\xi''\rho)^{\frac{1}{2}}}{6} (1 - i). \end{aligned} \quad (\text{III.33})$$

Since the real part of $D(\rho)$ is an even function and the imaginary part is an odd function of ρ ,

$$P(H_{\text{mol}}) = \frac{1}{\pi} \int_0^{\infty} \cos\{H_{\text{mol}}\rho - \frac{2\pi}{3} n (2\pi\xi''\rho)^{\frac{1}{2}}\} \exp\{-\frac{2\pi}{3} n (2\pi\xi''\rho)^{\frac{1}{2}}\} d\rho. \quad (\text{III.34})$$

This integral has the form

$$\int_0^{\infty} x e^{-px} \cos(x^2 - px) dx, \quad \text{wherein } x = (H_{\text{mol}})^{\frac{1}{2}}, \quad (\text{III.35})$$

so that $P(H_{\text{mol}})$ is given by

$$P(H_{\text{mol}}) = \frac{2}{3} \pi (\xi'')^{\frac{1}{2}} n H_{\text{mol}}^{-3/2} \exp\left(-\frac{4}{9} \frac{\pi^3 \xi'' n}{H_{\text{mol}}}\right). \quad (\text{III.36})$$

This is the so-called Pearson type V distribution function (121).

In fig. III.1 $P(H_{\text{mol}})$ is shown as a function of $x = 9H_{\text{mol}}/4\pi^3\xi''n^2$. The function attains its maximum value at $H_{\text{mol}} = (\frac{2}{3}\pi)^3\xi''n^2$, which value is proportional to n^2 , as was to be expected according to the $1/r^6$ dependence of the interaction strength. The half width of $P(H_{\text{mol}})$ equals $1.85 \pi^3 4\xi''n^2/9$, also proportional to n^2 , so that the relative width $\Delta H_{\text{mol}}/H_{\text{mol}}^{\text{max}}$ becomes about 2.7.

A disadvantage of this form for $P(H_{\text{mol}})$ is that $\int_0^{\infty} H_{\text{mol}} P(H_{\text{mol}}) dH_{\text{mol}}$ is not finite, obviously due to the assumed finite probability for small values of r , for which values $J(r)$ becomes very large. This difficulty can be avoided by incorporating a minimum allowed value for r .

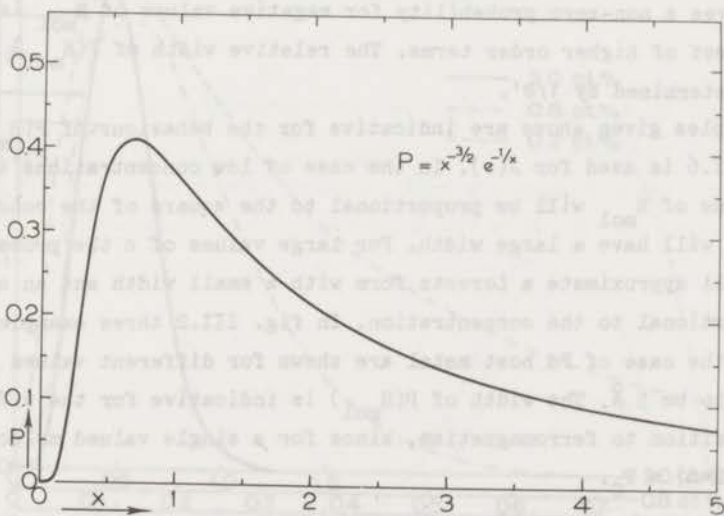


Fig. III.1. The Pearson type V distribution function.

In the limit of large concentrations $D(\rho)$ is given by

$$\begin{aligned}
 D(\rho) &= 4\pi \int_0^{\infty} r^2 (1 - e^{i\rho\xi'/r^3}) dr = \frac{4\pi\xi'\rho}{3} \int_0^{\infty} \frac{1}{x^2} (1 - e^{ix}) dx = \\
 &= \frac{4\pi\xi'\rho i}{3} + \frac{4\pi\xi'\rho}{3} \int_0^{\infty} \left(\frac{\sin x}{x} - \frac{i \cos x}{x} \right) dx \quad (\text{III.37})
 \end{aligned}$$

The imaginary part of $D(\rho)$, which part determines the value of H_{mol} at which $P(H_{\text{mol}})$ attains its maximum value, is infinite. This must be caused by the integral of ξ'/r^3 over an infinite volume, which integral is infinite. The result for $D(\rho)$ can be made finite by assuming a maximum allowed interaction distance, σ' , so that $J(r) = 0$ if $r > \sigma'$. In that case $D(\rho)$ can approximately be written as

$$D(\rho) = \frac{4\pi|\rho|\xi'}{3} \left(\frac{\pi}{2} - \frac{\xi'|\rho|}{2\sigma'^3} \right) + \frac{4\pi\xi'\rho i}{3} \left(2.03 - \frac{\xi'|\rho|}{2\sigma'^3} + \ln \frac{\xi'|\rho|}{\sigma'^3} \right) \quad (\text{III.38})$$

The leading terms in $D(\rho)$ are proportional to ρ , which means that $P(H_{\text{mol}})$ will approximate a Lorentzian form. The fact that such a distribution function gives a non-zero probability for negative values of H_{mol} is due to the neglect of higher order terms. The relative width of $P(H_{\text{mol}})$ is primarily determined by $1/\sigma'$.

The examples given above are indicative for the behaviour of $P(H_{\text{mol}})$ when eq. III.6 is used for $J(r)$. In the case of low concentrations the average value of H_{mol} will be proportional to the square of the concentration and $P(H_{\text{mol}})$ will have a large width. For large values of c the probability function will approximate a Lorentz form with a small width and an average value proportional to the concentration. In fig. III.2 three examples of $P(H_{\text{mol}})$ in the case of Pd host metal are shown for different values of c , assuming σ to be 5 \AA . The width of $P(H_{\text{mol}})$ is indicative for the width of the transition to ferromagnetism, since for a single valued molecular field $H_{\text{mol}}(T=0) \propto T_C$.

III.d.6.b. The non-zero temperature case.

Within the molecular field approximation it has to be assumed that the spins are statistically independent. Then the following equation holds for $\langle S^z \rangle$

$$\langle S^z \rangle = S \int_0^\infty P(H_{\text{mol}}, T) B_S(x) dH_{\text{mol}}, \quad (\text{III.39})$$

wherein $x = g\mu_B S(H_{\text{ex}} + H_{\text{mol}})/k_B T$.

The molecular field at a temperature T is assumed to be proportional to $\langle S^z \rangle$. Hence,

$$H_{\text{mol}}(r, T) = \langle S^z \rangle \frac{J(r)}{g\mu_B} \quad (\text{III.40})$$

Since at zero temperature $H_{\text{mol}}(r)$ was given by $SJ(r)/g\mu_B$, we should now insert in eq. III.31

$$H_{\text{mol}}(r, T) = \frac{\langle S^z \rangle}{S} H_{\text{mol}}(r, T=0). \quad (\text{III.41})$$

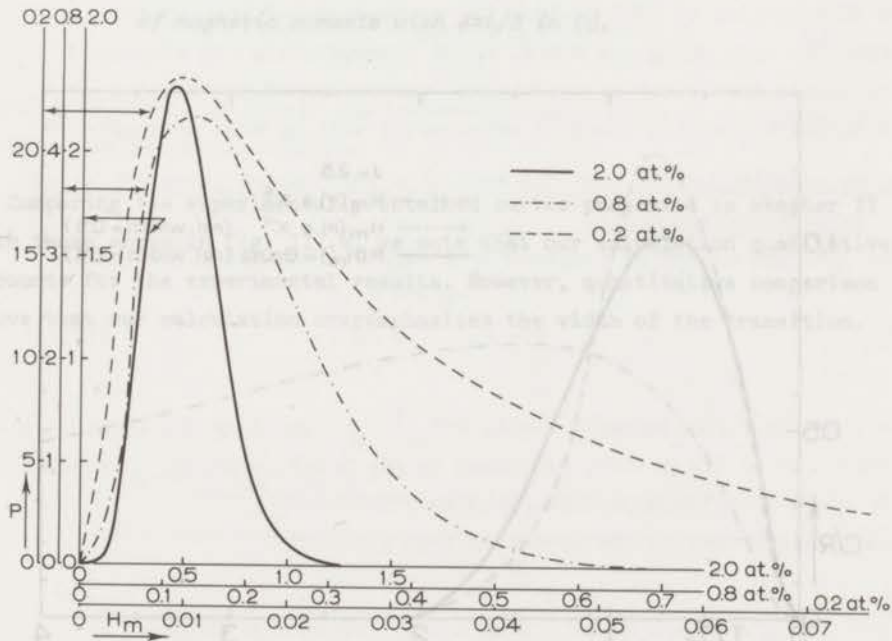


Fig. III.2. $P(H_{\text{mol}})$ as a function of H_{mol} for three different concentrations of magnetic moments in Pd.

In order to investigate the temperature dependence of $P(H_{\text{mol}}, T)$ it is convenient (since $\langle S^2 \rangle$ is not a function of r) to introduce the variable $\rho' = \rho \langle S^2 \rangle / S$. Then eq. III.30 becomes

$$P(H_{\text{mol}}, T) = \frac{1}{\pi} \frac{S}{\langle S^2 \rangle} \int_0^{\infty} \exp\left\{-i\rho' \frac{S}{\langle S^2 \rangle} H_{\text{mol}}(T) - n D(\rho')\right\} d\rho', \quad (\text{III.42})$$

which means that the probability is a function of $H_{\text{mol}}(T=0)$ only, or in other words not the shape of $P(H_{\text{mol}}, T)$ but only the scale is a function of temperature. The factor $S/\langle S^2 \rangle$ accounts for the normalization.

Regarding this fact, a calculation of the specific heat can be made straightforwardly. A detailed description will be given in chapter IV. Results for a Lorentz distribution, a Gauss distribution and a Pearson type V one are shown in fig. III.3. Results of the calculation of the specific heat for the distribution curves as shown in fig. III.2 are presented in fig. III.4.

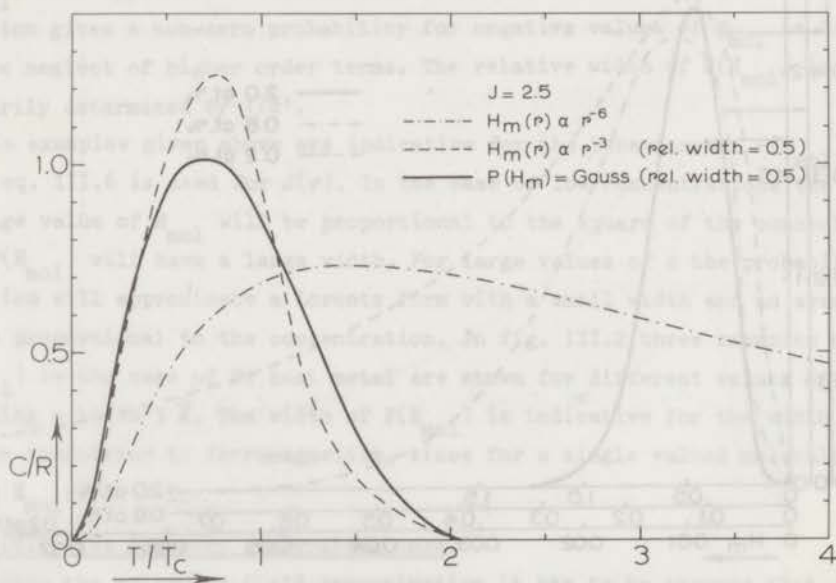


Fig. III.3. Specific heat calculated by means of the Weiss molecular-field model incorporating a gaussian distribution of molecular fields, a lorentzian distribution and a Pearson type V one, respectively.

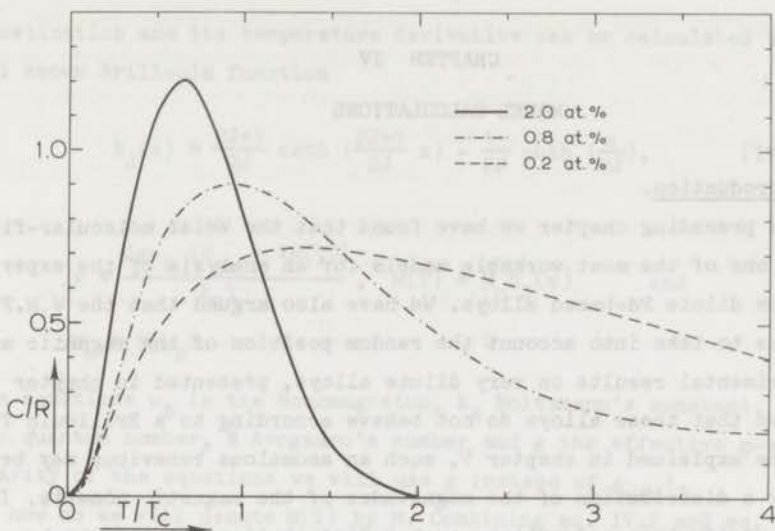


Fig. III.4. The specific heat calculated for three different concentrations of magnetic moments with $J=5/2$ in Pd.

Comparing the experimentally obtained curves presented in chapter II with those shown in fig. III.4, we note that our calculation qualitatively accounts for the experimental results. However, quantitative comparison shows that our calculation overemphasizes the width of the transition.

CHAPTER IV
MODEL CALCULATIONS

IV.a. Introduction.

In the preceding chapter we have found that the Weiss molecular-field model is one of the most workable models for an analysis of the experimental results on dilute Pd-based alloys. We have also argued that the W.M.F. model enables us to take into account the random position of the magnetic moments. The experimental results on very dilute alloys, presented in chapter II, have shown that these alloys do not behave according to a Brillouin function. As will be explained in chapter V, such an anomalous behaviour may be caused by a distribution of the magnitudes of the magnetic moments. In order to verify this assumption, such a distribution has also to be incorporated in the W.M.F. model.

In this chapter we will outline the mathematics of the calculation of the specific heat using the W.M.F. model incorporating the several modifications due to the distributions. Comparison of the results of these calculations with those of experiments will be made in chapter V.

IV.b. Calculation of the specific heat of a ferromagnet using the Weiss molecular-field model.

The internal energy of a system of N magnetic moments is given by

$$U = - \int_0^{M(T)} H \, dM, \quad (IV.1)$$

where H is the total magnetic field, $H = H_{\text{ex}} + H_{\text{mol}}$ and M is the total magnetization of the system. According to the W.M.F. model H_{mol} is equal to λM , where λ is the molecular-field coefficient.

The specific heat of the system is then given by

$$C = \frac{dU}{dT} = - \frac{d}{dT} \int_0^{M(T)} H \, dM = - H_{\text{ex}} \frac{dM(T)}{dT} - \lambda \frac{dM^2(T)}{dT} = - \{ H_{\text{ex}} + \lambda M(T) \} \frac{dM(T)}{dT} \quad (IV.2)$$

The magnetization and its temperature derivative can be calculated using the well known Brillouin function

$$B_J(x) = \frac{2J+1}{2J} \coth\left(\frac{2J+1}{2J}x\right) - \frac{1}{2J} \coth\left(\frac{x}{2J}\right), \quad (\text{IV.3})$$

where

$$x = \frac{Jg\mu_B \{H_{\text{ex}} + \lambda M(T)\}}{k_B T}, \quad M(T) = M_0 B_J(x) \quad \text{and}$$

$$M_0 = Ng\mu_B J.$$

In these equations μ_B is the Bohrmagneton, k_B Boltzmann's constant, J the magnetic quantum number, N Avogadro's number and g the effective g -value (for clarity of the equations we will use g instead of g_{eff}).

From now on we will denote $M(T)$ by M . Combining eq. IV.2 and eq. IV.3 the specific heat becomes

$$C = - \{H_{\text{ex}} + \lambda M_0 B_J(x)\} M_0 \frac{dB_J(x)}{dT}. \quad (\text{IV.4})$$

Denoting $dB_J(x)/dx$ by $B'_J(x)$, the temperature derivative of the Brillouin function can be calculated from

$$\frac{dB_J(x)}{dT} = B'_J(x) \frac{dx}{dT} = B'_J(x) \left(\frac{Jg\mu_B \lambda M_0}{k_B T} \frac{dB_J(x)}{dT} - \frac{Jg\mu_B \{H_{\text{ex}} + \lambda M_0 B_J(x)\}}{k_B T^2} \right) \quad (\text{IV.5})$$

so that C can be written as

$$C = \frac{Jg\mu_B \{H_{\text{ex}} + \lambda M_0 B_J(x)\}}{k_B T^2} \frac{M_0 \{H_{\text{ex}} + \lambda M_0 B_J(x)\} B'_J(x)}{1 - B'_J(x) \frac{Jg\mu_B \lambda M_0}{k_B T}}. \quad (\text{IV.6})$$

We have found it convenient to use the following equations in order to transform eq. IV.6 into a form applicable to a computer program:

$$p = \frac{H_{\text{ex}}}{\lambda M_0}, \quad x = \frac{3J}{J+1} \frac{T_C}{T} \{p + B_J(x)\} \quad \text{and} \quad T_C = \frac{(J+1)g\mu_B \lambda M_0}{3k_B}. \quad (\text{IV.7})$$

Using these equations the specific heat can be written as

$$C = \frac{R x^2 B_J'(x) \{p + B_J(x)\}}{p + B_J(x) - x B_J'(x)}, \quad (\text{IV.8})$$

where R is the gasconstant.

A number of results for $J=3/2$ and different values for p are shown in fig. IV.1. As can be seen the specific-heat curve for $p=0$ attains a sharp maximum equal to $5RJ(J+1)/\{J^2+(J+1)^2\}$ at T_C and approaches the Schottky specific-heat curve (122) for large values of p .

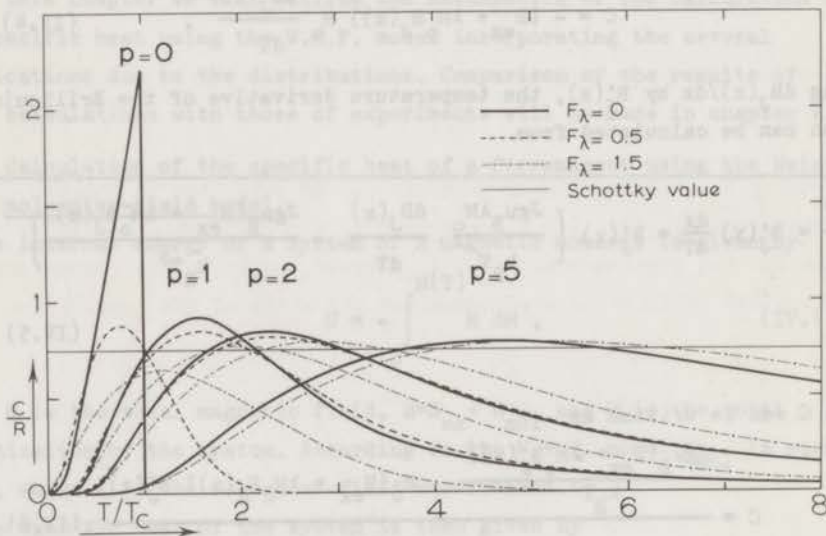


Fig. IV.1. Specific heat as a function of T/T_C calculated by means of W.M.F. model, incorporating a distribution of molecular fields with $F_\lambda=0$, $F_\lambda=0.5$ and $F_\lambda=1.5$.

Specific-heat curves calculated from eq. IV.8 have been compared with the experimental data on Pd-Mn dilute alloys obtained in strong external magnetic fields (9,13). These comparisons, which were quite successful, will be described in more detail in the next chapter in connection with the determination of the magnetic moment of Mn in Pd.

IV.c. Variant involving a distribution of molecular-field coefficients.

As outlined in section III.d.6, we should account for the random position of the magnetic moments in the alloys by incorporation of a distribution $P(H_{\text{mol}}, T)$ of molecular fields, or a distribution $P(\lambda)$ of molecular-field coefficients.

Calculations of the specific heat using the W.M.F. model incorporating a distribution of molecular-field coefficients have been performed and applied to Pd-based alloys by Takahashi and Shimizu (112) and by Boerstoeel (9). These authors have used a gaussian distribution of λ 's around a most probable value λ_0 . The weight of each value of λ is then given by

$$\frac{1}{\text{NORM}} \exp \left(- \frac{(\lambda - \lambda_0)^2}{2(F_\lambda \lambda_0)^2} \right), \quad (\text{IV.9})$$

where NORM is the normalization constant and F_λ is the relative width of the distribution (F_λ is not a function of λ).

For each value of λ the specific heat is given by

$$C(\lambda) = \frac{R x^2 B_J'(x) \{ p + \frac{\lambda}{\lambda_0} B_J(x) \}}{p + \frac{\lambda}{\lambda_0} B_J(x) - \frac{\lambda}{\lambda_0} B_J'(x)}, \quad (\text{IV.10})$$

where $x = \frac{3J}{(J+1)} \frac{T_C}{T} \{ p + \frac{\lambda}{\lambda_0} B_J(x) \}$ and $T_C = \frac{(J+1)g\mu_B \lambda_0 M_0}{3k_B}$.

It follows from eq. IV.9 and eq. IV.10 that

$$C = \frac{1}{\text{NORM}} \int_0^\infty C(\lambda) \exp \left(- \frac{(\lambda - \lambda_0)^2}{2(F_\lambda \lambda_0)^2} \right) d\left(\frac{\lambda}{\lambda_0}\right). \quad (\text{IV.11})$$

A number of examples of specific-heat curves calculated from eq. IV.11 are also shown in fig. IV.1. A common feature of these curves is that the influence of the distribution is at largest for the lower p -values, which was to be expected. A comparison between these curves and the experimental ones for Pd-Fe alloys has been made by Takahashi and Shimizu (112) and by Boerstoeel (9). Agreement between model and experiment appeared to be rather poor. Boerstoeel compared three curves obtained from the model with those from specific-heat experiments in external magnetic fields. The maximum values of the experimental specific-heat curves are much lower than those obtained from model calculations, as shown in fig. IV.2. This discrepancy becomes even more striking in the case of very dilute alloys measured in strong external fields (see also chapter II).

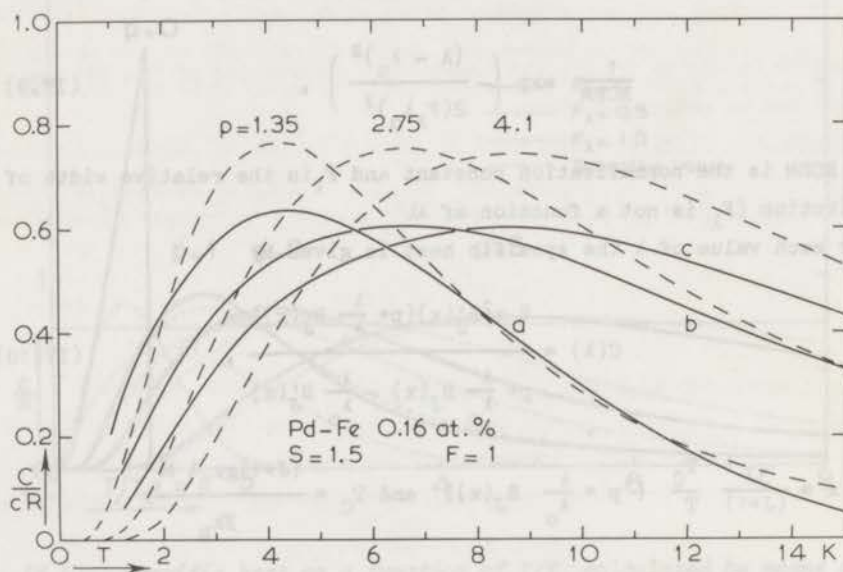


Fig. IV.2. Pd-Fe 0.16 at.%. Experimentally obtained curves (—) and calculated specific-heat curves (---). a, b and c represent results obtained in $H_{ex}=9, 18$ and 27 kOe, respectively (after Boerstoeel (9)).

IV.d. Variant involving a *macrodistribution* of g -values.

In order to diminish the discrepancy mentioned above, the model has to be modified in such a way as to influence the calculations of the specific heat in an external field. We attempted to achieve this by incorporation in the model a distribution of magnitudes of magnetic moments. In that case the excess specific heat of very dilute alloys measured in strong external fields will be a summation of "Schottky" curves with maxima at different temperatures, leading to a broader curve with a lower maximum value. Since rather normal values for the magnetic quantum number have been found from the entropy content of the excess specific heat, and also considering the Hirst model (26), each magnetic moment is supposed to have the same magnetic quantum number, but different effective g -values. In the course of the development of a more realistic model, we first used the so-called "*macrodistribution*" of g -values.

In this case the system is figuratively divided into a number of pieces (e.g. 200). Every magnetic moment in a particular piece is given the same effective g -value. The size of each piece is determined by the distribution of g -values, which is taken to be gaussian (see also ref. 51). This implies that magnetic moments with a certain g -value are sited in the neighbourhood of each other.

Applying this variant of the W.M.F. model eq. IV.8 becomes

$$C(g) = \frac{R x^2 B_J'(x) \left\{ \frac{g}{g_0} p + \left(\frac{g}{g_0} \right)^2 B_J(x) \right\}}{\frac{g}{g_0} p + \left(\frac{g}{g_0} \right)^2 B_J(x) - \left(\frac{g}{g_0} \right)^2 x B_J'(x)}, \quad (\text{IV.12})$$

where

$$x = \frac{3J}{J+1} \frac{T_C}{T} \left\{ \frac{g}{g_0} p + \left(\frac{g}{g_0} \right)^2 B_J(x) \right\} \text{ and } T_C = \frac{(J+1)g_0 \mu_B \lambda M_0}{3k_B}.$$

The total specific heat is then given by

$$C = \frac{1}{\text{NORM}} \int_0^{\infty} C(g) \exp \left[- \frac{(g - g_0)^2}{2(F_G g_0)^2} \right] d\left(\frac{g}{g_0}\right), \quad (\text{IV.13})$$

where F_G is the relative width of the *macrodistribution* of g -values.

A number of curves obtained from eq. IV.13 are shown in fig. IV.3 together with some curves obtained assuming the same values for p but incorporating a distribution of molecular-field coefficients with the same relative width. As can be seen from the graph this variant of the W.M.F. model influences the specific-heat curves for strong external fields.

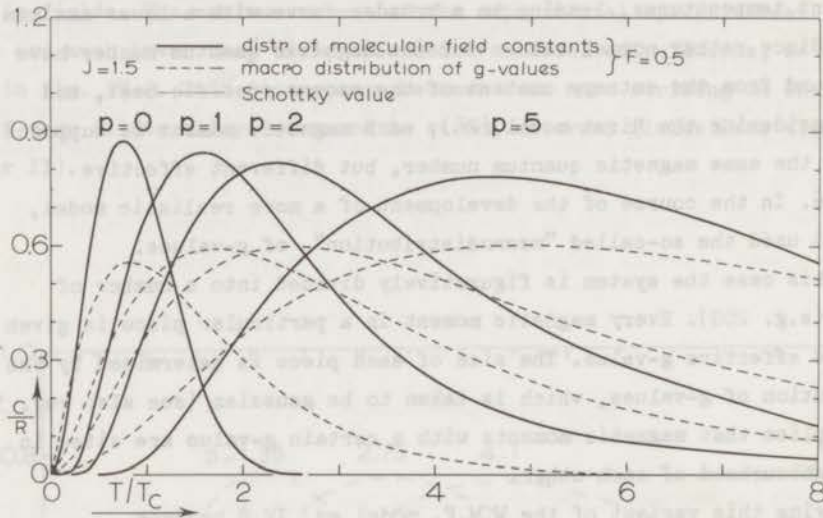


Fig. IV.3. Specific heat as a function of T/T_c obtained by application of the macrodistribution of g -values together with those obtained via the distribution of molecular fields.

IV.e. Variant involving a *microdistribution* of g -values.

The assumption of a *macrodistribution* is not supported by theoretical arguments nor by experimental results (although this variant seems to work rather well (51), see, however, chapter V). Therefore another variant involving a *microdistribution* of g -values has been elaborated. In this variant every magnetic moment is given a g -value and a statistical weight according to a gaussian distribution. However, in contrast to the case of the *macrodistribution*, they are randomly distributed in the alloy. The total magnetization M is calculated assuming the molecular field to be proportional to M . This implies that eq. IV.3 has to be transformed into

$$M = \frac{N\mu_B J}{\text{NORM}} \int_0^{\infty} g B_J(x) \exp\left(-\frac{(g - g_0)^2}{2(F_g g_0)^2}\right) d\left(\frac{g}{g_0}\right) \quad (\text{IV.14})$$

where $x = \frac{Jg\mu_B(H_{\text{ex}} + M)}{k_B T}$ and F_g is the relative width of the

microdistribution of g -values. Note that the index G refers to the *macrodistribution* and the index g to the *microdistribution*.

For the numerical calculations eq. IV.14 implies that the summation over the distribution must take place within the iterative procedure necessary for solving eq. IV.14. The calculation of the specific heat becomes a little more complicated in this case. Using the definition of T_C (see eq. IV.12) and eq. IV.2 the specific heat can be written as

$$c = -\frac{\lambda M_0^2}{T_C} \left(p + \frac{M}{M_0}\right) \frac{d(M/M_0)}{d(T/T_C)} = -\frac{3R_J}{J+1} \left(p + \frac{M}{M_0}\right) \frac{d(M/M_0)}{d(T/T_C)} \quad (\text{IV.15})$$

Taking into account that $x = \frac{3J}{J+1} \frac{T_C}{T} \frac{g}{g_0} \left(p + \frac{M}{M_0} \right)$ it is possible to calculate $\frac{d(M/M_0)}{d(T/T_C)}$ from the following implicit equation

$$\frac{d(M/M_0)}{d(T/T_C)} = \frac{1}{\text{NORM}} \int_0^\infty \frac{g}{g_0} B_J'(x) \left(-\frac{3J}{J+1} \frac{T_C^2}{T^2} \frac{g}{g_0} \left(p + \frac{M}{M_0} \right) + \frac{3J}{J+1} \frac{T_C}{T} \frac{g}{g_0} \frac{d(M/M_0)}{d(T/T_C)} \right) \exp \left(-\frac{(g - g_0)^2}{2(F_g g_0)^2} \right) d\left(\frac{g}{g_0}\right) \quad (\text{IV.16})$$

Equation IV.16 can be solved numerically to obtain values for the specific heat. Examples of specific-heat curves calculated from eq. IV.15 are shown in fig. IV.4 in the case of zero external field. In fig. IV.5 curves obtained by application of the *microdistribution* of g -values are shown together with curves obtained applying the *macrodistribution*. As is evident the difference between the curves is the largest for the lowest values of p .

Calculations for the paramagnetic phase can also be done using the *macro-* or the *microdistribution* of g -values by making the molecular-field coefficient zero. As should be expected, there is no difference between the *micro-* and *macrodistribution* for this phase.

Although this chapter does not concern the physical interpretation of the calculations, some remarks have to be made here. We have supposed the magnetic moments to sense the molecular fields via their g -value and we also assumed the molecular field caused by a particular magnetic moment to be proportional to its g -value. In view of the origin of the molecular field this may seem unreasonable, since the molecular field is not a real magnetic field; in most cases it is only an approximate description of the exchange interaction. However, as we are dealing with Pd-based alloys, the magnitude of the magnetic moment is proportional to $(1 + \alpha\chi_0)$. The term $\alpha\chi_0$ determines the extra moment induced in the Pd-band, and it is this induced magnetization which causes the interaction between the moments (see chapter III). If there is a distribution of g -values, and we will see in chapter V very strong experimental indication that there is, then this distribution is presumably caused by the term $\alpha\chi_0$.

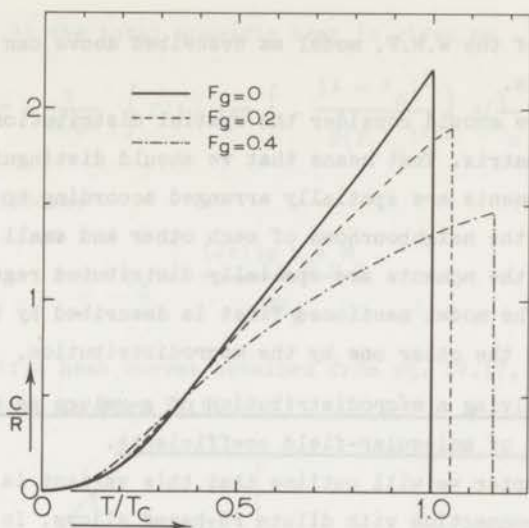


Fig. IV.4. Zero-field specific heat as a function of T/T_c calculated with the incorporation of the microdistribution of g -values.

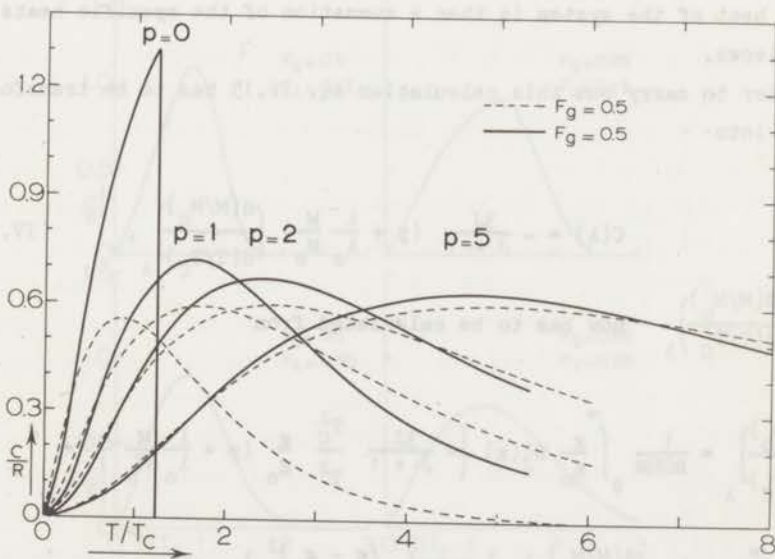


Fig. IV.5. Specific heat as a function of T/T_c calculated by means of the macrodistribution of g -values and that obtained via the microdistribution.

Thus the variant of the W.M.F. model as described above can be justified on physical grounds.

Consequently, we should consider the spatial distribution of the magnetic moments over the matrix. That means that we should distinguish between a model where the moments are spatially arranged according to their magnitude (large moments in the neighbourhood of each other and small moments too) and a model where the moments are spatially distributed regardless of their magnitude. The model mentioned first is described by the *macrodistribution*, the other one by the *microdistribution*.

IV.f. Variant involving a *microdistribution* of *g*-values as well as a *distribution* of molecular-field coefficients.

In the next chapter we will outline that this variant is the most realistic one in connection with dilute Pd-based alloys. In this case the system is divided into a number of pieces, each piece having its molecular-field coefficient. The size of the pieces is determined by the gaussian distribution of the molecular-field coefficients with F_λ as parameter. The specific heat of each piece is calculated according to the *microdistribution* of *g*-values (see preceding section). The total specific heat of the system is then a summation of the specific heats of all pieces.

In order to carry out this calculation eq. IV.15 has to be transformed a little into

$$C(\lambda) = - \frac{3J}{J+1} \left(p + \frac{\lambda}{\lambda_0} \frac{M}{M_0} \right) \left(\frac{d(M/M_0)}{d(T/T_C)} \right)_\lambda, \quad (IV.17)$$

where $\left(\frac{d(M/M_0)}{d(T/T_C)} \right)_\lambda$ now has to be calculated from

$$\left(\frac{d(M/M_0)}{d(T/T_C)} \right)_\lambda = \frac{1}{\text{NORM}} \int_0^\infty \frac{g}{g_0} B_J'(x) \left(- \frac{3J}{J+1} \frac{T_C}{T^2} \frac{g}{g_0} \left(p + \frac{\lambda}{\lambda_0} \frac{M}{M_0} + \frac{3J}{J+1} \frac{T_C}{T} \frac{g}{g_0} \frac{\lambda}{\lambda_0} \left(\frac{d(M/M_0)}{d(T/T_C)} \right)_\lambda \right) \exp \left(- \frac{(g - g_0)^2}{2(F_g g_0)^2} \right) d \left(\frac{g}{g_0} \right) \quad (IV.18)$$

Similarly to eq. IV.11 the total specific heat is given by

$$C = \frac{1}{\text{NORM}} \int C(\lambda) \exp \left[- \frac{(\lambda - \lambda_0)^2}{2(F_\lambda \lambda_0)^2} \right] d\left(\frac{\lambda}{\lambda_0}\right) \quad (\text{IV.19})$$

while T_C is now defined as

$$T_C = \frac{(J+1)g_0 u_B \lambda_0 M_0}{3k_B} \quad (\text{IV.20})$$

Examples of specific heat curves obtained from eq. IV.17, eq. IV.18 and eq. IV.19 are shown in fig. IV.6.

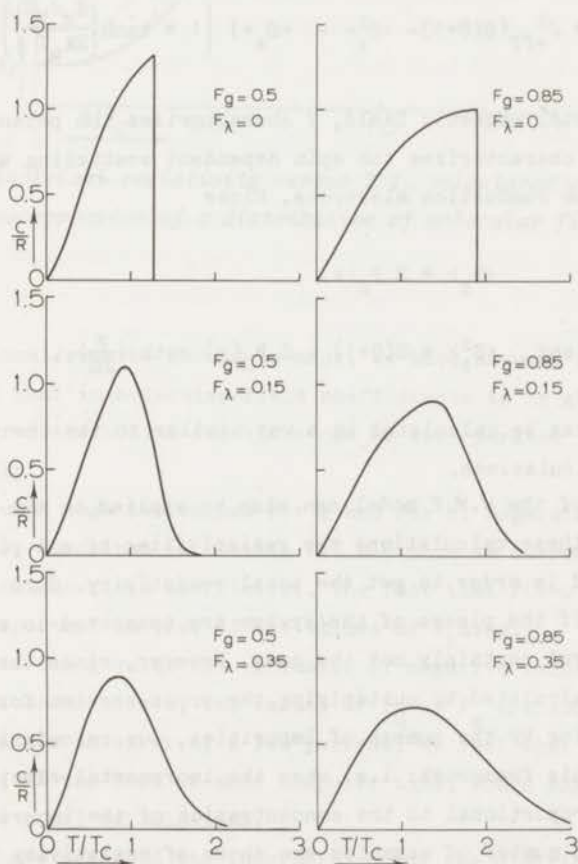


Fig. IV.6. Specific heat as a function of T/T_C calculated with incorporation of a distribution of molecular fields and a microdistribution of g -values.

IV.g. Calculation of the electrical resistivity using the W.M.F. model.

According to the calculations by Yosida (72) and by Long and Turner (49) the electrical resistivity within the molecular-field approximation is given by (we have to replace J by S because the orbital contribution to the scattering amplitude has been neglected, due to the assumed quenching of the orbital angular momentum) :

$$\Delta\rho(T,H) \propto V^2 + J_{\text{eff}}^2 \langle S_z^2 \rangle + J_{\text{eff}}^2 \{S(S+1) - \langle S_z^2 \rangle - \langle S_z \rangle\} \left(1 + \tanh \left(\frac{g_e \mu_B H}{2k_B T} \right) \right) - \frac{4 J_{\text{eff}}^2 V^2 \langle S_z \rangle^2}{V^2 + J_{\text{eff}}^2 \langle S_z^2 \rangle + J_{\text{eff}}^2 \{S(S+1) - \langle S_z^2 \rangle - \langle S_z \rangle\} \left(1 + \tanh \left(\frac{g_e \mu_B H}{2k_B T} \right) \right)}, \quad (\text{IV.21})$$

where H is the total magnetic field, V characterizes the potential scattering, J_{eff} characterizes the spin dependent scattering and g_e is the g -value of the conduction electrons. Since

$$\langle S_z \rangle = S B_S(x)$$

$$\text{and } \langle S_z^2 \rangle = S(S+1) - S B_S(x) \coth \left(\frac{x}{2S} \right), \quad (\text{IV.22})$$

the resistivity can be calculated in a way similar to the one used for the specific-heat calculations.

The variants of the W.M.F model can also be applied to the resistivity calculation. In these calculations the resistivities of all pieces of the system are summed in order to get the total resistivity. Such a summation is only correct if the pieces of the system are connected in series, which is in general certainly not the case. However, since the resistivity of an alloy is calculated by multiplying the cross-section for electron impurity scattering by the number of impurities, our calculation is correct within this framework: i.e. when the incremental electrical resistivity is proportional to the concentration of the impurities.

In fig. IV.7 a number of examples are shown of resistivity versus T/T_C curves calculated from eq. IV.21 involving a distribution of molecular coefficients.

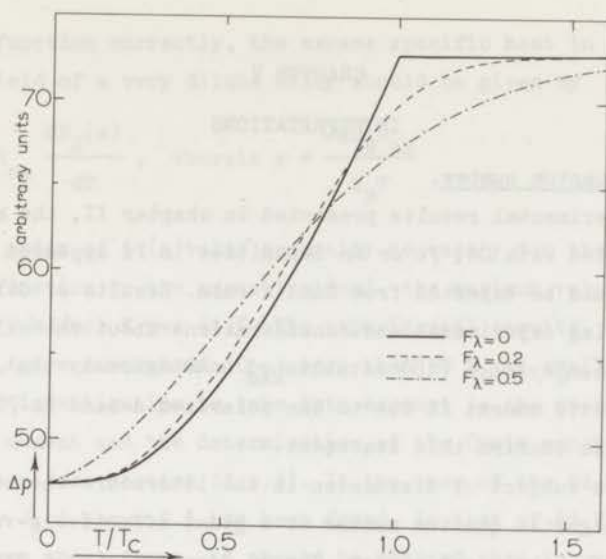


Fig. IV.7. Electrical resistivity versus T/T_c calculated with the incorporation of a distribution of molecular fields.

A few additional remarks should be made. We have assumed the distribution in g -values and that in molecular-field coefficients to be gaussian. Of course, other distribution functions can be incorporated straightforwardly.

We have excluded negative values for g and for λ . Regarding the function $P(H_{mol})$, described in section III.d.6 this is correct in the case of the molecular-field coefficient. The fact that $P(\lambda=0) \neq 0$ is not really important in view of the values of F_λ used.

With regard to the g -value the exclusion of negative values has no physical ground. Nevertheless, the values of F_G or F_g are such that the exclusion causes an error of a few percent. We feel that a correction for this effect, at the cost of more computer time, would exaggerate the value of the model calculations.

Finally, we have defended the incorporation of the distribution of g -values in the molecular-field term via the term $\alpha\chi_0$ in the effective g -value. In principle we should use a distribution in $\alpha\chi_0$ values, however, since $\alpha\chi_0 \approx 2$ in the cases of Co or Fe in Pd, we feel again that this more laborious calculation would exaggerate the value of the model.

CHAPTER V

INTERPRETATIONS

V.a. Magnetic quantum number.

From the experimental results presented in chapter II, the magnetic moments associated with Co, Fe or Mn impurities in Pd appeared to be larger than should be expected from Hund's rule. Results of diffuse neutron scattering experiments and considerations about the values for the transition temperature (18) established unambiguously that part of this large magnetic moment is due to the polarized d-band in Pd. Theoretical calculations also confirm this statement.

It has been a subject of discussion in the literature whether a giant value for the magnetic quantum number or a giant effective g-value should account for the giant moment. Theory does not give a decisive answer to this problem. Nevertheless, some arguments may be advanced:

In view of the Hirst model (26) one should hardly expect a large difference between the electronic configuration of the free atom and that of the atom implanted in the host metal. In other words, the impurity will obey Hund's rule in the metallic environment as well.

Nevertheless, in addition to an explicit change in the electronic configuration of the impurity atom, there may be another possibility for the existence of a giant magnetic quantum number. When the d-electrons of Pd and those of the impurities are coupled so strongly that their magnetic quantum numbers should be added, a large value for J may be obtained. Such a strong (albeit antiferromagnetic) coupling exists probably in the ground states of Kondo systems (123).

A normal value for the multiplicity and thus for the magnetic quantum number has been deduced from the entropy content of the excess specific heat. On the other hand, results of magnetization experiments and of Mössbauer-effect investigations have successfully been fitted to Brillouin functions involving a large magnetic quantum number. The source of this discrepancy may be found in two ways: (i) the excess specific heat, as evaluated from experiments at temperatures up to 20 K, does not contain the total magnetic entropy; (ii) the magnetization of the alloys cannot be described by a Brillouin function at all.

In order to pass a judgement on these statements results of two experiments should be discussed. First, if the magnetization follows a

Brillouin function correctly, the excess specific heat in an external magnetic field of a very dilute alloy should be given by

$$\Delta C = - H_{\text{ex}} \frac{dB_J(x)}{dT}, \quad \text{wherein } x = \frac{Jg\mu_B H_{\text{ex}}}{k_B T} \quad (\text{V.1})$$

If J is of order of 5 (a value generally necessary for the fit of the Brillouin function to the magnetization), the maximum value of ΔC turns out to be 79 mJ/mol K per at.%. The experimental results, described in chapter II, give a value of ΔC_{max} more than 30 % too small in all cases.

A second investigation to take into account is the measurement of the saturation moment and the determination of the Curie constant of the same specimen (see section II.c.3). In the case of the Pd-Mn system a value for J of about 2.5 has been found, in that of Pd-Fe 1.5 ± 0.5 (18).

Apart from these facts, it should be noticed that in order to obtain a good fit of a Brillouin function to the experimental magnetization and magnetoresistance data, a quite large value for J had to be assumed (27,28,79, see also table II.I). This value for J was so large that the product J times g_{eff} strongly exceeds the value of the magnetic moment (expressed in μ_B). Such a choice of J passes over the physical origin of the Brillouin function.

In view of the arguments given above we conclude that the values of the magnetic quantum number as deduced from the specific-heat investigations are correct. This conclusion implies that one cannot describe the magnetization of Pd-Fe and of Pd-Co alloys as a function of temperature and external magnetic field by a Brillouin function. An exception, however, should be made for Pd-Mn alloys, as will be outlined in the next section.

In order to find the cause of the inadequacy of the Brillouin function in accounting for the magnetization and for the specific heat in external fields, we should go through the derivation of the formulae for the bulk magnetization. In calculating the entropy of an assembly of magnetic moments, we started by writing the entropy of one magnetic moment as

$$S'_m = k_B \ln(2J+1). \quad (\text{V.2})$$

Then we assumed all the magnetic moments to have the same value of J ,

so that

$$S_m = cR \ln(2J+1). \quad (V.3)$$

If the average value of the z-component of J of a single magnetic moment is given by $\langle J^z \rangle = J B_J(x)$ ($x = g_{\text{eff}} \mu_B J H_{\text{ex}} / k_B T$, H_{ex} in the z-direction) then the magnetization along the z-axis is given by

$$M'_z = g_{\text{eff}} \mu_B J B_J(x). \quad (V.4)$$

If all the magnetic moments have the same value of J and of g_{eff} the total magnetization may be written as

$$M_z = cN g_{\text{eff}} \mu_B J B_J(x). \quad (V.5)$$

We have to conclude that either $\langle J^z \rangle$ is not given by the Brillouin function or the effective g-values are not the same for all moments. Since the experiments sense the average magnetization of a large number of magnetic moments we do not expect to be able to distinguish between these possibilities on the basis of experimental results.

The values of the magnetic quantum number deduced from specific-heat investigations are:

Pd-Co : 1.4,

Pd-Fe : 2,

Pd-Mn : 2.3.

Since J should be a half integer the values 3/2, 2 and 5/2 should be accepted as the correct ones. It is remarkable that these values are equal to those for the spin only quantum numbers of the free atoms. Assuming no change in the electronic configuration of Co, Fe and Mn on alloying, it follows that no contribution of the orbital angular momentum has been found.

According to Hirst (96) the contribution of the orbital angular momentum of Co and Fe may be quenched in a f.c.c. lattice when the coefficient of the fourth degree terms of the crystalline electric field, C_4 , is negative. The coefficient C_4 is defined in cartesian coordinates by the following equation for the electric field (124)

$$V_L(x,y,z) = C_4 \{x^4 + y^4 + z^4\} - \frac{3}{5} r^4 \quad (V.6)$$

$$C_6 \{ (x^6 + y^6 + z^6) + \frac{15}{4} (x^2 y^4 + x^2 z^4 + y^2 x^4 + y^2 z^4 + z^2 x^4 + z^2 y^4) - \frac{15}{14} r^6 \} + \dots$$

The negative value for C_4 is in agreement with point charge calculations by Lacroix (125) and with the results of E.P.R. experiments on Pd-Dy single crystals by Devine (126,127).

V.b. Paramagnetic behaviour.

Discussing the paramagnetic behaviour, we will only focus our attention on results of experiments carried out on alloys with such a concentration that $T/T_C > 5$ (T being the temperature at which the measurements are made) or $H_{ex}/H_{mol}(T=0) > 5$ (H_{ex} being the external field in which the experiment is done). Nevertheless, when a comparison with calculations is made, the interaction between the magnetic moments will be taken into account by applying the Weiss molecular-field model. The shortcomings of this model will have a negligible effect on the results of the calculations, since the interactions are only of minor importance (always less than 20%)

We will sometimes use the term 'Schottky calculation (122)' when "paramagnetic properties" are concerned. These calculations of course also incorporate a molecular field in order to account for the interaction, however, they do not include any of the other modifications described in chapter IV.

V.b.1. Paramagnetic behaviour of Pd-Mn.

The paramagnetic behaviour of Pd-Mn alloys is not at all peculiar, although it deviates from that of the other two systems, and therefore quite important for the understanding of the behaviour of dilute Pd-based alloys.

As mentioned in chapter II, the excess specific heat as well as the magnetization can be described by the molecular-field model involving $J=5/2$ and $g_{eff}=3$ (13,18). In ref. 13 examples are shown of a comparison between the calculated and the experimental curves of the specific heat. It should be emphasized again that the excellent quality of the fit has been obtained without any artifice. In ref. 18 examples are shown of comparisons between calculated and experimental results for the magnetization. In this case even no adjustable parameters have been used.

The Pd-Mn system may be called a 'corner-stone' for the assumption of a normal value for J and a large value for g_{eff} .

V.b.2. Paramagnetic behaviour of Pd-Co and Pd-Fe.

When the values $3/2$ and 2 for the magnetic quantum number of Co and Fe in Pd are accepted, we should recognize that it is impossible to

describe the magnetization and the specific heat according to a Brillouin function involving these values for J . The maximum of ΔC as a function of temperature or as a function of external field turned out to be much lower than the calculated values (40 % in the case of Co, 20 % in that of Fe). The ΔC versus T curves are also much broader, in agreement with entropy considerations. The amount of deviation from a Schottky curve does not depend on the temperature of the maximum nor on the magnetic field strength.

Such a broadened specific-heat curve suggests a superposition of Schottky curves with maxima at different temperatures or, what is similar, at different external field strengths. This supposition physically implies the assumption that the effective g -value of the magnetic moments differ from one to the other.

In such a case the magnetization should be written as

$$M(T, H_{ex}) = cN J\mu_B \int_0^{\infty} g_{eff} B_J(x) f(g_{eff}) dg_{eff} \quad (V.7)$$

where $x = Jg_{eff}\mu_B H_{ex} / k_B T$ and $f(g_{eff}) dg_{eff}$ is the probability of finding a magnetic moment with an effective g -value between g_{eff} and $g_{eff} + dg_{eff}$. From eq. V.7 the specific heat can be calculated according to

$$\Delta C = -J\mu_B cN H_{ex} \int_0^{\infty} g_{eff} \frac{dB_J(x)}{dT} f(g_{eff}) dg_{eff} \quad (V.8)$$

In order to compare results of eq. V.7 and of eq. V.8 with the experimental data a gaussian function for $f(g_{eff})$ has been rather arbitrarily chosen, i.e. $f(g_{eff}) \propto \exp \{-(g_{eff} - g_{eff,0})^2 / (2F_G g_{eff,0})^2\}$. The interaction between the magnetic moments has been taken into account according to the *macrodistribution* of g -values as described in chapter IV.

First we have made fits of the results of eq. V.8 to results of separate specific-heat measurements by choosing the best value for F_G and for $g_{eff,0}$. It appeared from these fits that neither F_G nor $g_{eff,0}$ depends strongly on the concentration, the external field strength or the temperature. Also the method used for the measurement (adiabatic or a.c.) was of no importance. The best values for F_G and $g_{eff,0}$ were determined mainly by the kind of magnetic impurity, Co or Fe. Therefore, comparison between calculations and experimental data will be made here by use of the average values $F_G = 0.85$ and $g_{eff,0} = 5.5$ in the case of Co and $F_G = 0.5$ and $g_{eff,0} = 4.7$

in the case of Fe impurities. Because negative values of g_{eff} have been excluded, these values of $g_{\text{eff},0}$ imply that the average of g_{eff} is 4.9 in the case of Fe and 6.3 in the case of Co. These values are in fair agreement with the results from magnetization measurements (see table II.I). Figures V.1-V.6 show the experimental data for the excess specific heat together with curves calculated according to eq. V.8. Note that in those cases where the experimental data have been obtained from adiabatic experiments, the measured values have been plotted in order to avoid effects due to 'wishful thinking' at drawing curves through these points.

It is evident from these graphs that eq. V.8 describes the specific heat of paramagnetic alloys rather well, or at least much better than the 'Schottky calculation' (with $F_G=0$).

Irrespective of the significance of the distribution of effective g -values, it is in view of the large values of $g_{\text{eff},0}$ obvious from these figures that large magnetic moments should account for the experimental curves. Thus these specific-heat investigations confirm the existence of the giant moments. The large value of the bulk magnetization of these alloys could possibly be ascribed to localized moments plus itinerant magnetism. However, the specific-heat results do not fit in such a picture; the localized model should be preferred.

If the excess specific heat can be described according to eq. V.8 then eq. V.7 should be in agreement with the data from magnetization measurements. A comparison between experimentally obtained curves on a Pd-Co 0.1 at.% alloy, as measured by Star, and points calculated according to eq. V.7 using $F_G=0.85$ and $g_{\text{eff},0}=5.5$, is shown in fig. V.7. The curve obtained by Maley et al. (31) from a fit to their Mössbauer-effect data on Pd-Fe has been drawn in fig. V.8 together with a curve calculated according to eq. V.7. In fig. V.9 a fit by Grassie et al. (71) to magnetoresistance data has been compared to results of our calculations with the parameters mentioned above. These three graphs show a rather fair agreement.

A description of the Mössbauer-effect results by eq. V.7 implies that we find a lower value for the saturation moment than originally has been evaluated from these results, since the value as deduced from these experiments is proportional to $3J/(J+1)$. The choice of the lower value of the magnetic quantum number for the description of the magnetoresistance

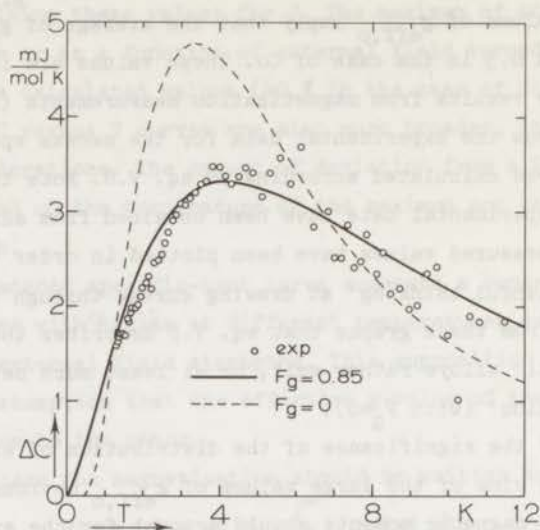


Fig. V.1. Specific-heat curves as obtained from our calculation (—) together with the experimental results as obtained by Boerstoel (9) for Pd-Co 0.075 at.% in an external magnetic field of 18 kOe. The dashed line represents the "Schottky" behaviour.

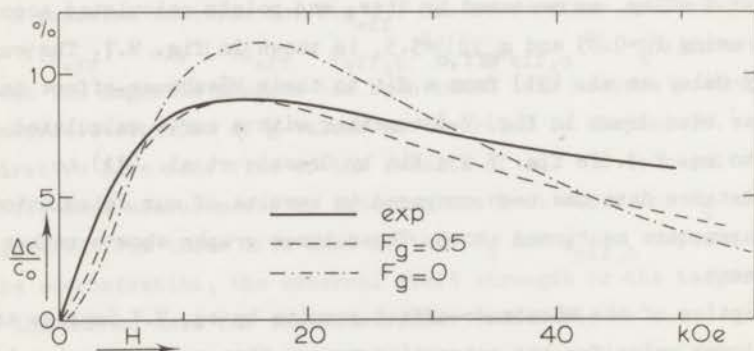


Fig. V.2. ΔC versus H_{ex} of Pd-Fe 0.05 at.% at $T=3.46$ K as obtained from experiment (—) and that as obtained from our calculation (- - - -). The dash-dotted line represents the "Schottky" behaviour.

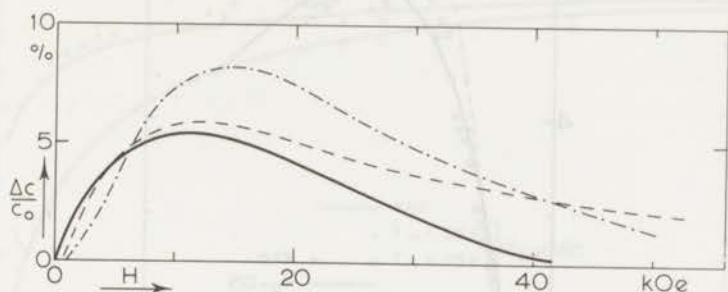


Fig. V.3. ΔC versus H_{ex} of Pd-Co 0.05 at.% at $T=3.46$ K as obtained from experiment (—) and that as obtained from our calculation (---). The dash-dotted line represents the "Schottky" behaviour.

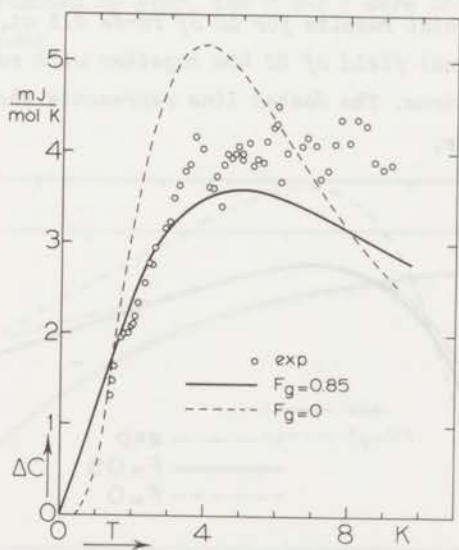


Fig. V.4. Experimental results for ΔC of Pd-Co 0.081 at.% s.c. in an external field of 20 kOe together with results of our calculations. The dashed line represents the "Schottky" behaviour.

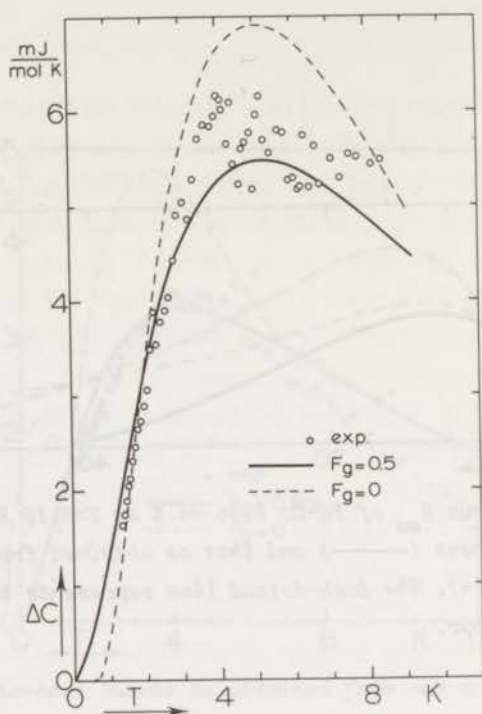


Fig. V.5. Experimental results for ΔC of Pd-Fe 0.1 at.% s.c. in an external field of 20 kOe together with results of our calculations. The dashed line represents the "Schottky" behaviour.

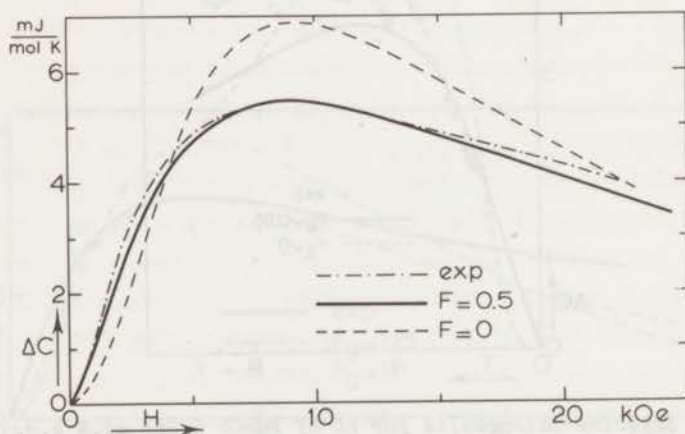


Fig. V.6. ΔC of Pd-Fe 0.1 at.% s.c. as a function of H_{ex} at 3.16 K. The solid line is obtained from experiment, the dashed one from our calculation. The dash-dotted line represents the "Schottky" behaviour.

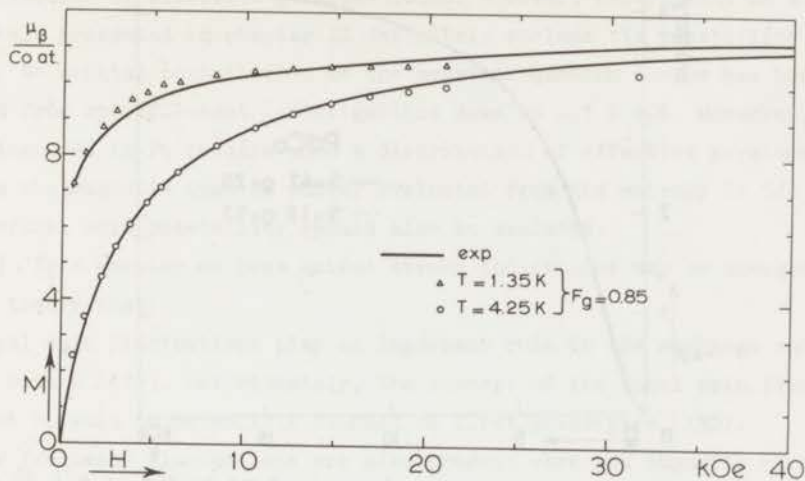


Fig. V.7. Magnetization of Pd-Co 0.1 at.% as a function of H_{ex} at $T=1.35$ K and 4.25 K. The solid line represents the experimental result obtained by Star, the \circ and Δ were obtained from our calculations

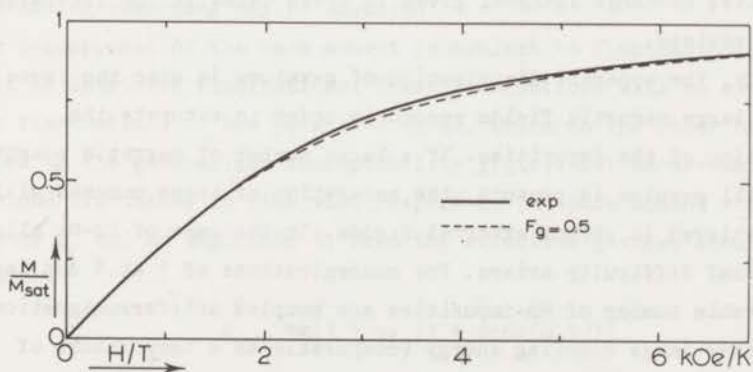


Fig. V.8. Magnetization of Pd-Fe ($c < 0.1$ at.%). The solid line is a Brillouin function with $J=3.76$ and $g=2.95$ as obtained by Maley et al. (31), the dashed line represents the result of our calculation.

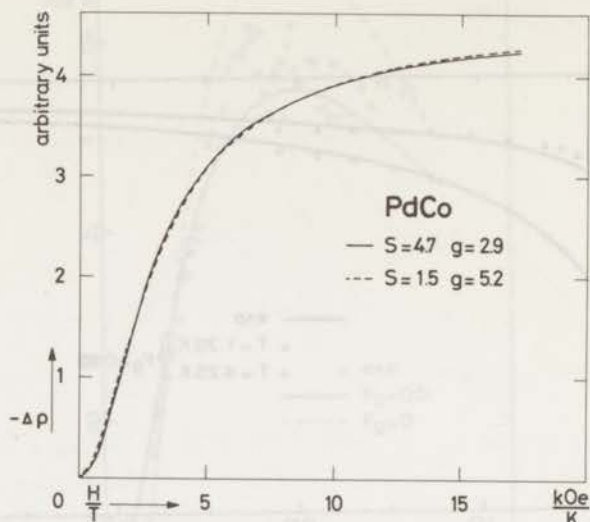


Fig. V.9. Results for the magnetoconductance of Pd-Co 0.1 at.% (—) calculated by application of Yosida's equation with $S=4.7$ and $g=2.9$ (after Grassie et al. (71)) together with the result of our calculation (---).

data results in a different value for the effective exchange integral between the conduction electrons and the giant moment. The value of this integral as deduced from magnetoconductance measurements is approximately proportional to $1/J$. Therefore, values of the saturation moment and for the effective exchange integral given in these cases in the literature should be revised.

Probably, the apparent distribution of g -values is also the cause of the quite large magnetic fields needed in order to saturate the magnetization of the impurities. If a large number of magnetic moments with a small g -value is present, the saturation of these moments will only be achieved in strong external fields. In the case of Pd-Mn alloys an additional difficulty arises. For concentrations of 1 at.% and larger a considerable number of Mn-impurities are coupled antiferromagnetically with a rather large coupling energy (comparable to a temperature of 50 K (18)). The decoupling of these moments will also only occur in strong external fields.

Possible causes of the observed distribution of effective g -values are: (i) magnetic anisotropy, (ii) influence of the orbital angular momentum and (iii) influences of fluctuations.

(i). Since the original investigations had been carried out on polycrystalline samples, magnetic anisotropy might be the cause of the distribution of effective g -values found. However, experiments on single crystals presented in chapter II definitely exclude this possibility.

(ii). No orbital contribution to the magnetic quantum number has been found from specific-heat investigations down to 0.1 K (9). Moreover, Mn dissolved in Pt reveals also a distribution of effective g -values, while the magnetic quantum number evaluated from the entropy is 5/2 (128). Therefore, this possibility should also be excluded.

(iii). In a greater or less extent strong indications may be emerged from theory that:

- Local spin fluctuations play an important role in the exchange enhanced host metals (129). Unfortunately, the concept of the local spin fluctuation cannot be said to be solidly founded on first principles (130).
- Low frequency fluctuations are also present when the impurity carries a magnetic moment (131). The frequency ω_f is such that $h\omega_f/2\pi k_B \sim 0.1$ K.
- The z -component of the bare moment is subject to thermal fluctuations.
- The generalized magnetic susceptibility $\chi(q, \omega)$ of pure Pd attains a maximum value for low values of ω (depending on q) (50). Roughly, Pd metal, and especially that part of the metal in the neighbourhood of a magnetic impurity, wobbles between the paramagnetic and ferromagnetic state.

It is not possible to found a theory on these assumptions. Nevertheless, if we allowed to let our imagination loose in the rest of this section, the following reasoning may be advanced:

The z -component of the bare moment is subject to fluctuations, thermal as well as intrinsic fluctuations. These fluctuations will be coupled to the fluctuations of the polarized cloud, which on the other hand are governed by the generalized susceptibility $\chi(q, \omega)$. Let us assume that this cloud fluctuates in time with respect to the bare moment with a frequency ω_f and an amplitude β . Then the effective g -value should be written as

$$g_{\text{eff}} = g \left(1 + \alpha \chi_0 \{ 1 + \beta \cos(\omega_f t) \} \right) \quad (\text{V.9})$$

In principle we should use a spectral density function $\beta(\omega_f)$, but we feel that incorporation of such a function would exaggerate the importance of this reasoning. According to eq. V.9 the bare moment senses a magnetic field equal to

$$H = H_{ex} \left[1 + \alpha \chi_0 \{ 1 + \beta \cos(\omega_f t) \} \right]. \quad (V.10)$$

The question, whether this expression for the magnetic field should be incorporated in the argument of the Brillouin function, depends strongly on the ability of the z-component of the bare moment to follow the time dependence of the magnetic field. Note that this argument only holds at temperatures larger than $h\omega_f/2\pi k_B$, below this temperature the use of the Brillouin function itself is not allowed.

The ability of the z-component of a magnetic moment to follow a time dependent magnetic field depends on its longitudinal relaxation time T_1 (132). Two cases should be distinguished:

- 1) the adiabatic limit, where $T_1 \omega_f \gg 2\pi$.
- 2) the isothermal limit, where $T_1 \omega_f \ll 2\pi$.

ad.1. In the adiabatic limit the time dependence of the magnetic field should *not* be incorporated in the argument of the Brillouin function, since the z-component is not able to follow the fluctuations. Only the average value $H_{ex}(1 + \alpha \chi_0)$ is important. In this case a normal Brillouin function behaviour for the magnetization is expected. The adiabatic limit is probably applicable to Pd-Mn alloys.

ad 2. In the isothermal limit, where the z-component of the moment is able to follow the fluctuation, the time dependent field should be incorporated in the argument of the Brillouin function. In that case the magnetization is given by

$$M = J\mu_B cN \int_0^\pi g \left[1 + \alpha \chi_0 \{ 1 + \beta \cos(\omega_f t) \} \right] B_J(x) d(\omega_f t), \quad (V.11)$$

wherein $x = J\mu_B H_{ex} g \left[1 + \alpha \chi_0 \{ 1 + \beta \cos(\omega_f t) \} \right] / k_B T$.

Equation V.11 can also be written as

$$M = J\mu_B cN \int_0^\infty g' B_J(J\mu_B H_{ex} g' / k_B T) f(g') dg', \quad (V.12)$$

where

$$f(g') = \frac{\pi}{4\beta\alpha\chi_0} \cos \left(\frac{(g' - \alpha\chi_0)\pi}{2\beta\alpha\chi_0} \right) \text{ if } \alpha\chi_0(1-\beta) < g' < \alpha\chi_0(1+\beta) \text{ and}$$

$f(g') = 0$ for all other values of g' .

It is evident that eq. V.12 gives results similar to those of eq. V.7, especially when a range of fluctuation frequencies is involved.

Unfortunately, our knowledge about ω_f and T_1 is rather poor. The only experimental data can be obtained from E.P.R. investigations on dilute Pd-Mn alloys (85-87). These investigations reveal a value of 10^{-10} s for T_1 . The electron paramagnetic resonance of Fe and of Co in Pd has not been observed. Assuming this fact to be due to a small value of T_1 , we should remark that Pd-Co and Pd-Fe probably should be treated in the isothermal limit. If the value of T_1 of Mn in Pd is long enough to treat this alloy in the adiabatic limit, it can be said that the reasoning given above is in agreement with our experimental observations.

Some additional support to these ideas may be obtained from the following observations. Mössbauer-effect investigations on Fe dissolved in Ni_3Ga (133), which compound has an even larger paramagnetic susceptibility than Pd, resulted in a magnetization curve which deviates more from $B_2(x)$ than the curves obtained for Pd-Fe. Since the importance of fluctuations increase at increasing paramagnetic susceptibility, this seems to fit in our picture. Electrical-resistance measurements by Loram et al. (134) are indicative of spinfluctuation effects in Pt-Fe with $h\omega_f/2\pi k_B = 0.4 \pm 0.2$ K.

Although we are unable to place this argument on a firm theoretical ground, we feel that the balance between fluctuations and relaxations determines the deviations from the Brillouin function behaviour of Fe and Co in Pd. Investigations of the excess specific heat as a function of external field at temperatures higher and lower than $h\omega_f/2\pi k_B$ and measurements of the magnetic susceptibility of transition metal impurities dissolved in host metals with various degrees of exchange enhancement may be of value for the elucidation of this problem.

V.c.1. Transition temperature.

As has been mentioned in section V.b. the localized picture should be applied to the magnetic ordering in dilute Pd-based alloys. The occurrence of ferromagnetism down to very small concentrations in this alloy system evidently implies that the interaction between the magnetic moments is caused by the d-band electrons in Pd. The calculations by Takahashi and Shimizu (110), assuming a spatially homogeneous polarization of the band, result in the following expression for T_C

$$T_C = cNJ(J+1)g^2 \mu_B^2 \alpha^2 \chi_0 / 3k_B \quad (V.13)$$

If g is assumed to be 2, the value of $\alpha\chi_0$ can be determined from $g_{\text{eff}} = g(1 + \alpha\chi_0)$. Using for χ_0 the value $7.26 \cdot 10^{-4}$ emu/mol the results for T_C are:

Pd-Mn	15 K/at.%,
Pd-Fe	93 K/at.%,
Pd-Co	183 K/at.%.

These results are in disagreement with experiments: T_C is predicted to be proportional to the concentration (which has not been found) and it is overestimated by a factor 5-8. The disagreement between the calculations and the experimental results is obviously caused by the assumed spatial homogeneity of the polarization.

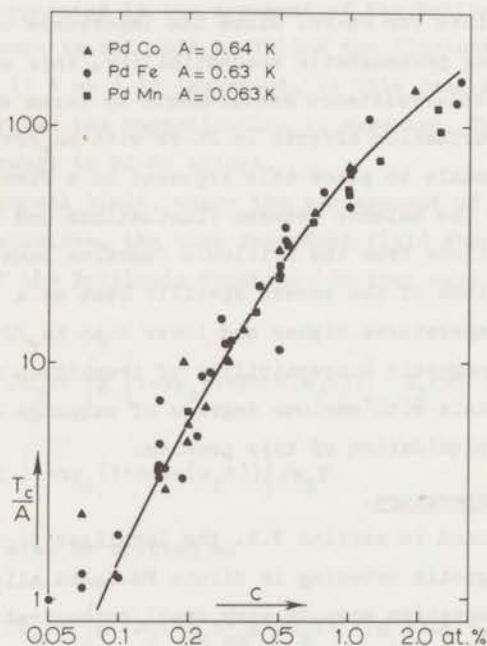


Fig. V.10. The ferromagnetic transition temperature of Pd-Co (\blacktriangle), of Pd-Fe (\bullet) and of Pd-Mn (\blacksquare) as a function of the concentration. The solid line results from our calculation.

The calculation of the concentration dependence of T_C presented in chapter III is based on a more realistic spatial dependence of the matrix polarization. Fig. V.10 shows a comparison between the experimental data and the result of this calculation. The comparison has been made by handling the magnitude of T_C as a parameter. In view of the scatter in the experimental data, we consider agreement between the calculated and experimental concentration dependence satisfactory. Estimates of the ratio between the magnitude of T_C as obtained from eq. V.13 and values obtained from our calculations using eq. III.6 result in a number between 5 and 9 (at $c=0.5$ at.%), which is not contradicted by the experiments.

The fact that the concentration dependence of T_C in the case of Pd-Mn alloys is analogous to that of Pd-Co and of Pd-Fe strongly indicates that the spatial extension of the matrix polarization is also similar, at least at distances larger than 5 \AA . The assumption of a homogeneous polarization, made by Boerstoel et al. (13) in connection with their specific-heat results, is not supported. Since no diffuse neutron scattering experiments have been reported yet, evidence for our conclusion could not be obtained. During completion of this thesis we have started this experiment in collaboration with the "Reactor Centrum Nederland".

V.c.2. The character of the transition.

The onset of magnetic ordering in random dilute alloys is spread out over a wide temperature range in most cases. In the last section of chapter III we discussed the width of the transition and its concentration dependence, and related it to the distance dependence of the interaction between giant moments in Pd.

Since the distribution of g -values, as described in the preceding section, must have its influence on the magnetic ordering, we should focus our attention on Pd-Mn alloys. The increasing width of the transition in these alloys with decreasing concentration is evident from the experimental results presented in chapter II. A comparison with our calculations in chapter III indicates that the model used there overestimates the width of the transition. This is presumably due to the fact that we considered the alloy as a continuum instead of a collection of discrete lattice sites. Nevertheless, the introduction of a distribution of molecular-field coefficients in the W.M.F. model accounts qualitatively for the width of the transition.

On the other hand, comparison between fig. II.24 and fig. IV.1 demonstrates that the pure W.M.F. model, which should be appropriate to more concentrated Pd-Mn alloys, is not able to describe the experimental results. As pointed out by Boerstoeel et al. (13), the ratios between the entropy and energy contents in the temperature ranges below and above T_C is rather remarkable in as much as more energy and entropy is found at $T > T_C$ than predicted by various calculations. This effect increases with decreasing concentration and may indicate that the magnetic ordering of dilute alloys (~ 1 at.%) has a rather low coordination number.

As to the character of the transition of Pd-Co and Pd-Fe alloys, we have to check to what extent the distribution of effective g -values has to be taken into account. In a number of preliminary reports on the present investigation (51,128,135) we used the *macrodistribution* of g -values. This implies that the magnetic moments were assumed to be spatially ordered according to their value of g_{eff} .

The results of this model are in good agreement with the zero- and finite external field specific heat of Pd-Co alloys, as shown in fig. V.11 and V.12. Also qualitative agreement with magnetization results has been obtained as is shown in fig. V.13.

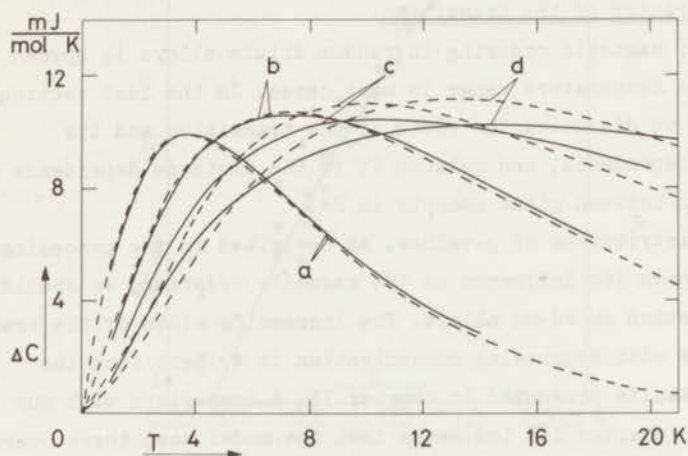


Fig. V.11. The excess specific heat of Pd-Co 0.24 at.%, experimental (—) and calculated (---) curves. The calculated curves have been obtained for $T_C=4.16$ K, $F_G=0.6$ and $H_{mol}(T=0)=10$ kOe. The characters a, b, c and d refer to external magnetic fields of 0, 9, 18 and 27 kOe, respectively.

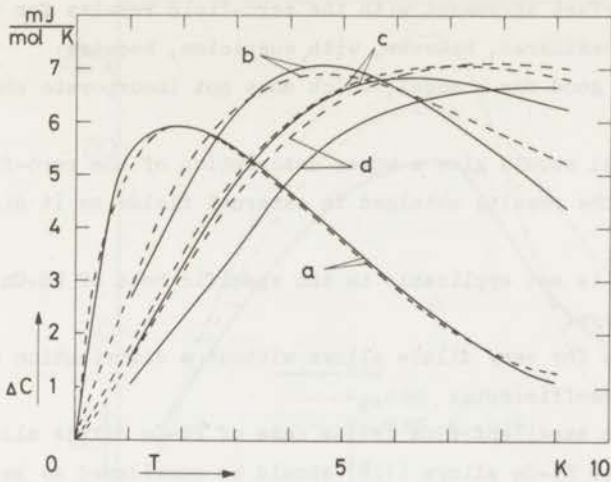


Fig. V.12. The excess specific heat of Pd-Co 0.16 at.%, experimental (—) and calculated (---) curves. The calculated curves have been obtained for $T_C=1.84$ K, $F_G=0.71$ and $H_{mol}(T=0)=6.2$ kOe. The characters a, b, c and d refer to external magnetic fields of 0, 9, 18 and 27 kOe, respectively.

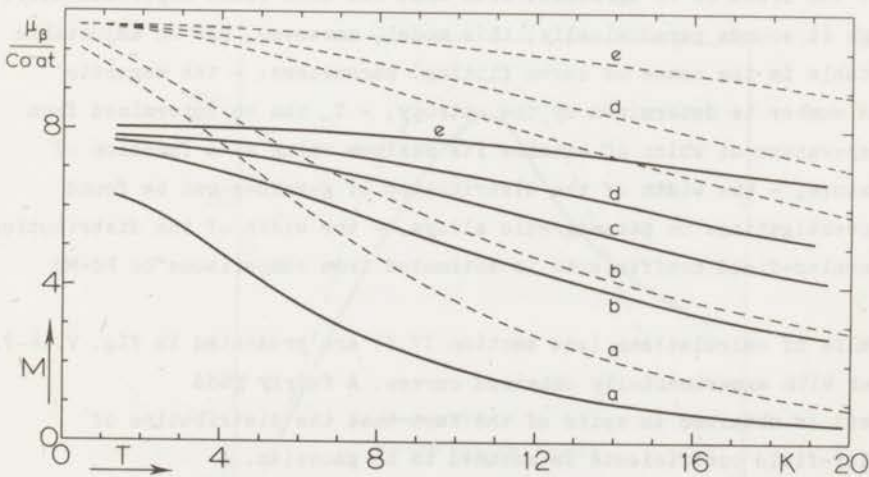


Fig. V.13. Magnetization of Pd-Co 0.24 at.% as a function of temperature. Experimental results (—) and results obtained from a calculation with the same parameters as used for the calculation of the specific heat. The characters a, b, c, d and e refer to external magnetic fields of 1, 9, 18, 27 and 54 kOe, respectively.

The almost perfect agreement with the zero-field results for the specific heat should be considered, however, with suspicion, because:

- the fit is too good for a model, which does not incorporate short-range order;
- The W.M.F. model should give a worse description of the zero-field results than of the results obtained in external fields as it did in the case of Pd-Mn;
- The same model is not applicable to the specific heat of Pd-Co 0.35 at.% and of Pd-Fe alloys;
- The model works for very dilute alloys without a distribution of molecular-field coefficients.

Therefore, the excellent fits in the case of Pd-Co dilute alloys and in the case of dilute Pt-Co alloys (128) should be considered as being fortuitous. We will come back to this point later.

The model involving the *micro*distribution of g -values is more likely to be appropriate to Pd-Co and Pd-Fe alloys. Obviously, an additional distribution of molecular-field coefficients should be applied, since we are dealing with random dilute alloys.

The influence of the various parameters is shown in fig. IV.6 and as is evident the trend is in agreement with what has been found experimentally. Although it sounds paradoxically, this model, moreover, has no adjustable (adjustable in the sense of curve fitting) parameters: - the magnetic quantum number is determined by the entropy, - T_C can be determined from the temperature at which ΔC attains its maximum value as a function of temperature, - the width of the distribution of g -values can be found from investigations on paramagnetic alloys, - the width of the distribution of molecular-field coefficients is estimated from comparisons on Pd-Mn alloys.

Results of calculations (see section IV.f) are presented in fig. V.14-V.16 together with experimentally obtained curves. A fairly good agreement is obtained in spite of the fact that the distribution of molecular-field coefficients is assumed to be gaussian.

The statistical calculation presented in chapter III indicates that this distribution becomes broader and asymmetric at decreasing concentration. Calculations show that application of such a type of distribution enhances the agreement with the experimental results indeed.

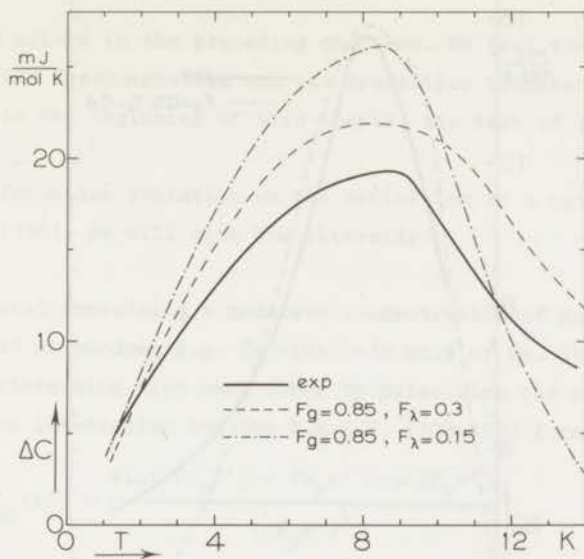


Fig. V.14. The results for ΔC versus T of Pd-Co 0.35 at.% as obtained experimentally by Boerstael (9) together with those of our calculation.

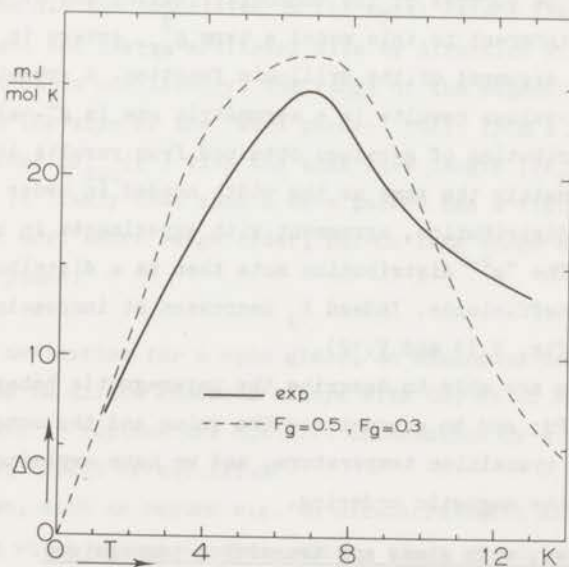


Fig. V.15. Experimental and calculated results for ΔC of Pd-Fe 0.35 at.% as a function of temperature.

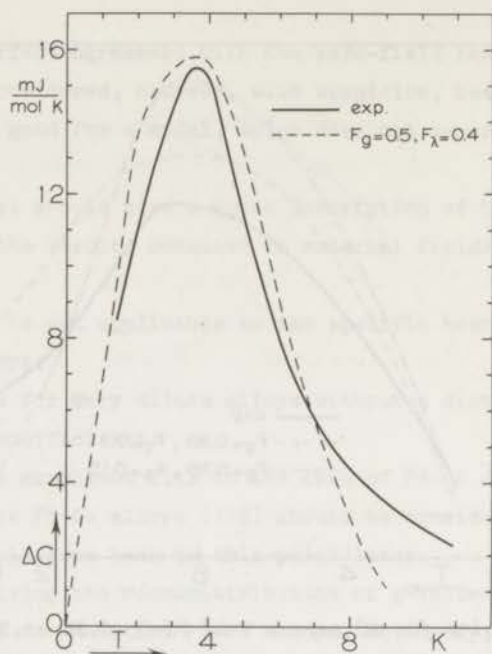


Fig. V.16. Experimental and calculated results for ΔC of Pd-Fe 0.23 at.% as a function of temperature.

Consequently, the success of the *macrodistribution* can be understood. In the equations inherent to this model a term g_{eff}^2 enters in the molecular field part of the argument of the Brillouin function. A symmetric distribution of g -values results in a asymmetric one in g^2 -values. If the width of the distribution of g -values obtained from results in external fields is approximately the same as the width needed in order to get an appropriate " g^2 " distribution, agreement with experiments in zero field may be expected. The " g^2 " distribution acts then as a distribution of molecular-field coefficients. Indeed F_G decreases at increasing concentration (see captions to fig. V.11 and V.12).

Summarizing, we are able to describe the paramagnetic behaviour of Mn, Fe and Co in Pd; and to account for the value and the concentration dependence of the transition temperature, and we have explained qualitatively the character of the magnetic ordering.

V.d. Ferromagnetism, spin glass and transition temperature.

The reader will have certainly remarked that we have not defined the concepts ferromagnetism, spin glass and transition temperature with

regard to dilute alloys in the preceding chapters. We feel that if we had been able to define ferromagnetism and the transition temperature in dilute Pd-based alloys in the beginning of this thesis, the rest of it would have been superfluous.

Let us first focus our attention on the definition of a spin glass as given by Rivier (136). We will cite him literally:

"Consider a metal containing a moderate concentration of magnetic impurities located at random, e.g. Cu with 1-10 at.% of Mn. Those impurities are interacting with each other by polarizing the conduction electrons, and the interaction has the R.K.K.Y. (103-105) form

$$J_{\text{int}}(r') \propto \frac{\sin(2k_F r') - 2k_F r' \cos(2k_F r')}{(2k_F r')^4} \quad (\text{V.14})$$

which is: 1° oscillatory, 2° of infinite range. What sort of magnetic order, if any, do we expect?

To be more specific: the magnetic impurities have statistically independent positions as long as the concentration is sufficiently low. At any point, the effective molecular field is a superposition of contributions from *all* the impurities in the metal (since the interaction has infinite range) and has an arbitrary size or direction since the R.K.K.Y. interaction is oscillatory. The range of the magnetic order corresponds to the size of the 'wave packet' built from a superposition of the contributions $\vec{\mu} J_{\text{int}}(r')$ with the same wave length $(2k_F)^{-1}$ but a random phase. It is likely that such a wave packet has a finite size, i.e. the system has at most short range order, but no long range order. We then have a *spin glass*."

Adopting this definition for a spin glass, an analogous definition for ferromagnetism in dilute Pd-based alloys with Co, Fe or Mn can be given; we only have to replace the R.K.K.Y. interaction by a function as presented in eq. III.5 or eq. III.6:

'Ferromagnetism, such as occurs e.g. in dilute Pd-based alloys, is a magnetic ordering which arises in these alloys since at any point an effective molecular field prevails originating from contributions of all the magnetic moments and having a random magnitude.'

We may call such a ferromagnet a random ferromagnet. Note that in this case the order at $T=0$ is of a long range type (although not uniform), since the interaction is not oscillatory.

The definition of the transition temperature is not that simple, since the transition to ferromagnetism occurs in a wide temperature range due to the random magnitude of the effective molecular field. In fact, we cannot give a model-independent definition; we shall define a mean transition temperature in terms of the molecular-field approximation.

If the magnetization of the i -th single magnetic moment as a function of temperature and magnetic field is given by $M_i = f_i(H, T)$ then the total magnetization is given by $M = \sum_i M_i$. Note that $f_i(H, T)$ is not necessarily a Brillouin function. The molecular field acting in the i -th moment is assumed to be $\xi_i M$. Then, in the molecular-field approximation the magnetization in zero external field can be calculated from

$$M = \sum_i f_i \left(\frac{\xi_i M}{T} \right). \quad (V.15)$$

From eq. V.15 the mean transition temperature can be defined as that temperature at which

$$\left(\frac{\delta}{\delta M} \sum_i f_i \left(\frac{\xi_i M}{T} \right) \right)_{M=0} = 1. \quad (V.16)$$

This definition is in agreement with those given in chapter IV, and obviously reduces to the molecular-field definition of the Curie temperature for a uniform system, for which $\xi_i = \lambda$ and $f_i(x)$ is the Brillouin function.

V.e. Note added in proof.

Just before the finishing of this thesis a number of interesting results of diffuse neutron scattering experiments on Pd-Mn became available. These experiments were carried out in the context of the present investigation in collaboration with De Pater of the metals group and with Van Dijk and other workers of the "Reactor Centrum Nederland" at Petten.

It is not possible to give a complete report on the results of these measurements. Nevertheless a few facts should be given: The measurements were carried out with a crystal spectrometer using neutrons with $\lambda = 2.6 \text{ \AA}$, the alloy was a Pd-Mn 0.25 at.% alloy (KOL 73122), the temperature was about 1.5 K and the magnetic field 10 kOe. The preliminary results confirm

our predictions (and those in ref. 18) about the spatial extension of the giant moment of Mn in Pd.

The first is concerned with the results of the present study on the spatial extension of the giant moment of Mn in Pd. The second is concerned with the results of the present study on the spatial extension of the giant moment of Mn in Pd. The third is concerned with the results of the present study on the spatial extension of the giant moment of Mn in Pd.

The first is concerned with the results of the present study on the spatial extension of the giant moment of Mn in Pd. The second is concerned with the results of the present study on the spatial extension of the giant moment of Mn in Pd. The third is concerned with the results of the present study on the spatial extension of the giant moment of Mn in Pd.

The first is concerned with the results of the present study on the spatial extension of the giant moment of Mn in Pd. The second is concerned with the results of the present study on the spatial extension of the giant moment of Mn in Pd. The third is concerned with the results of the present study on the spatial extension of the giant moment of Mn in Pd.

The first is concerned with the results of the present study on the spatial extension of the giant moment of Mn in Pd. The second is concerned with the results of the present study on the spatial extension of the giant moment of Mn in Pd. The third is concerned with the results of the present study on the spatial extension of the giant moment of Mn in Pd.

The first is concerned with the results of the present study on the spatial extension of the giant moment of Mn in Pd. The second is concerned with the results of the present study on the spatial extension of the giant moment of Mn in Pd. The third is concerned with the results of the present study on the spatial extension of the giant moment of Mn in Pd.

CHAPTER VI

INFLUENCE OF ADDITION OF RH OR AG ON THE BEHAVIOUR OF DILUTE PD-BASED ALLOYS WITH CO, FE OR MN IMPURITIES

VI.a. Introduction.

Susceptibility measurements on Pd-Ag and Pd-Rh alloys (137-140) have shown an increase in the susceptibility compared to that of pure Pd upon alloying with Rh ($c < 5$ at.%) and a decrease upon alloying with Ag. Specific-heat investigations (137, 141-143) revealed qualitatively the same behaviour for the contribution of electrons. As the host susceptibility plays a decisive role in the model of Takahashi and Shimizu (110), the change in the susceptibility provides an opportunity to test this model, if one assumes that the Pd-Rh and Pd-Ag hosts can be described by the same uniform model as Pd itself. Such an assumption has been made by Takahashi and Shimizu.

Unfortunately, the behaviour of Pd-Rh and Pd-Ag alloys is rather complicated. Detailed descriptions and possible explanations may be found in refs. 2 and 12 and in refs. quoted therein. We will restrict ourselves to a brief summary of the experimental results on dilute alloys ($c < 4$ at.%).

The change in the susceptibility measured at room temperature can be

written as $\frac{1}{\chi_0} \frac{d\chi_0}{dc} = 5.2$ %/at.% in the case of Rh and -5.2 %/at.% in the case

of Ag. At $T=4.2$ K these numbers turn out to be 2.8 and -2.8 , respectively.

The change of $\eta(\epsilon_F)$ can be deduced from the change in the contribution of the electrons to the specific heat; one finds, neglecting changes in

the mass enhancement, $\frac{1}{\eta(\epsilon_F)} \frac{d\eta(\epsilon_F)}{dc} = 2.8$ %/at.% in the case of Rh and

-2.8 in the case of Ag. Bearing in mind that $\chi_P = 2\mu_B^2 \eta(\epsilon_F)$ and $\chi_0 = \chi_P(1 - \gamma\chi_P)^{-1}$ the change in the susceptibility can be calculated from these changes in the density of states according to

$$\frac{1}{\chi_0} \frac{d\chi_0}{dc} = (1 - \gamma\chi_P)^{-1} \frac{1}{\chi_P} \frac{d\chi_P}{dc}.$$

The results of this calculation is 28 in the case of Rh and -28 in the case of Ag. Note that these values are not in agreement with the results of susceptibility experiments at room temperature. A better agreement might be obtained if a non-uniform model for the alloys is applied. In spite of these difficulties, and maybe just because of them, an investigation on the influence of Rh and Ag on the properties of magnetic alloys may be worthwhile. In view of the measured susceptibility a decrease of μ and T_C is to be expected upon alloying with Ag and an increase of both values upon alloying with Rh.

This kind of investigation has been carried out by Clogston et al. (32), by Bozorth et al. (144), by Guertin and Foner (81) and by Levy et al. (145). Clogston et al. found μ and T_C of Pd-Co and of Pd-Fe alloys to decrease with increasing concentration of Ag. Bozorth et al. investigated Pd-Co 1 at.% alloys and Pd-Fe 1 at.% alloys as a function of the addition of Rh, Ag and Cu. They found that the magnetic moment associated with Co or Fe as well as the transition temperature decreases upon addition of either of the three elements Rh, Ag or Cu. Note that this observation contradicts the prediction by Takahashi and Shimizu (110) that T_C should be proportional to the host susceptibility.

Guertin and Foner (81) measured the saturation moment of Fe in various base materials; they found μ to decrease upon addition of Ag to Pd and also upon addition of Rh to Pd. Clearly, they did not find the induced moment to be proportional to the host susceptibility.

Levy et al. (145) investigated Pd-Fe 1 at.% alloys with several amounts of Ag (up to 50 at.%) by means of the Mössbauer effect. Their results demonstrate that the transition temperature varies linear with the host susceptibility. The authors conclude that these results are in agreement with the calculations by Takahashi and Shimizu (110) and by Kim (102). However, this conclusion is ill-founded and should be discarded, since these calculations predict T_C to be *proportional* to the host susceptibility, not only to *vary linear* with it. The results of Levy et al. (145) certainly do not show such a *proportionality*.

VI.b. Results.

Results of resistivity measurements on Pd-Mn 1 at.% alloys with Ag (KOL 7035, KOL 7150, KOL 7151 and KOL 7152) are presented in fig. VI.1. In order to be sure about the equal amount of Mn in the specimens, the three

specimens with Ag have been prepared from a Pd-Mn 1 at.% master alloy. No difference in the Mn content of these specimens could be detected from chemical analysis. As can be deduced from the figure, T_C decreases

with increasing concentration of Ag; $\frac{1}{T_C} \frac{dT_C}{dc} = -18 \%/at.\%$. This decrease

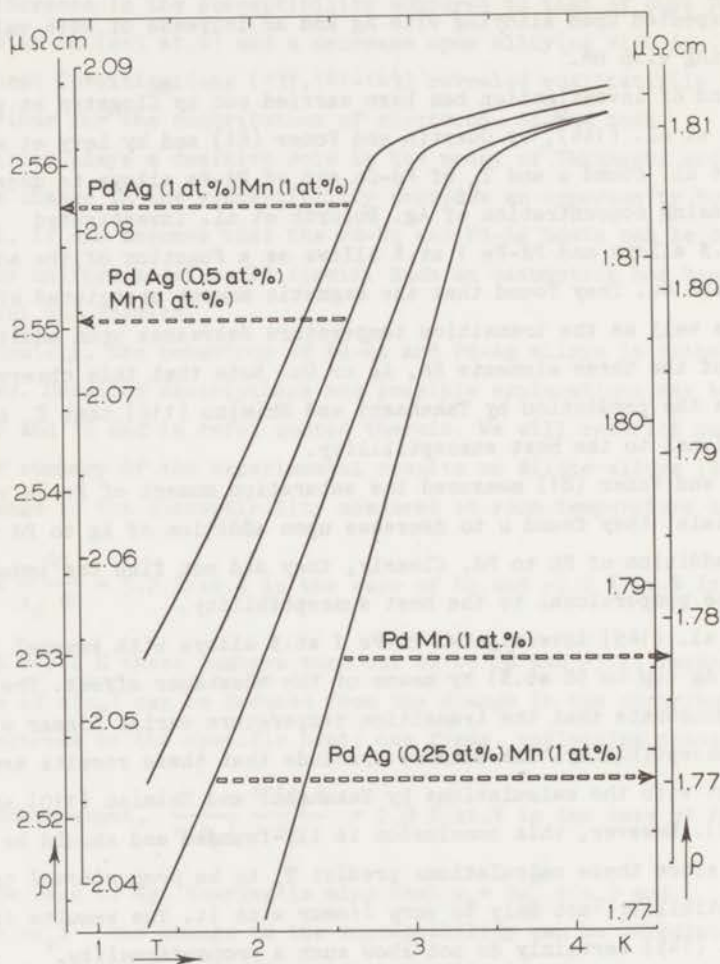


Fig. VI.1. Electrical resistivity of Pd-Mn 1 at.%, of Pd-Ag(0.25 at.%) - Pd-Ag(0.25 at.%) - Mn(1 at.%), of Pd-Ag(0.5 at.%) - Mn(1 at.%) and of Pd-Ag(1 at.%) - Mn(1 at.%) plotted versus temperature. (Note the different vertical scales.)

is more than three times as large as the decrease of the host susceptibility. Thus no proportionality between T_C and χ_0 has been found.

Resistivity results on ternary Pd-Rh-Mn alloys (KOL 73078-73081 and KOL 73101-73104) are shown in figs. VI.2 and VI.3. Concentrations are indicated in the graphs. From these figures the remarkable effect can be deduced that T_C is hardly increased by small amounts of Rh, and beyond 1 at.% decreases rapidly (-13 %/at.%) with increasing Rh concentration up to 6 at.%. Thus in the case of Rh as well, T_C is not found to be proportional to the host susceptibility. The transition to ferromagnetism becomes much broader at increasing Rh concentration. Such a broadening has not been observed in the case of Ag, however the amount of Ag did not exceed 1 at.%. The observations described above and summarized in table VI.I are in qualitative agreement with those reported in the literature.

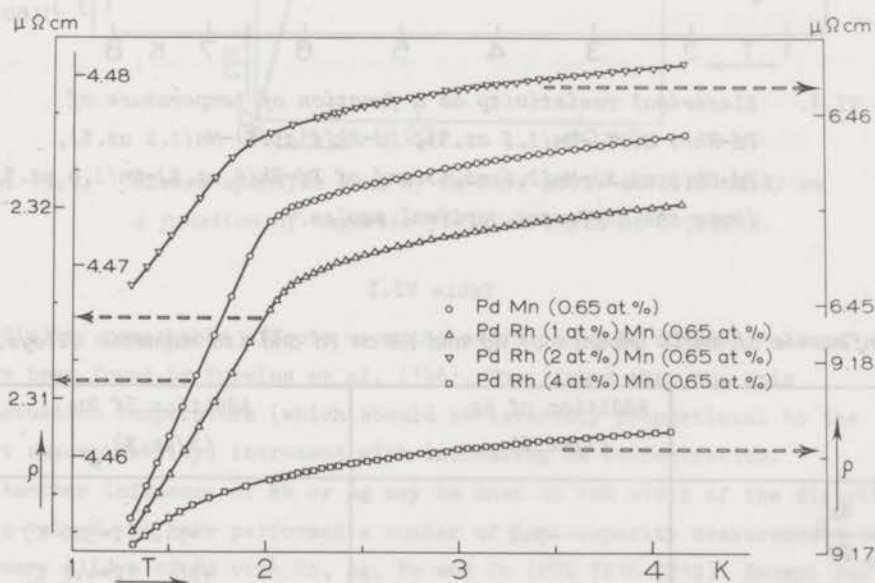


Fig. VI.2. Electrical resistivity as a function of temperature of Pd-Mn 0.65 at.%, Pd-Rh(1 at.%) - Mn(0.65 at.%), Pd-Rh(2 at.%) - Mn(0.65 at.%) and of Pd-Rh(4 at.%) - Mn(0.65 at.%). (Note the different vertical scales.)

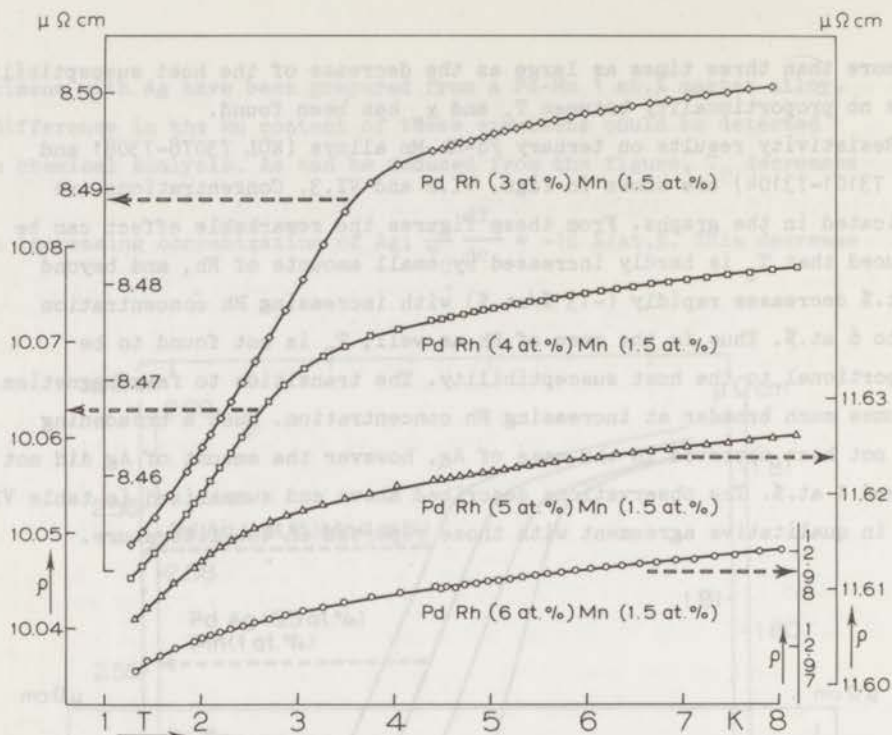


Fig. VI.3. Electrical resistivity as a function of temperature of Pd-Rh(3 at.%) - Mn(1.5 at.%), Pd-Rh(4 at.%) - Mn(1.5 at.%), Pd-Rh(5 at.%) - Mn(1.5 at.%) and of Pd-Rh(6 at.%) - Mn(1.5 at.%). (Note the different vertical scales.)

Table VI.I

Influence of small amounts of Ag and Rh on Pd and its magnetic alloys.

	Addition of Ag (%/at.%)	Addition of Rh (%/at.%)
$\frac{1}{\chi_0} \frac{d\chi_0}{dc}$	-5.2	+5.2 (T=300 K) +28 (T=4.2 K)
$\frac{1}{\eta(\epsilon_F)} \frac{d\eta(\epsilon_F)}{dc}$	-2.8	+2.8
$\frac{1}{T_C} \frac{dT_C}{dc}$	-18	-13 (c>1 at.%)

A measurement of the heat capacity as a function of external magnetic field on Pd-Rh(6 at.%) - Mn(0.16 at.%) (KOL 73119), presented in fig. VI.4, yielded a normal, Schottky-like, behaviour with a value for g_{eff} only 5 % smaller than in the case of Pd-Mn 0.2 at.%. Magnetization measurements on Pd-Ag(1 at.%) - Mn(1 at.%), carried out by Star, showed only a slight decrease of μ relative to Pd-Mn.

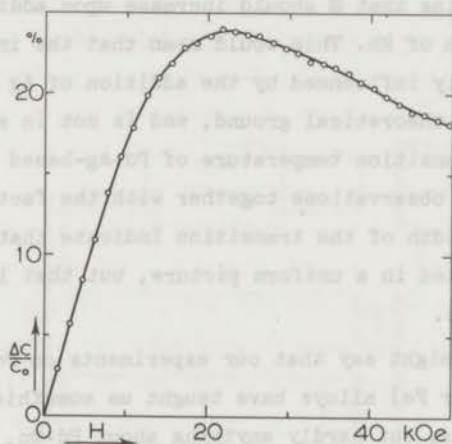


Fig. VI.4. Excess specific heat of Pd-Rh(6 at.%) - Mn(0.16 at.%) as a function of magnetic field strength at $T=3.46$ K.

Similar remarkable effects upon the addition of Rh to Pd-Ni alloys have been found by Purwins et al. (146). They found that the spin fluctuation temperature (which should be inversely proportional to the host susceptibility) increased with increasing Rh concentration.

Another influence of Rh or Ag may be that on the width of the distribution of g -values. We have performed a number of heat-capacity measurements on ternary alloys of Pd with Rh, Ag, Fe and Co (KOL 7216-7219). Except for a small change in the field dependence, due to the change in the magnetic moment, and a change in T_C , no remarkable effects have been observed within experimental accuracy. Also a.c. heat-capacity measurements on alloys with a very small amount of magnetic impurities (KOL 73110-73113) did not reveal a difference in the width of the distribution of g -values beyond the experimental error.

VI.c. Discussion.

Evidently, addition of Rh strongly influences the interactions between the giant moments. However, the change in the host susceptibility cannot account for this influence. The same pertains to the case of Ag, since the decrease of T_C is much larger than the decrease of the susceptibility. Since $J_{int}(r) \propto \exp\{-2k_F r / (S/3)^{1/2}\}$ we may assume that a change of the Stoner enhancement factor, S , should account for the behaviour of T_C . If this is the case, the change in S should also account for the magnetic susceptibility, implying that S should increase upon addition of Ag and decrease upon addition of Rh. This would mean that the interaction parameter γ is strongly influenced by the addition of Ag or Rh, which is not to be expected on theoretical ground, and is not in agreement with the results of the transition temperature of Pd-Ag-based alloys.

We feel that these observations together with the fact that addition of Rh increases the width of the transition indicate that Pd-Ag and Pd-Rh alloys cannot be treated in a uniform picture, but that local effects play an important role.

In conclusion, we might say that our experiments on Pd-Rh-Mn (Co or Fe) and on Pd-Ag-Mn (Co or Fe) alloys have taught us something about Pd-Rh and about Pd-Ag alloys, but hardly anything about Pd-Mn, Pd-Fe or Pd-Co alloys. Therefore, a detailed analysis is beyond the scope of this thesis.

(A) To study the effect of the frequency of the alternating current on the rate of the reaction between the hydrogen and the oxygen. The rate of the reaction was measured by the volume of gas evolved in a fixed time. The results are shown in Table I.

(B) To study the effect of the concentration of the hydrogen on the rate of the reaction. The rate of the reaction was measured by the volume of gas evolved in a fixed time. The results are shown in Table II.

(C) To study the effect of the concentration of the oxygen on the rate of the reaction. The rate of the reaction was measured by the volume of gas evolved in a fixed time. The results are shown in Table III.

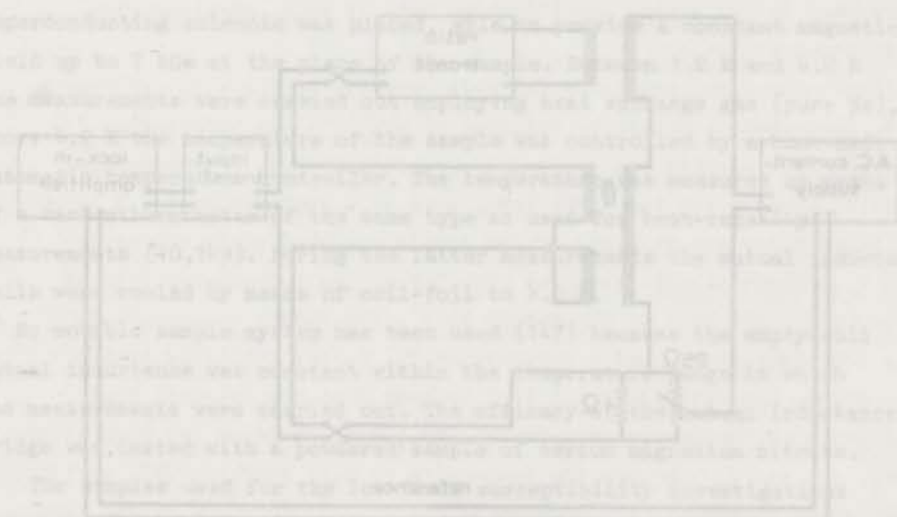


Fig. 1. Schematic diagram of the apparatus used for the study of the reaction between hydrogen and oxygen.

A constant current supply of constant voltage (varied from 10 mA) operating at a frequency of 50 Hz provided the primary current. The standard solution of 10 M was used as an electrolyte. The rate of the reaction was measured by the volume of gas evolved in a fixed time. The results are shown in Table I.

(*) Some of the experiments will be mentioned in the text.

APPENDIX 1.

APPARATUS FOR THE MEASUREMENT OF LOW-FIELD SUSCEPTIBILITY.

(G.E.L. van Vliet)⁺

The susceptibility was measured by means of a mutual inductance method, generally used for the temperature measurements below 1 K, but as was shown by Canella (147) also very suitable for examining dilute magnetic alloys. The mutual inductance bridge used in this experiment is quite similar to that described by Maxwell (148); a circuit diagram is shown in fig.A.1.1.

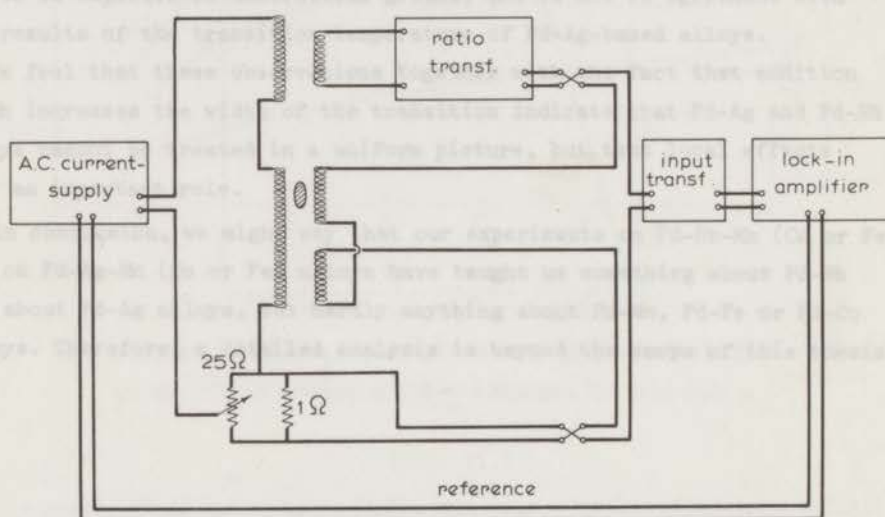


Fig. A.1.1. Circuit diagram for low-field susceptibility measurements.

A home-made current supply of constant amplitude (maximal 10 mA) operating at a frequency of 210 Hz provided the primary current. The standard mutual inductance of 10 mH was wound on an evacuated glass tube, which could be cooled with liquid nitrogen in order to decrease the resistance of the coils.

⁺) Names of the collaborators will be mentioned between brackets.

The secondary voltage was fed into a ratiotransformer (E.S.I., type DT 72 A). The primary and secondary coils in the cryostat were wound around an ebonite cylinder. The sample, which had the shape of a foil parallel to the magnetic field of the primary coil, was kept in place by a pure copper fork, serving also for controlling the temperature of the sample. As a null-detector a phase sensitive voltmeter (Automatic Systems Lab., type 1100) was used connected to the secondary circuit via an input-transformer (P.A.R., type AM 1). Applying this input-transformer the null-detector had a sensitivity of 10^{-8} volt.

The cryostat mutual inductance and the sampleholder were placed in a vacuumvessel immersed in liquid helium. The vacuumvessel was the same as that used for the resistance measurements. Around this vessel a superconducting solenoid was placed, able to provide a constant magnetic field up to 7 kOe at the place of the sample. Between 1.2 K and 4.2 K the measurements were carried out employing heat exchange gas (pure He), above 4.2 K the temperature of the sample was controlled by a home-made automatic temperature controller. The temperature was measured by means of a carbonthermometer of the same type as used for heat-capacity measurements (10,149). During the latter measurements the mutual inductance coils were cooled by means of coil-foil to 4.2 K.

No movable sample system has been used (147) because the empty-coil mutual inductance was constant within the temperature range in which the measurements were carried out. The efficacy of the mutual inductance bridge was tested with a powdered sample of cerium magnesium nitrate.

The samples used for the low-field susceptibility investigations were cut from the same ingot from which the wires were drawn for the resistance measurements as reported in chapter II.

APPENDIX 2

THE A.C. SYSTEM FOR HEAT-CAPACITY MEASUREMENTS

(J. Turenhout and J.F. Benning)

Heat-capacity data can be obtained, using the conventional d.c. or adiabatic technique (10), with an error of 0.5 %. In order to obtain the contribution of the impurities to the specific heat of alloys, the heat capacity of the host metal has to be subtracted from the measured value (see also section II.c.1). In the case of very dilute alloys the contribution of the impurities may even amount to 5 % only. Consequently, the accuracy in the excess specific-heat data is poor, particularly at high temperatures.

Another method for measuring the heat capacity is the a.c. calorimetry method, described in detail by Sullivan et al. (150). In this method the sample is connected via a thermal conductance κ_b to a temperature reservoir, usually the liquid-He bath, kept at a temperature T_b . A heater and a thermometer are attached to the sample via heat conductances κ_h and κ_{th} , respectively. The heat capacity of the thermometer will be denoted by C_{th} and that of the heater by C_h . The sample is assumed to have a heat capacity C_s and a temperature T_s . In the following analysis of the method the simplification will be made that the internal heat conductances of the sample, the heater and the thermometer are much larger than κ_b , κ_{th} and κ_h . Through the heaterwire an a.c. current, $I = I_0 \cos(\omega t/2)$, is led, which causes: 1) an increase of the mean temperature of the sample, \bar{T}_s , such that $\kappa_b (\bar{T}_s - T_b)$ equals the amount of heat dissipated per second in the heater; 2) a temperature oscillation with frequency ω and mean temperature \bar{T}_s . When the amount of heat dissipated per second in the heater is denoted by $\dot{Q} = \dot{Q}_0 \{\cos(\omega t/2)\}^2$, the temperature T_s will be given according to Sullivan et al. (150) by

$$T_s = T_b + \frac{\dot{Q}}{2} \left\{ \frac{1}{\kappa_b} + \frac{1}{\omega C} \left[1 + \frac{\tau_{th}^2 + \tau_h^2}{\tau_s^2} + \frac{1}{\omega^2 \tau_s^2} + \omega^2 \left(\tau_h^2 + \tau_{th}^2 + \frac{\tau_{th}^2 \tau_h^2}{\tau_s^2} \right) + \omega^4 \tau_{th}^2 \tau_h^2 \right]^{-\frac{1}{2}} \cos(\omega t - \phi) \right\}, \quad (A.2.1.)$$

wherein $C = C_S + C_h + C_{th}$, $\tau_S = C_S / \kappa_b$, $\tau_{th} = C_{th} / \kappa_{th}$ and $\tau_h = C_h / \kappa_h$.

Considering the a.c. part of eq. A.2.1 it can be seen that the amplitude of the temperature oscillation is proportional to C^{-1} when $\omega^2(\tau_{th}^2 + \tau_h^2) \ll 1$ and $\omega^2 \tau_S^2 \gg 1$. It should be noted that in this case the other correction terms are even less important. The first condition means that the sample, the heater and the thermometer should come into thermal equilibrium in a time much shorter than the inverse of the heating frequency, and requires that the heater and the thermometer have a very small heat capacity and are closely coupled to the sample. The second condition implies that the coupling to the temperature reservoir should be slower than the inverse of the heating frequency, so that the temperature oscillations are not damped out by the leak to the reservoir. This condition is equivalent to the condition that the temperature oscillations should be much smaller than $\bar{T}_S - T_D$.

Assuming these conditions to be fulfilled, this method enables us to measure the heat capacity of the sample at the temperature \bar{T}_S as a function of e.g. an external magnetic field. Relative to e.g. the zero-field heat capacity this can be done with a random error of 0.2 %. Absolute measurements of the heat capacity, however, require measurements of a low frequency a.c. voltage, which cannot be carried out with great accuracy. Therefore, for absolute measurements the adiabatic method prevails.

On the other hand the a.c. method provides an exciting opportunity in the case of very dilute alloys. These alloys have a zero-field heat capacity almost equal to that of the host metal, a value known from adiabatic measurements (77). The change in the heat capacity of these alloys due to an external magnetic field may amount to 5 to 20 % of the zero-field value, which variation can be determined by the a.c. technique. Another advantage of this relative method is that, if an error is introduced by neglecting the correction terms in eq. A.2.1, this error will vary only slightly with the magnetic field. Also the phase angle ϕ of the a.c. signal is giving no rise to problems, since ϕ varies only by 1 % for a change in the heat capacity of 20 %.

As an example, it may be worthwhile to give the conditions under which a 20 grams single crystal of Pd-Fe 0.1 at.% has been investigated. The heat capacity of this sample was 9 mJ/K at 3.5 K and the thermal conductance of the link to the liquid-He bath was 3×10^{-3} W/K, so that τ_S became 3 s. The relaxation times of the thermometer and of the heater were

approximately 0.03 s, and $\omega/2\pi$ was 5.5 Hz. Then the correction terms are estimated to be

$$\frac{1}{\omega^2 \tau_S^2} \approx 7 \times 10^{-4} \quad \text{and} \quad \omega^2 (\tau_h^2 + \tau_{th}^2) \approx 0.01 \quad (\text{A.2.2})$$

It should be noticed that the second correction is not influenced by the heat capacity of the sample nor by the heat conductance of the link to the bath. When the temperature of the bath is 1.2 K a heat input of 9 mW is causing a temperature oscillation with an amplitude of 15 mK compared to a temperature difference between sample and bath of 2 K.

The electronics.

In fig. A.2.1 a circuit diagram is shown of the electronics of the system. A function generator (Philips, type PM 5168) acts as a source for the heater. The function generator is connected to the heater circuit via a home-made amplifier in order to match the impedance. The null detector of the d.c. Wheatstone bridge containing the thermometer was a high impedance voltmeter (Fluke, 845 A.B.). The a.c. temperature oscillation was detected by means of a lock-in amplifier (P.A.R. type 126)

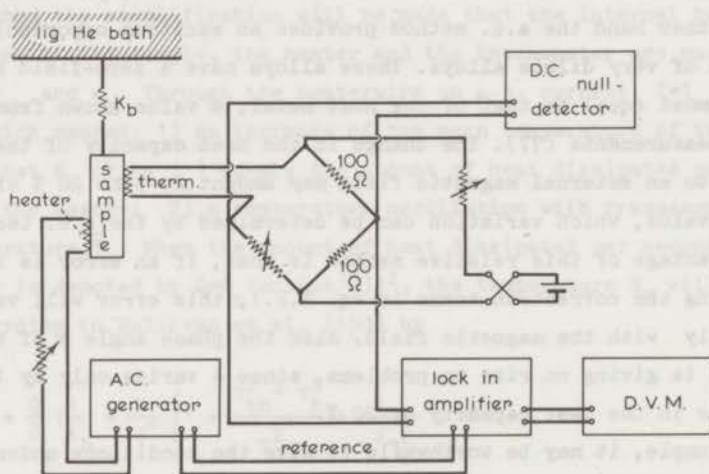


Fig. A.2.1. Circuit diagram for a.c. heat-capacity measurements.

connected to the Wheatstone bridge via a high impedance preamplifier (P.A.R., type 225, input impedance = 100 M Ω). The variable arm of the Wheatstone bridge is formed by a decade box (E.S.I., type DB 645 A ohmsupply). The output of the lock-in amplifier was fed into a digital voltmeter (Solartron, type LM 1619) making the reading of the output more convenient.

The cryotechnical set-up.

In the case of the investigation of single crystals the same cryostat assembly and iron-core magnet has been used as for the adiabatic heat-capacity measurements (10). The direction of the external magnetic field could be varied over an angle of 120°. During the search for anisotropy of the heat capacity in external fields data were taken at constant temperature and constant field strength as a function of the field direction, so that the full advantage of the a.c. method could be achieved. The success of this investigation (although with a negative result for the anisotropy) initiated the building of a new cryostat for measurements in magnetic fields up to 50 kOe.

A sketch of this cryostat assembly is shown in fig. A.2.2. The magnetic field was provided by a superconducting coil from Oxford Instruments Ltd., which firm also furnished the outer dewar. The coil has a core of 25 mm. The inner dewar was home-made from stainless steel; it can contain about one liter of liquid He enough to keep the cryostat at 1.2 K for about 10 hours.

The current supply, its programming unit and its protecting unit (sensing the level of the liquid He and the voltage over the coil) were built by the "Laboratorium voor Instrumentele Electronica". The instability of the current supply was less than 2 ppm. The sampleholder, drawn in fig. A.2.3, was made from photosensitive printed circuitry board (Nelco). The heat link to the bath was part of the sampleholder, so that the heat conduction could easily be dimensioned by properly choosing the length and the width of the path on the board. The heat conductance of such a copper strip was measured separately following the method of de Jong and Gubbens (151). The result of this measurement is shown in fig. A.2.4.

The specimens used for these heat-capacity measurements were cylinders with a height and a diameter of approximately 7 mm. The specimen was

glued to the sampleholder with bison kit (Perfecta Chemie B.V., Goes, Holland) (152). For this purpose bison kit was diluted 1:3 by bison kit thinner. The glue has been dried for at least 12 hours at 60°C. The heater consisted of 1 m of constantan wire with a diameter of 0.03 mm and a resistance of 750 Ω , bifilarly wound on the sample and glued to it with bison kit for better heat contact.

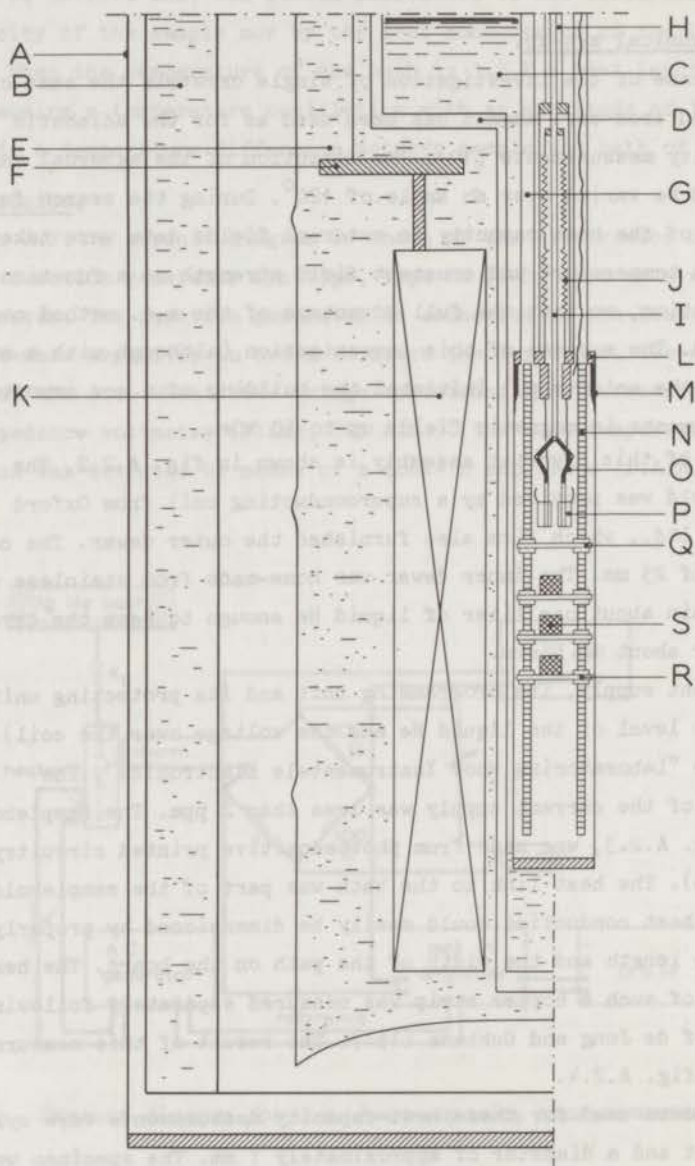


Fig. A.2.2. Cryostat assembly for a.c. heat-capacity measurements.

The meaning of the letters is: A outer vacuum vessel, B liquid N_2 , C liquid He at 1.2 K, D vacuum space of inner dewar, E liquid He at 4.2 K, F magnet support, G pumping line, H coaxial aligning tube, I heat-switch control tube, J bellows, K magnet solenoid, L lid of inner vacuum vessel, M Wood's solder joint, N support for sampleholders, O heat switch for adiabatic heat-capacity measurements, P gold plated copper jaws, Q brass ring for sample support for adiabatic heat-capacity measurements, R sampleholders, S samples.

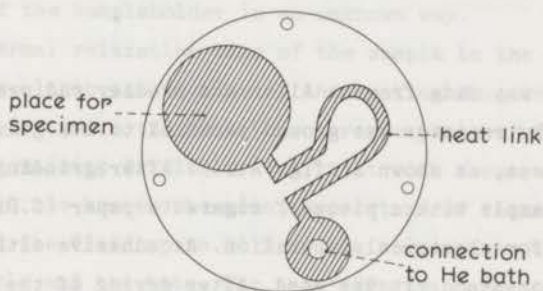


Fig. A.2.3. Sampleholder for a.c. heat-capacity measurements.

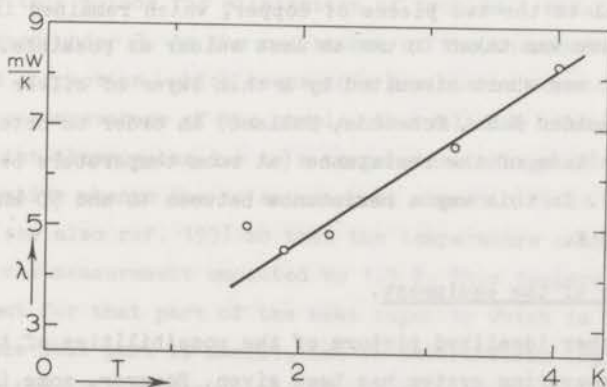


Fig. A.2.4. Heat conductivity of copper strip as a function temperature.

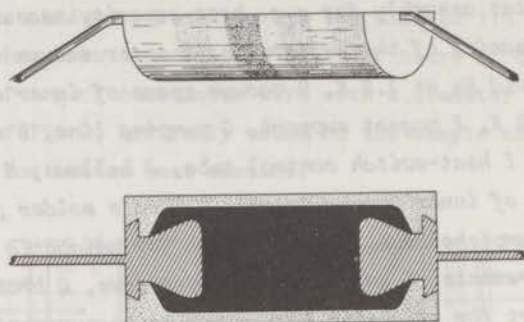


Fig. A.2.5. Thermometer for a.c. heat-capacity measurements.

The thermometer was made from an Allen and Bradley radioresistor of 330Ω , $1/8$ W. The resistor was ground parallel to its geometric axis to half its thickness, as shown in fig. A.2.5. After grinding the resistor was glued to the sample with a piece of cigarette paper (S.D. Modiano, Italy) in between for electrical insulation. As adhesive either G.E. varnish type 7031 or bison kit was used. After drying of the adhesive the resistor was ground as far as possible parallel to the surface of the sample, so that only a very thin layer of the resistor remained on the sample. The average thickness of the thermometers was 0.02 mm. The electrical leads (constantan wire of 0.05 mm diameter) were soldered with Wood's metal to the two pieces of copper, which remained in the carbonlayer. Care was taken to use as less solder as possible. A part of the thermometer was short circuited by a thin layer of silver paint (DAG 1415, Colloiden N.V., Scheenda, Holland) in order to obtain a convenient magnitude of the resistance (at room temperature between 500 and 2000Ω). In this way a resistance between 10 and 50 k Ω was obtained at 3.5 K.

The performance of the equipment.

So far a rather idealized picture of the possibilities of the a.c. heat-capacity measuring system has been given. However, some important experimental problems remained. These were the magnetic field dependences of : 1) the heat conductance of the link to the bath; 2) the resistance

of the heater; 3) the resistance of the thermometer; 4) the temperature derivative of the resistance of the thermometer. Fortunately the heat contact of the heater and the thermometer to the sample appeared to give no rise to problems, for the a.c. signal was within 1 % proportional to ω^{-1} in the range of $\omega/2\pi=2.7$ Hz to $\omega/2\pi=20$ Hz. From test measurements of the field dependence of the heat capacity of pure Pd and from separate measurements of the heat conductance of copper it was found that the first problem was the largest; field dependences up to 20 % in a field of 50 kOe were determined. Although it was possible to decrease this field dependence by application of a less pure material (e.g. brass) for the heat link, this possibility was deleted because in that case the heat link had to be quite thick, which would seriously increase the heat capacity of the sampleholder in an unknown way.

Since the thermal relaxation time of the sample to the He bath was chosen much larger than the inverse of the heating frequency, the 20 % change does not influence the amplitude nor the phase of the a.c. signal. Therefore, the remaining difficulty was, that with a current of constant amplitude through the heater the mean temperature of the sample changes as a function of the field up to 20 % of the temperature difference between the sample and the bath. For this effect a correction was made by adjusting the current through the heater at each value of the magnetic field in such a way, that the resistance of the thermometer remained the same. Afterwards the results for the measured a.c. voltage were corrected for these changes in the heater current.

A choice of this method for elimination of problem 1 reduces this to that mentioned under 3. As the resistance of the thermometer depends on the field a correction, which keeps this resistance constant, causes a change in the temperature of the sample. The relative change in the resistance of the thermometer due to a temperature change of 1 K is about 200 %, the relative change due to an external magnetic field of 50 kOe is about 3 % (see also ref. 153) so that the temperature change of the sample during the measurement amounted to 1.5 %. This temperature variation is not important for that part of the heat capacity which is field dependent (since this part is small), but is nevertheless important because of the temperature dependence of the heat capacity in zero field.

It is possible to correct for this effect and for the problems 2, 3 and 4 by a careful calibration of the thermometer and a measurement of the resistance of the heater as a function of temperature and magnetic field. Since the accuracy of the thermometer calibration still gave some trouble this way of correction has not been used. On the contrary an "experimental" method was applied. The starting points of this method were: 1. for each specimen measured the same type of thermometer was used; 2. all specimens were dilute Pd-based alloys, so that the temperature dependence of the zero-field specific heat was approximately the same as that for pure Pd; 3. for all heaters mounted on the specimens the same batch of constantan wire was used. Therefore, it seems reasonable to measure the apparent field dependence of the specific heat of pure Pd. From magnetization measurements and from a specific-heat measurement by Boerstoeel et al. it is known that the specific heat of pure Pd is independent of an external magnetic field up to at least 50 kOe. The result of this measurement on pure Pd was used to correct the results on the alloys. For fields up to 22 kOe two separate Pd specimens have been measured. The results were in agreement within the random experimental error, so that this "experimental" method may be considered to be correct within 0.5 %.

The determination of the heat capacity of the sampleholder, the heater and the thermometer and the testing of the equipment were carried out by investigating the field dependence of the heat capacity of a Pd-Mn 0.2 at.% sample (KOL 73118) of which the specific heat is accurately known from adiabatic measurements by Boerstoeel et al. (13). The result of this measurement is shown in fig. A.2.6. It appeared that the heat capacity of the sampleholder was about 0.03 mJ/K at 3.4 K, thus about 3 % of the total heat capacity.

Besides the problems mentioned before, which are inherent with the a.c. method, there are two external sources of error: 1. the long term stability of the amplitude of the function generator (the frequency stability turned out to be better than 0.01 %); 2. the long term stability and the linearity of the preamplifier (P.A.R. 225) and of the lock-in amplifier (P.A.R. 126). Certainly these deficiencies of the electronic system give rise to an additional error in the final results.

From what is mentioned before it can be concluded that the systematic error in the a.c. measurement is still larger than the random error.

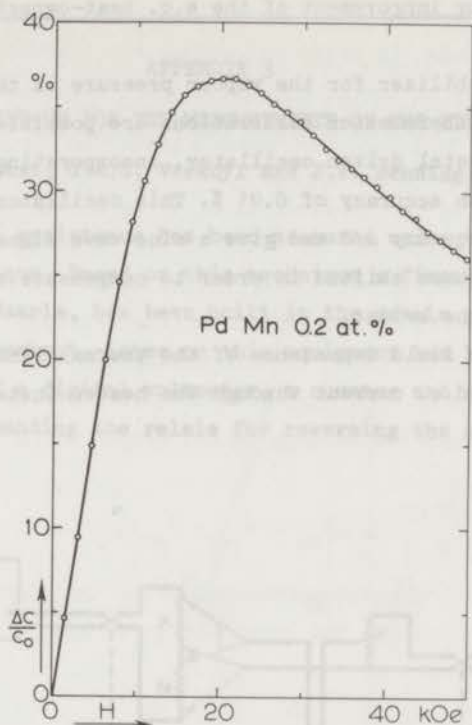


Fig. A.2.6. Excess specific heat of Pd-Mn 0.2 at.% at 3.46 K as a function of the external magnetic field.

Unfortunately it was not possible to improve the performance of the system within the course of the present work. On the other hand this improvement was not that necessary, since our aim with the equipment was:

1. looking for magnetic anisotropy of the samples, in which case a lot of errors should be eliminated by measuring at constant temperature and constant field strength ;
2. examination of the agreement between the results of the measurements of the heat capacity as a function of temperature at constant external field and those of measurements of the heat capacity as a function of the field at constant temperature. In this case the accuracy of the results was determined by the error in the adiabatic measurements.

Three suggestions for improvement of the a.c. heat-capacity measuring equipment.

1. Building of a stabilizer for the vapour pressure in the inner dewar, so that accurate thermometer calibrations are possible.
2. Building of a crystal driven oscillator, incorporating an amplitude stabilizer with an accuracy of 0.01 %. This oscillator should power the heater at frequency $\omega/2$ and give a sine-wave signal with frequency ω , which can be phase shifted in order to compensate the a.c. signal from the Wheatstone bridge.
3. Correction of the field dependence of the thermal link to the bath by an additional d.c. current through the heater instead of adjusting the a.c. current.

APPENDIX 3

EXPERIMENTAL SET-UP FOR THE MEASUREMENTS OF THE ELECTRICAL RESISTANCE

(G.E.L. van Vliet, J.A.G. Verkuyl and J.F. Benning).

The electrical resistance has been measured using the conventional four-probe technique. Based on this technique a first-rate equipment, designed by Van Baarle, has been built in the metals group by Star, De Vroede and Turenhout. Later on this equipment has been automatized by application of a digital voltmeter, a counter and a pulse generator, the last one commanding the relays for reversing the currents.

The electronics.

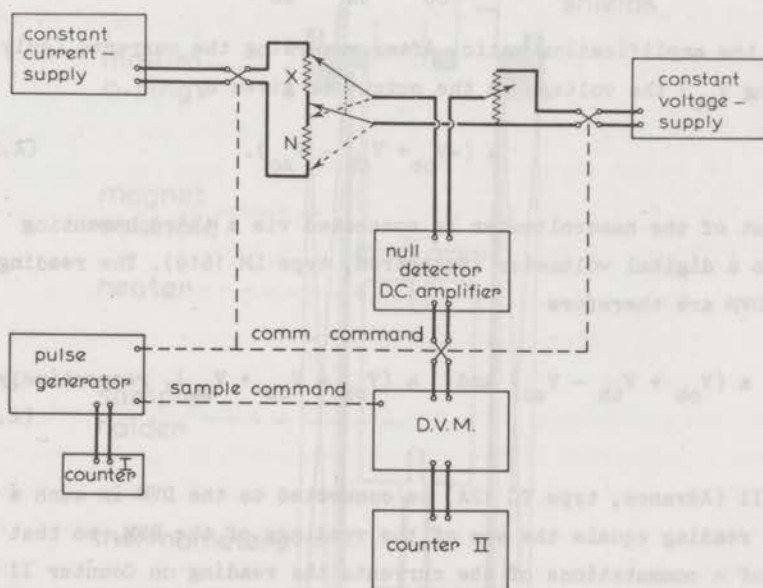


Fig. A.3.1. Circuit diagram for the measurements of the electrical resistance.

Fig. A.3.1 shows a circuit diagram of the set-up. The constant current supply, providing the current through the sample, has been built by Electhermo. The constant voltage supply, powering the nanopotentiometer (Guildline, type 9176), has been obtained from the

"Laboratorium voor Instrumentele Electronica". Both powersupplies have a stability within 2 ppm. In order to reverse the current through the sample and the voltage on the nanopotentiometer, mercury-wetted relais (Clare, type HG 50045) have been used. The nulldetector of the system is a nanovoltmeter (Keithly, type 147) with a linearity within 1 %. This d.c. amplifier has the possibility of using a zero off-set, so that thermoelectricpower in the circiut could be compensated.

The measurements are carried out by adjusting the potentiometer to such a value that a small out-of-balance voltage (usually less than 0.5 μ V) can be read on the nulldetector. If this voltage, due to the out-of-balance adjustment, is denoted by V_{ob} , the thermoelectricpower by V_{th} and the zero offset by V_{zo} , then the voltage on the output of the nulldetector is given by

$$a (V_{ob} + V_{th} - V_{zo}), \quad (A.3.1)$$

a being the amplification ratio. After reversing the currents (only effecting V_{ob}) the voltage on the output is given by

$$a (-V_{ob} + V_{th} - V_{zo}). \quad (A.3.2)$$

The output of the nanovoltmeter is connected via a third commuting relais to a digital voltmeter (Solartron, type LM 1619). The readings on this DVM are therefore

$$a (V_{ob} + V_{th} - V_{zo}) \text{ and } a (V_{ob} - V_{th} + V_{zo}), \text{ respectively.} \quad (A.3.3)$$

Counter II (Advance, type TC 12A) is connected to the DVM in such a way that its reading equals the sum of the readings of the DVM, so that at the end of n commutations of the currents the reading on Counter II is given by

$$\frac{n}{2} a (2 V_{ob}), \quad (A.3.4)$$

from which an average value of aV_{ob} is calculated.

From a calibration of aV_{ob} versus the out-of-balance value of the nanopotentiometer the original out-of-balance adjustment is corrected. Using this equipment, measurements of the electrical resistance can be carried out with an inaccuracy of less than a few ppm in an easy way.

The cryotechnical set-up.

For the measurements of the electrical resistance a simple cryostat as drawn in fig. A.3.2 has been built. The cryostat consists of a vacuum vessel sealed by an Indium O-ring, surrounded by a superconducting solenoid able to give a magnetic field up to 7 kOe. The solenoid was

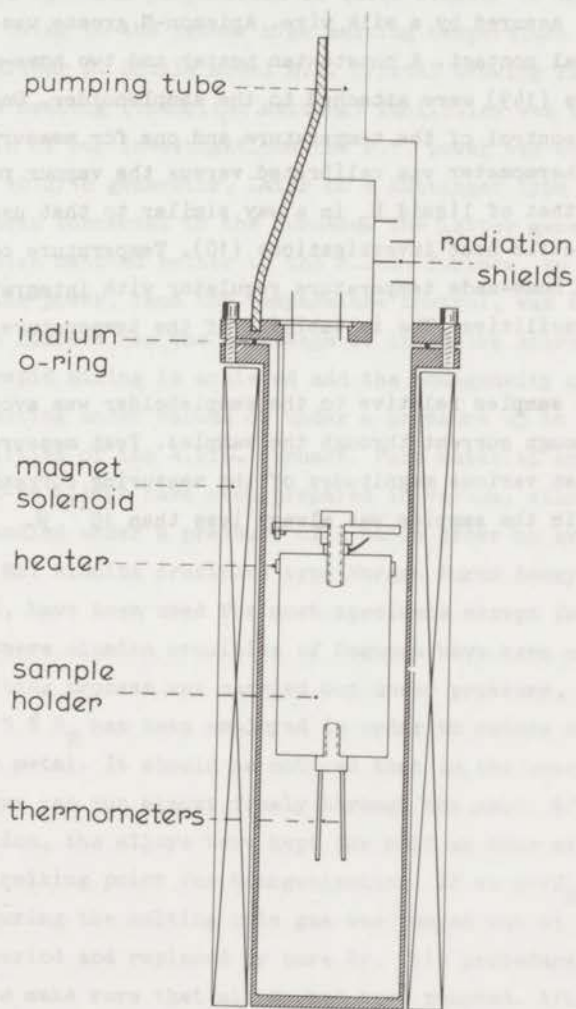


Fig. A.3.2. Cryostat for electrical resistance measurements.

powered by the same current supply as mentioned in A.2. In the vacuum vessel a support of stainless steel (for thermal insulation) for the sampleholder was mounted. The sampleholder was thermally connected to the liquid He bath by a copper wire of suitable heat conductance.

The sampleholder was a solid copper cylinder around which the samples could be wound. Cigarette paper was used for electrical insulation between the sample and its holder. Electrical insulation between the windings of the sample was assured by a silk wire. Apiezon-N grease was used to improve the thermal contact. A constantan heater and two home-made carbonthermometers (149) were attached to the sampleholder. One thermometer was used for the control of the temperature and one for measuring it. The "measuring" thermometer was calibrated versus the vapour pressure of liquid He and that of liquid H_2 in a way similar to that used for the adiabatic specific-heat investigations (10). Temperature control was achieved by a home-made temperature regulator with integration and differentiation facilities. The instability of the temperature was less than 0.02 %.

Heating of the samples relative to the sampleholder was avoided by choosing a low enough current through the samples. Test measurements were carried out at various magnitudes of the measuring current. The power dissipated in the samples was always less than 10^{-5} W.



APPENDIX 4

PREPARATION OF THE SPECIMENS

The polycrystalline alloys.

(B. Knook, C.E. Snel, H.J. Tan and T.J. Gortenmulder)

The method of specimen preparation is quite similar to that used by Boerstoeel (9). Owing to the rather high melting temperature of Pd and its alloys an Arthur D. Little model M.P. Crystal Growing Furnace with radio frequency heating (induction melting) facilities was used throughout. During the begin of our investigations the r.f. power was obtained from a Philips type 1012/16 generator. Later on a Hüttinger type JG 25/800 generator has been connected to the furnace. The latter generator had an impedance which matched better to the A.D.L. furnace, so that the regulation of the power, thus the temperature control, was improved.

An induction furnace has the advantage of intensive stirring of the melt, so that rapid mixing is achieved and the homogeneity of the specimens is enhanced. Melting under vacuum or under a pressure up to 20 at belongs to the possibilities of the A.D.L. furnace. Pure material and a number of Pd-Co and Pd-Fe alloys have been prepared in vacuum, alloys containing Mn have been handled under a pressure of 2 at/in order to avoid excessive evaporation of Mn. Alumina crucibles type Morgan Purox Recrystallized Alumina, 99.7 %, have been used for most specimens except for the smaller ones, where alumina crucibles of Degussa have been applied.

When the melting process was carried out under pressure, a mixture of 95 % Ar and 5 % H₂ has been employed in order to reduce any oxides of the impurity metal. It should be noticed that in the case of Pd-based alloys the H₂-gas can run almost freely through the melt. After melting and solidification, the alloys were kept for half an hour at a temperature just below the melting point for homogenization. If an Ar/H₂ mixture had been used during the melting this gas was pumped out at 800°C after the annealing period and replaced by pure Ar. This procedure was repeated several times to make sure that all H₂ had been removed. Afterwards the alloys cooled down to room temperature after switching off the power of the r.f. generator. No quenching has been applied.

Knowledge of the homogeneity after this preparation process is quite poor. According to literature (154,155) Pd forms a continuous series of

solid solutions with Co; the solid solubility limit of Fe and Mn in Pd is 20 at.%. Therefore, it is assumed that the low concentrated alloys investigated, have a fair homogeneity. This assumption is supported by experiments by Boerstael on alloys after additional annealing. However, Zweers (69) has found rather important effects on additional annealing of alloys with higher concentrations of Mn (5- 9 at.%).

The high demands upon the purity and the correct composition of the alloys require special care in order to avoid any contamination. The starting-materials and crucibles were first cleaned by means of an appropriate etchant (except when the starting-material was in the form of a sponge). Removal of the etchant was carried out by ultrasonic cleaning subsequently in distilled water and in alcohol. Whenever the specimen had been machined after melting (and if necessary also just before the measurement) the whole cleaning procedure was repeated.

The concentration of the alloys has been determined chemically in our laboratory in the case of alloys containing Mn and spectrographically by Johnson-Matthey in all other cases. The inaccuracy of the determination was a few percent for both methods. The concentration from these analysis was in agreement with the nominal concentrations in almost all cases. Whenever disagreement was found, the cause could be traced.

If the specimen had to be used for a measurement of the electrical resistance, they were rolled by means of a profile roller into rods with a square cross-section with sides of 0.6 mm. These rods were drawn into wires through diamond dies, using oil (Octoil-8) as a lubricant. Diameters of the wires used for the experiment were between 0.1 and 0.15 mm, depending on the concentration of the impurities. In most cases the lengths were about 1 m, leading to a resistance at low temperatures of order of 1 Ω . After drawing the wires were cleaned in order to remove the lubricant and were annealed at 600°C for at least 3 hours in order to diminish mechanical stress caused by cold working. During the whole procedure care was taken to preclude contamination of the specimens.

The single Crystals.

(B. Knook, A.W.A. van der Hart and E. Walker (University of Geneva))

For reasons evident from the results obtained on polycrystalline alloys (see chapter V) specific-heat measurements on single crystals

of Pd with Co and Fe appeared to be indispensable.

Three important techniques exist for growing single crystals (156):

1) the Bridgeman technique; 2) the Czochralski technique; 3) the molten-zone technique.

ad.1.

In the Bridgeman technique the material to be crystallized is contained in a cylindrical crucible with a conical bottom, which is lowered through a temperature gradient. Or the heater is raised along the crucible, or the moving temperature gradient is artificially obtained by means of a special construction of the furnace. Large single crystals can be grown in this way, but the following deficiencies are important: a. there is no preferred direction of crystallization; b. sometimes the first nucleation will be of several crystallines; c. the growing crystal is in contact with the crucible, so that roughnesses may initiate new nuclei.

ad.2.

In this technique the crystal is made by pulling it from the melt. The advantage is that the crystal is grown free of physical constraints imposed by the crucible. A preferred orientation is possible when a seed crystal is used. The Czochralski technique can be applied to dilute Pd-based alloys, but as the volume of the melt must be larger than that of the crystal to be grown, large quantities of Pd are necessary, which leads to financial problems.

ad.3.

Although this technique is mainly thought of as a purification technique, it may be used for growing of single crystals even of alloys. If a preferred direction of the crystal orientation is requested (as it was in our case) the procedure is the following: the seed crystal and the vertically placed rod of polycrystalline material are brought into a heater, usually an induction heater consisting of only one winding and are molten together. As the effect of the heating is only locally, the length of the molten zone can be small. Therefore, the surface tension can be in equilibrium with the force of gravity, so that the liquid will stay between the seed crystal and the polycrystalline rod. Then the seed crystal and the rod are moved simultaneously through the r.f. winding causing the material to crystallize on the seed crystal, while the volume of the liquid remains constant by melting off the rod.

Of course we should be careful in applying the molten-zone technique to alloys, since zone refining may result into a single crystal of a nearly pure metal. The amount of zone refining depends on the equilibrium distribution coefficient, k_0 , being the ratio between the concentration in the liquid and that in the solid. In the cases of Pd-Co and of Pd-Fe the value of k_0 is near to one. Moreover, complete segregation as determined by k_0 will only occur if there is complete mixing in the melt and if the freezing is sufficiently rapid to make solute diffusion in the solid negligible. In practice these conditions are not fulfilled. Therefore, it is to be expected that only the begin of the crystal will have a concentration which is lower and the last part will have a concentration which is higher than that of the polycrystalline starting material (157). The middle part of the crystal will have a uniform composition. In our case the lengths of the crystals obtained were large enough to have a sufficiently long part with the correct concentration.

The zone-melting technique has the advantage of being crucibleless and causing a small loss of material. On the other hand, owing to the marginal equilibrium between surface tension and gravity it demands much of the mechanical and thermal stability and of the dexterity of the operator.

Since there was no experience with this method at the metallurgical department of the metals group in Leiden and bearing in mind the expensiveness of pure Pd, it has been decided to call in the help of the metallurgical department of the University of Geneva. Fortunately two single crystals with 0.5 at.% Co and Fe, respectively, were available there and could be borrowed for our investigations. Besides this helpfulness the University of Geneva extended hospitality to one of our co-workers in order to prepare at its department two single crystals with 0.1 at.% Co and Fe, respectively. Single crystals of good quality have been obtained. Nominal concentration of the starting material being 0.1 at.%, the concentration of the Pd-Co single crystal became 0.081 at.% and that of the Pd-Fe s.c. 0.10 at.%.

Analysis of the orientations were carried out in our laboratory by means of an X-ray diffraction apparatus (Philips, type PW 1011/00).

Tables.

Two tables are submitted with this appendix; one tabulating the specimens used for our investigations and one reporting the quality

of the base metals. In the left column of table A.4.I the number of the specimen has been given (these numbers have also been mentioned in chapter II), the middle column contains the description of the specimen, the last column the lot or code number of the starting materials. In this column KOL stands for Kamerlingh Onnes Laboratory, J.M. for Johnson Matthey Chemicals Ltd., London and Cominco for Consolidated Mining and Smelting Company of Canada Ltd., Montreal. Owing to the fair agreement between the analyzed and the nominal concentration, no distinction has been made between these numbers.

In table A.4.II the lot or code numbers of the base metals (all of J.M.) are given together with the spectrographical analysis of the manufacturer.

Specimen No.	Description	Lot/Code No.
7100
7101
7102
7103
7104
7105
7106
7107
7108
7109
7110
7111
7112
7113
7114
7115
7116
7117
7118
7119
7120
7121
7122
7123
7124
7125
7126
7127
7128
7129
7130
7131
7132
7133
7134
7135
7136
7137
7138
7139
7140
7141
7142
7143
7144
7145
7146
7147
7148
7149
7150
7151
7152
7153
7154
7155
7156
7157
7158
7159
7160
7161
7162
7163
7164
7165
7166
7167
7168
7169
7170
7171
7172
7173
7174
7175
7176
7177
7178
7179
7180
7181
7182
7183
7184
7185
7186
7187
7188
7189
7190
7191
7192
7193
7194
7195
7196
7197
7198
7199
7200

TABLE A.4.I

Preparation of the specimens.

code-number	specimen	starting material
7035	Pd-Mn(1 at.%)	Pd : J.M. S 8750
		Mn : J.M. S 6759
7070	Pd-Fe(0.2 at.%)	Pd : J.M. S 8750
		Fe : J.M. 7037x
7071	Pd-Co(0.2 at.%)	Pd : J.M. S 8750
		Co : J.M. 9139x
7090	Pd-Fe(1.25 at.%)	Pd-Fe : KOL 6944(=0.16 at.%)
		Fe : J.M. 7037x
7123	Pd-Co(0.3 at.%)	Pd-Co : KOL 7114(=1 at.%)
		Pd : J.M. S 8750
		Co : J.M. 9123x
7138	Ag-Mn(10 at.%)	Ag : Cominco
		Mn : J.M. S 6759
7140	Pd-Ag(10 at.%) - Mn(1 at.%)	Ag-Mn : KOL 7138
		Pd : J.M. S 8750
7141	Pd-Ag(20 at.%) - Mn(1 at.%)	Ag-Mn : KOL 7138
		Pd : J.M. S 8750
		Ag : Cominco
7150	Pd-Ag(0.25 at.%) - Mn(1 at.%)	Pd : J.M. S 8750
		Mn : J.M. S 6759
		Ag : J.M. 12137 (grain)
7151	Pd-Ag(0.5 at.%) - Mn(1 at.%)	Pd : J.M. S 8750
		Mn : J.M. S 6759
		Ag : J.M. 12137 (grain)
7152	Pd-Ag(1 at.%) - Mn(1 at.%)	Pd : J.M. S 8750
		Mn : J.M. S 6759
		Ag : J.M. 12137 (grain)
7153	Pd-Fe(0.3 at.%)	Pd : J.M. S 8750
		Fe : J.M. S 7037x
7157	Pd-Rh(0.5 at.%) - Mn(1 at.%)	Pd : J.M. S 8750
		Rh : J.M. 9007
		Mn : J.M. S 6759

code-number	specimen	starting material
7158	Pd-Rh(1 at.%) - Mn(1 at.%)	Pd : J.M. S 8750
		Rh : J.M. 9007
		Mn : J.M. S 6759
7159	Pd-Rh(2 at.%) - Mn(1 at.%)	Pd : J.M. S 8750
		Rh : J.M. 9007
		Mn : J.M. S 6759
7160	Pd-Rh(4 at.%) - Mn(1 at.%)	Pd : J.M. S 8750
		Rh : J.M. 9007
		Mn : J.M. S 6759
7168	Pd-Ag(1 at.%)	Pd : J.M. S 8750
		Ag : J.M. 12137 (grain)
7169	Pd-Rh(2 at.%)	Pd : J.M. S 8750
		Rh : J.M. 9007
7182	Pd-Mn(0.15 at.%)	Pd-Mn : KOL 7173(=0.2 at.%)
		KOL 7174(=0.1 at.%)
7192	Pd-Rh(2 at.%) - Fe(0.07 at.%)	Pd-Rh : KOL 7169
		Fe : J.M. 7037
7193	Pd-Rh(2 at.%) - Mn(0.15 at.%)	Pd-Rh : KOL 7169
		Mn : J.M. S 6759
7194	Pd-Rh(2 at.%) - Co(0.07 at.%)	Pd-Rh : KOL 7194
		Co : J.M. 9319
7195	Pd-Ag(1 at.%) - Fe(0.07 at.%)	Pd-Ag : KOL 7168
		Fe : J.M. 7037
7196	Pd-Ag(1 at.%) - Mn(0.15 at.%)	Pd-Ag : KOL 7168
		Mn : J.M. S 6959
7197	Pd-Ag(1 at.%) - Co(0.07 at.%)	Pd-Ag : KOL 7168
		Co : J.M. 9319
7216	Pd-Rh(2 at.%) - Co(0.25 at.%)	Pd-Rh-Co: KOL 7194
		Co : J.M. 9319x
7217	Pd-Rh(2 at.%) - Fe(0.25 at.%)	Pd-Rh-Fe: KOL 7192
		Fe : J.M. 7037
7218	Pd-Ag(2 at.%) - Fe(0.25 at.%)	Pd-Ag-Fe: KOL 7195
		Fe : J.M. 7037
7219	Pd-Ag(1 at.%) - Co(0.25 at.%)	Pd-Ag-Co: KOL 7197
		Co : J.M. 9319x

code-number	specimen	starting material
7228	Pd-Mn(0.4 at.%)	Pd : J.M. S 56291 G.F. Mn : J.M. S 6759
7229	Pd-Mn(0.3 at.%)	Pd : J.M. S 56291 G.F. Mn : J.M. S 6759
7230	Pd-Mn(0.2 at.%)	Pd-Mn : KOL 7228 Pd : J.M. S 56291 G.F.
7231	Pd-Mn(0.1 at.%)	Pd-Mn : KOL 7229 Pd : J.M. S 56291 G.F.
7232	Pd-Mn(0.05 at.%)	Pd-Mn : KOL 7229 Pd : J.M. S 56291 G.F.
7240	Pd-Rh(2 at.%) - Mn(1.4 at.%)	Pd-Rh-Mn: KOL 7193 Mn : J.M. S 6759
7241	Pd-Ag(1 at.%) - Mn(1.4 at.%)	Pd-Ag-Mn: KOL 7196 Mn : J.M. S 6759
7273	Pd-Fe(0.25 at.%)	Pd : J.M. S 56291 G.F. Fe : J.M. 7037x
7286	Pd-Co(250 p.p.m.)	Pd-Co : KOL 6825(=0.075 at.%) Pd : J.M. S 57233
7287	Pd-Co(100 p.p.m.)	Pd-Co : KOL 6825(=0.075 at.%) Pd : J.M. S 57233
7288	Pd-Co(50 p.p.m.)	Pd-Co : KOL 6825(=0.075 at.%) Pd : J.M. S 57233
-	Pd-Fe(0.5 at.%) single crystal	Borrowed from Geneva
-	Pd-Co(0.5 at.%) single crystal	Borrowed from Geneva
73014	Pd-Fe(0.1 at.%) single crystal	Pd-Fe : KOL 7090 Pd : J.M. S 56291 G.F. J.M. S 57870
73015	Pd-Co(0.1 at.%) single crystal	Pd : J.M. S 57233 J.M. S 57870 Co : J.M. 9319
73044	Pd-Fe(0.35 at.%)	Pd-Fe : KOL 7273 Pd : J.M. S 52733 Fe : J.M. 7037x

code-number	specimen	starting material
73076	Pd (pure)	Pd : J.M. S 52733
73077	Pd-Mn(0.7 at.%)	Pd : J.M. S 52733 J.M. S 56291 Mn : J.M. S 6759
73078	Pd-Mn(0.7 at.%)	Pd-Mn : KOL 73077
73079	Pd-Rh(1 at.%) - Mn(0.7 at.%)	Pd-Mn : KOL 73077 Rh : J.M. 16813/1
73080	Pd-Rh(2 at.%) - Mn(0.7 at.%)	Pd-Mn : KOL 73077 Rh : J.M. 16813/1
73081	Pd-Rh(4 at.%) - Mn(0.7 at.%)	Pd-Mn : KOL 73077 Rh : J.M. 16813/1
73086	Pd-Fe(0.05 at.%)	Pd-Fe : KOL 73044 Pd : J.M. S 57233
73087	Pd-Co(0.05 at.%)	Pd : J.M. S 57233 Co : J.M. 9319
73100	Pd-Mn(1.5 at.%)	Pd : J.M. S 58899 J.M. S 56291 Mn : J.M. S 6759
73101	Pd-Rh(3 at.%) - Mn(1.5 at.%)	Pd-Mn : KOL 73100 Rh : J.M. 16813/1 (wire)
73102	Pd-Rh(4 at.%) - Mn(1.5 at.%)	Pd-Mn : KOL 73100 Rh : J.M. 16813/1 (wire)
73103	Pd-Rh(5 at.%) - Mn(1.5 at.%)	Pd-Mn : KOL 73100 Rh : J.M. 16813/1 (wire)
73104	Pd-Rh(6 at.%) - Mn(1.5 at.%)	Pd-Mn : KOL 73100 Rh : J.M. 16813/1 (wire)
73110	Pd-Ag(1 at.%) - Co(0.05 at.%)	Pd-Co : KOL 73087 Ag : J.M. 12137
73111	Pd-Rh(1 at.%) - Co(0.05 at.%)	Pd-Co : KOL 73087 Rh : J.M. 16813/1 (wire)
73112	Pd-Ag(1 at.%) - Fe(0.05 at.%)	Pd-Fe : KOL 73086 Ag : J.M. 12137
73113	Pd-Rh(1 at.%) - Fe(0.05 at.%)	Pd-Fe : KOL 73086 Rh : J.M. 16813/1 (wire)

code-number	specimen	starting material
73114	Pd-Mn(0.2 at.%)	Pd : J.M. S 58899 Mn : J.M. S 6759
73115	Pd-Mn(0.2 at.%)	Pd-Mn : KOL 73114
73118	Pd-Mn(0.2 at.%)	Pd-Mn : KOL 73114
73119	Pd-Rh(6 at.%) - Mn(0.25 at.%)	Pd-Mn : KOL 73114 Rh : J.M. S 8627
73122	Pd-Mn(0.25 at.%)	Pd-Mn : KOL 73115 Pd : J.M. S 58899 Mn : J.M. S 6759

TABLE A.4.II

*Estimated quantity of impurity present in p.p.m.
Other impurities have been searched for, but were not found.*

Source of base metal	Na	Mg	Al	Si	Ca	Mn	Fe	Ni	Cu	Ag	Pt	Pb	Pd
Pd: J.M. S 8750	<1	<1		8	<1		<1		<1	<1			
S 56291 GF	<1	<1		5	<1		3		<1				
S 57233	<1	<1		1	<1		<1		<1	<1			
S 57870	<1	<1		<1	<1		1		<1	3	10		
S 58899		<1		7	<1		<1		<1	<1			
Ag: J.M. 12137	<1	<1		<1	<1		2		<1			<1	
Rh: J.M. S 5071	3	<1		2	<1		3		<1	<1		5	
16813/1	3	1	10	5	1	3	20		5	<1			<1
9007	2	<1		1	2				<1				
S 8627		<1	1	2	<1		4		1	<1			
Mn: J.M. S 6759		40		2			5		<1				
Co: J.M. 9319		<1	2	<1			5		2				
Fe: J.M. S 7037	<1	<1		<1		<1	1	<5	<1				

BIBLIOGRAPHY

1. B.M. Boerstoel, J.E. van Dam and G.J. Nieuwenhuys, Proc. Nato Summerschool, La Colle sur Loupe, 1970, to be published.
2. J.E. van Dam, thesis, University of Leiden, 1973.
3. J.C. McLennan and H. Grayson Smith, Proc. Roy. Soc. A 112 (1926) 110.
4. L. Hodges, R.E. Watson and H. Ehrenreich, Phys. Rev. B 5 (1972) 3953.
5. F.M. Mueller and J.W. Garland, Bull. Am. Phys. Soc. II 13 (1968) 58.
6. F.M. Mueller, Phys. Rev. 153 (1967) 659.
7. O.K. Anderson, Phys. Rev. B 2 (1970) 883.
8. E.C. Stoner, Proc. Roy. Soc. (London) A 154 (1936) 656; *ibid.* A 165 (1938) 372; Rep. Progr. Phys. 11 (1947) 43.
9. B.M. Boerstoel, thesis, University of Leiden, 1970.
10. B.M. Boerstoel, W.J.J. van Dissel and M.B.M. Jacobs, Physica 38 (1968) 287, Comm. Kamerlingh Onnes Lab., Leiden, No. 363a.
11. B.H. Verbeek and G.J. Nieuwenhuys, Phys. Letters 46 A (1973) 147; B.H. Verbeek, M.F. Pikart and G.J. van den Berg, to be published.
12. P.F. de Chatel and E.P. Wohlfarth, Comm. Solid State Phys. 5 (1974) 133.
13. B.M. Boerstoel, J.J. Zwart and J. Hansen, Physica 57 (1972) 397, Comm. Kamerlingh Onnes Lab., Leiden, No. 388b.
14. G.J. van den Berg, Proc. Nato Summerschool, La Colle sur Loupe, 1970, to be published.
15. W.M. Star, E. de Vroede and C. van Baarle, Physica 59 (1972) 128, Comm. Kamerlingh Onnes Lab., Leiden, No. 390c.
16. S. Foner and E.J. McNiff, Jr, Rev. Sci. Instr. 39 (1968) 171.
17. J.E. van Dam, P.C.M. Gubbens and G.J. van den Berg, Physica 61 (1972) 389, Comm. Kamerlingh Onnes Lab., Leiden, No. 394b.
18. W.M. Star, S. Foner and E.J. McNiff, Jr, to be published.
19. H. Hasegawa, Prog. Theor. Phys. 21 (1959) 483.
20. G.J. Nieuwenhuys, Scriptie, Leiden, 1969.
21. P. Monod and S. Schultz, Phys. Rev. 173 (1968) 645.
22. P. Weiss and M. Forrer, Ann. Physique 5 (1926) 153.
23. A. Arrott, Phys. Rev. 108 (1957) 1394.
24. M.P. Kawatra and J.I. Budnick, Intern. J. Magnetism 1 (1970) 61.
25. M.E. Fisher and J.S. Langer, Phys. Rev. Letters 20 (1968) 665.
26. L.L. Hirst, Phys. Kond. Mat. 11 (1970) 255.

27. M. McDougald and A.J. Manuel, *J. appl. Phys.* 39 (1968) 961.
28. M. McDougald and A.J. Manuel, *J. Phys. C* 3 (1970) 147.
29. R.M. Bozorth, P.A. Wolff, D.D. Davis, V.B. Compton and J.H. Wernick, *Phys. Rev.* 122 (1961) 1157.
30. P.P. Craig, D.E. Nagle, W.A. Steyert and R.D. Taylor, *Phys. Rev. Letters* 9 (1962) 12.
31. M.P. Maley, R.D. Taylor and J.L. Thompson, *J. appl. Phys.* 38 (1967) 1249.
32. A.M. Clogston, B.T. Matthias, M. Peter, H.J. Williams, E. Corenzwit and R.C. Sherwood, *Phys. Rev.* 125 (1962) 541.
33. J.W. Cable, E.O. Wallan and W.C. Koehler, *Phys. Rev.* 138 (1965) A 755.
34. W.C. Phillips, *Phys. Rev.* 138 (1965) A 1649.
35. G.G. Low, *Proc. int. Conf. Magnetism, Nottingham, 1964, I.P.P.S., London, 1965, p. 133.*
36. G.G. Low and T.M. Holden, *Proc. Phys. Soc.* 89 (1966) 119.
37. T.J. Hicks, T.M. Holden and G.G. Low, *J. Phys. C* 1 (1968) 528.
38. Thanks are due to Dr. I. Riesz, Ottawa, for his remarks on this point.
39. B.D. Dunlap and J.G. Dash, *Phys. Rev.* 155 (1967) 460.
40. W.L. Trousdale, T.A. Kitchens and G. Longworth, *J. appl. Phys.* 38 (1967) 922.
41. M.P. Sarachik and D. Shaltiel, *J. appl. Phys.* 38 (1967) 1155.
42. G. Williams and J.W. Loram, *Solid State Comm.* 7 (1969) 1261.
43. G. Williams, G.A. Swallow and J.W. Loram, *Phys. Rev. B* 3 (1971) 3863.
44. G. Williams and J.W. Loram, *J. Phys. F* 1 (1971) 434.
45. G. Williams, *Phys. Rev. B* 5 (1972) 236.
46. M.E. Colp and G. Williams, *Phys. Rev. B* 5 (1972) 2599.
47. G. Williams, G.A. Swallow and J.W. Loram, *Phys. Rev. B* 7 (1973) 257.
48. H.S.D. Cole and R.E. Turner, *J. Phys. C* 2 (1969) 124.
49. P.D. Long and R.E. Turner, *J. Phys. C* 3 (1970) S 127.
50. S. Doniach and E.P. Wohlfarth, *Proc. Roy. Soc. (London) A* 296 (1967) 442.
51. G.J. Nieuwenhuys, B.M. Boerstael, J.J. Zwart, H.D. Dokter and G.J. van den Berg, *Physica* 62 (1972) 278, *Comm. Kamerlingh Onnes Lab., Leiden, No. 395c.*
52. D. Gerstenberg, *Ann. Physik* 2 (1958) 236.
53. G. Grube and D. Winckler, *Z. Electrochem.* 41 (1935) 52.
54. G. Chouteau and R. Tournier, *J. de Physique*, 32 (1971) C 1002.

55. M.P. Kawatra, J.I. Budnick and J.A. Mydosh, Phys. Rev. B 2 (1970) 1587.
56. J. Crangle and W.R. Scott, J. appl. Phys. 38 (1965) 921.
57. M.D. Wilding, Proc. Phys. Soc. 90 (1967) 801.
58. G. Williams and J.W. Loram, J. Phys. Chem. Solids 30 (1969) 1827.
59. B.R. Coles, J.H. Waszink and J.W. Loram, Proc. int. Conf. Magnetism, Nottingham, 1964, I.P.P.S., London, 1965, p. 165.
60. D.M.S. Bagguley and J.A. Robertson, Phys. Letters 27 A (1968) 516.
61. J.A. Mydosh, J.I. Budnick, M.P. Kawatra and S. Skalski, Phys. Rev. Letters 21 (1968) 1346.
62. J. Crangle, Phil. Mag. 5 (1960) 335.
63. P.P. Craig, R.C. Perisho, R. Segnan and W.A. Steyert, Phys. Rev. 138 (1965) A 1460.
64. J.S. Carlow and R.E. Meads, J. Phys. C 2 (1969) 2120.
65. M.P. Kawatra, S. Skalski, J.A. Mydosh and J.I. Budnick, J. appl. Phys. 40 (1969) 1202.
66. J. Rault and J.P. Burger, C.R. Acad. Sc. (Paris) 269 Serie B (1969) 1085.
67. G.J. Nieuwenhuys and B.M. Boerstoel, Phys. Letters 33 A (1970) 147.
68. G. Williams, J. Phys. Chem. Solids 31 (1970) 529.
69. H.A. Zweers, to be published.
70. Thanks are due to Dr. E. Walker, University of Geneva, for kindly putting this specimen to our disposal.
71. A.D.C. Grassie, G.A. Swallow, G. Williams and J.W. Loram, Phys. Rev. B 3 (1971) 4154.
72. K. Yosida, Phys. Rev. 107 (1957) 396.
73. D.E. Nagle, P.P. Craig, P. Barrett, D.F.R. Cochran, C.E. Olsen and R.D. Taylor, Phys. Rev. 125 (1962) 490.
74. J.W. Loram, G. Williams and G.A. Swallow, Phys. Rev. B 3 (1971) 3060.
75. B.W. Veal and J.A. Rayne, Phys. Rev. 135 (1964) A 442.
76. G. Chouteau, R. Fourneaux and R. Tournier, Proc. 12th Conf. Low Temp. Phys., Kyoto, Japan, 1970, Academic Press of Japan, p. 769.
77. B.M. Boerstoel, J.J. Zwart and J. Hansen, Physica 54 (1971) 442, Comm. Kamerlingh Onnes Lab., Leiden, No. 385c.
78. C. Herring, Magnetism, Vol. IV, ed. G.T. Rado and H. Suhl, Academic Press, New York, 1966, Chapter VI.
79. N.C. Koon, A.I. Schindler and D.L. Mills, Phys. Rev. B 6 (1972) 4241; N.C. Koon and A.I. Schindler, Phys. Rev. B 8 (1973) 5257.

80. F.W.D. Woodhams, R.E. Meads and J.S. Carlow, *Phys. Letters* 23 A (1966) 419.
81. R.P. Guertin and S. Foner, *J. appl. Phys.* 41 (1970) 917.
82. B.R. Coles, H. Jamieson, B.D. Rainford, A. Tari and R.H. Taylor, to be published in *J. Phys. F.*
83. W.M. Star and G.J. Nieuwenhuys, *Phys. Letters* 30 A (1969) 22.
84. W.M. Star, F.B. Basters, G.M. Nap, E. de Vroede and C. van Baarle, *Physica* 58 (1972) 585, Comm. Kamerlingh Onnes Lab., Leiden, No. 390a.
85. D. Shaltiel, J.H. Wernick, H.J. Williams and M. Peter, *Phys. Rev.* 135 (1964) A 1346;
D. Shaltiel and J.H. Wernick, *Phys. Rev.* 136 (1964) A 245.
86. H. Cottet, thesis, University of Geneva, 1971.
87. R.A.B. Devine, private comm.
88. R.M. Bozorth, *Ferromagnetism*, D. van Nostran Company, Inc., New York, 1951.
89. N. Heizum and K. Stierstadt, *Intern. J. Magnetism* 3 (1973) 39.
90. A.J. Heeger, *Proc. Nato Summerschool, La Colle sur Loupe, 1970*, to be published.
91. J. Friedel, *Nuovo Cim.* 7 (1958) 287.
92. P.W. Anderson, *Phys. Rev.* 124 (1961) 41.
93. P.A. Wolff, *Phys. Rev.* 124 (1961) 1030.
94. D.K. Wohlleben and B.R. Coles, *Magnetism*, Vol. V, ed. H. Suhl, Academic Press, New York, 1973, Chapter I.
95. A. Blandin, *Magnetism*, Vol. V, ed. H. Suhl, Academic Press, New York, 1973, Chapter II.
96. L.L. Hirst, *Z. Physik* 241 (1971) 9.
97. T. Moriya, *Prog. Theor. Phys.* 34 (1965) 329.
98. I.A. Campbell, *J. Phys. C* 1 (1968) 687.
99. J.A. Schrieffer, *J. appl. Phys.* 39 (1968) 642.
100. J. Lindhard, *Kgl. Danske Videnskab. Selskab. Mat.-fys. Medd.* 28 (1954) 8.
101. J.B. Diamond, thesis, University of Pennsylvania, 1971;
J.B. Diamond, *Intern. J. Magnetism* 2 (1972) 241.
102. D.J. Kim, *Phys. Rev.* 149 (1966) 434.
103. T. Kasuya, *Prog. Theor. Phys.* 16 (1956) 45.
104. M.A. Ruderman and C. Kittel, *Phys. Rev.* 96 (1954) 99.

105. K. Yosida, Phys. Rev. 106 (1957) 893.
106. R. Brout, Phys. Rev. 115 (1959) 824.
107. G.J. Nieuwenhuys, Phys. Letters 43A (1973) 301.
108. J.S. Smart, Effective Field Theories of Magnetism, W.B. Saunders Company, Philadelphia and London, 1966.
109. H. Eugene Stanley, Introduction to Phasetransitions and Critical Phenomena, International Series of Monographs on Physics, ed. W. Marshall and D.H. Wilkinson, Oxford University Press, 1970.
110. T. Takahashi and M. Shimizu, J. Phys. Soc. Japan 20 (1965) 26.
111. M.E. Zuckermann, Solid State Comm. 9 (1971) 1861.
112. T. Takahashi and M. Shimizu, J. Phys. Soc. Japan 23 (1967) 945.
113. I.Ya. Korenblitz and E.F. Shender, Sov. Phys. JETP 35 (1972) 1017.
114. W. Marshall, Phys. Rev. 118 (1960) 1519.
115. M.W. Klein and R. Brout, Phys. Rev. 132 (1963) 2412.
116. R.J. Harrison and M.W. Klein, Phys. Rev. 154 (1967) 540.
117. M.W. Klein, Phys. Rev. 173 (1968) 552.
118. M.W. Klein, Phys. Rev. 188 (1969) 933.
119. S. Chandrasekhar, Rev. Mod. Phys. 15 (1943) 1.
120. H. Margenau, Phys. Rev. 48 (1935) 755.
121. M.G. Kendall, The Advanced Theory of Statistics, Charles Griffin and Company, Ltd., London.
122. W. Schottky, Phys. Z. 23 (1922) 448.
123. A.J. Heeger, Solid State Physics, eds. F. Seitz, D. Turnbull and H. Ehrenreich, Vol. 23, p. 283, Academic Press, New York, 1969.
124. R.M. White, Quantum Theory of Magnetism, McGraw Hill Book Company, 1970.
125. J. Lacroix, private comm. to R.A.B. Devine.
126. R.A.B. Devine, J.M. Moret, J. Ortelli, D. Shaltiel, W. Zingg and M. Peter, Solid State Comm. 10 (1972) 575.
127. R.A.B. Devine, Solid State Comm. 13 (1973) 935.
128. G.J. Nieuwenhuys, M.F. Pikart, J.J. Zwart, B.M. Boerstoel and G.J. van den Berg, Physica 69 (1973) 119, Comm. Kamerlingh Onnes Lab., Leiden, No. 403a.
129. D.L. Mills, M.T. Beal-Monod and P. Lederer, Magnetism, Vol. V, ed. H. Suhl, Academic Press, New York, 1973, Chapter III.
130. N. Menyhard, Solid State Comm. 11 (1972) 423.
131. B. Giovannini, A.J. Heeger and M. Peter, Helv. Phys. Acta 43 (1970) 101.

132. C.J. Gorter, Paramagnetic Relaxation, Elsevier Publishing Company, 1947.
133. H. Maletta, Z. Physik 250 (1972) 68.
134. J.W. Loram, R.J. White and A.D.C. Grassie, Phys. Rev. B 5 (1972) 3659.
135. G.J. Nieuwenhuys, B.M. Boerstoel and W.M. Star, Proc. 13th Int. Conf. low Temp. Phys., Boulder, U.S.A., 1972, Vol. II, p. 510, to be published.
136. N. Rivier, to be published in Wiss. Z. der T.U. Dresden 3 (1974).
137. D.W. Budworth, F.E. Hoare and J. Preston, Proc. Roy. Soc. A 257 (1960) 250.
138. F.E. Hoare, J.C. Matthews and J.C. Walling, Proc. Roy. Soc. A 216 (1953) 502.
139. R. Doclo, thesis, University of Gent, 1968.
140. R. Doclo, S. Foner and A. Narath, J. appl. Phys. 40 (1969) 1206.
141. F.E. Hoare and B. Yates, Proc. Roy. Soc. A 240 (1957) 42.
142. A. Junod, private comm. to J.E. van Dam.
143. B.H. Verbeek, private comm.
144. R.M. Bozorth, D.D. Davis and J.H. Wernick, J. Phys. Soc. Japan 17 Suppl. B-I (1962) 112.
145. R.A. Levy, J.J. Burton, D.I. Paul and J.I. Budnick, Phys. Rev. B 9 (1974) 1085.
146. H.G. Purwins, Y. Taylor, J. Sierro and F.T. Hedgcock, Solid State Comm. 11 (1972) 361.
147. V. Canella, thesis, Fordham University, 1971.
148. E. Maxwell, Rev. Sci. Instr. 36 (1965) 553.
149. W.M. Star, J.E. van Dam and C. van Baarle, J. Phys. E (J. Sci. Instr.) 2 (1969) 257.
150. P.F. Sullivan and G. Seidel, Phys. Rev. 173 (1968) 679.
151. J.J. de Jong and P.C.M. Gubbens, scriptie, Leiden, 1970.
152. J.N. Haasbroek, thesis, University of Leiden, 1971.
153. H.H. Sample, L.J. Neuringer and L.G. Rubin, Rev. Sci. Instr. 45 (1974) 64.
154. M. Hansen, Constitution of Binary Alloys, McGraw Hill Book Company Inc., New York, 1958.
155. R.P. Elliot, Constitution of Binary Alloys, First Supplement, McGraw Hill Book Company. Inc., New York, 1965.
156. R.A. Laudise, The Growth of Single Crystals, Prentise Hall Inc., New Jersey, 1971.

157. P.H. Thornton, Techniques of Material Research, ed. R.F. Bunshah,
Vol. I, part II, p. 1077, Interscience Publishers, 1968.

SAMENVATTING

Elementen uit de eerste lange periode van overgangsmetalen van het periodiek systeem vertonen een aantal opmerkelijke verschijnselen, wanneer zij worden opgelost in palladium. Dit wordt veroorzaakt door de bijzonder grote paramagnetische susceptibiliteit van deze gastheer; tot op zekere hoogte kan Pd een bijna ferromagnetisch metaal worden genoemd. Verdunde oplossingen van Cr in Pd vertonen het zogenaamde Kondo effect, terwijl Pd-Ni legeringen bij een concentratie kleiner dan 2 at.% de karakteristieke invloed van lokale spinfluctuaties weergeven.

De elementen Co, Fe en Mn behouden min of meer hun magnetische eigenschappen als zij worden opgelost in Pd; hun aanwezigheid gaat namelijk gepaard met de aanwezigheid van permanente magnetische momenten. Magnetisatie metingen aan deze soort legeringen hebben echter aangetoond, dat het magnetisch moment per opgelost atoom nogal groot is, ongeveer $10\mu_B$ per Co- en Fe-atoom en $7,5\mu_B$ per Mn-atoom. Dit laatste is pas kort geleden gevonden.

Er zijn sterke aanwijzingen vanuit de theorie dat een atoom opgelost in een niet magnetische matrix ook moet voldoen aan de regel van Hund. Deze regel staat evenwel de opbouw van dergelijke grote momenten, zoals zijn gevonden, niet toe. Daarom moet worden verondersteld, dat een gedeelte van het "reuze moment" wordt veroorzaakt door de gepolariseerde d-band van Pd-metaal. Experimenten met behulp van diffuse verstrooiing van neutronen hebben inderdaad aangetoond dat dergelijke momenten, die samen gaan met Co- en Fe-atomen, een ruimtelijke uitbreiding over meer dan 200 Pd-atomen hebben. Het is jammer dat dergelijke experimenten aan Pd-Mn nog niet zijn gepubliceerd.

Onontkoombaar rijst de vraag op hoe groot de multiplicititeit (of wel het magnetisch quantum getal J) van deze momenten is. En als een waarde voor J wordt vastgesteld moeten wij ons afvragen of, als de verzadigingswaarde van het moment wordt geschreven als $g_{\text{eff}}J\mu_B$, de magnetisatie en de soortelijke warmte in een uitwendig magnetisch veld zich gedragen volgens een Brillouin functie met deze waarden van J en g_{eff} . De theorie, hoewel in staat het bestaan, de grootte en de ruimtelijke uitgebreidheid van de reuze momenten te verklaren, blijft het antwoord op deze vragen schuldig. In het algemeen leiden de interpretaties van magnetische metingen tot een grote waarde van J en een kleine waarde van g_{eff} .

Entropie berekeningen op grond van metingen van de soortelijke warmte zijn daarmee in tegenspraak. Deze tegenspraak was de voornaamste reden voor het huidige onderzoek.

In legeringen van Pd met Co, Fe en Mn treedt ferromagnetische ordening op bij lage temperatuur, zelfs indien de concentratie kleiner is dan 0.1 at.%. De oorzaak van deze ordening moet ongetwijfeld worden gezocht in de grote ruimtelijke uitgebreidheid van de magnetische momenten. De waarde van de overgangstemperatuur en het karakter van de ordening is het onderwerp geweest van vele onderzoeken. Aan meer dan 100 legeringen van Pd met Co, Fe of Mn zijn experimenten gedaan. Om een ruw beeld te schetsen kunnen wij het volgende opmerken: voor kleine hoeveelheden Fe en Co in Pd is T_C evenredig met c^2 en in het geval van grotere concentraties is T_C een lineaire functie van c . Het begin van de magnetische ordening treedt niet op bij een scherp gedefinieerde temperatuur, maar is uitgespreid over een temperatuurgebied van de orde van $0.5 T_C$. Deze breedte is groot voor kleine concentraties en kleiner door grotere concentraties. Ook is de breedte van de overgang in het geval van Co groter dan in dat van Fe. Daar tegenover staan de soortelijke warmte metingen van Boerstool c.s. aan Pd-Mn ($c < 2.5$ at.%), die hebben laten zien dat in deze legering een scherpe overgang plaats vindt. Verder scheen T_C voor deze legering evenredig met de concentratie te zijn. In dit proefschrift wordt verder ingegaan op de vraag of Pd-Mn werkelijk een uitzonderlijk systeem is.

Omdat de magnetische momenten, die aan de ordening deelnemen, verbonden zijn aan gastatomen, lijkt het gelokaliseerde model voor ferromagnetische ordening hier van toepassing. Aan de andere kant moet worden bedacht dat een groot gedeelte van het moment zijn oorsprong vindt in een gepolariseerde geleidingsband. De veronderstelling kan daarom worden geopperd dat de aanwezigheid van de magnetische gastatomen palladium juist over de grens naar het bandferromagnetisme helpt. Theorieën en argumentaties, gebaseerd op een van beide modellen of op een vermenging daarvan, kunnen in de literatuur worden gevonden. In dit proefschrift wordt een keuze tussen deze theorieën gemaakt voor legeringen met een kleine concentratie.

Een samenvatting van de belangrijkste resultaten van het onderhavige onderzoek en van onderzoek dat hiermee direct verband houdt kan als volgt in telegramstijl worden gegeven.

- Het reuze moment moet worden toegeschreven aan normale waarden van het magnetische quantum getal ($3/2$ voor Co, 2 voor Fe en $5/2$ voor Mn) en een grote waarde van g_{eff} .
- Paramagnetische Pd-Co en Pd-Fe legeringen gedragen zich niet in overeenstemming met een Brillouin functie, legeringen van Pd-Mn doen dit wel. Daarom moeten een aantal interpretaties van magnetische metingen als onjuist worden beschouwd.
- Het gelokaliseerde model voor ferromagnetische ordening kan de verschijnselen, die in verdunde Pd legeringen optreden, redelijk beschrijven. Het moleculaire veld model van Weiss kan, zij het met enige veranderingen, worden toegepast.
- De overgangstemperatuur van Pd-Mn legeringen is niet evenredig met de concentratie, maar na herschaling is het gedrag analoog aan dat van Pd-Co en Pd-Fe. De concentratie afhankelijkheid kan worden verklaard uitgaande van een berekening van de sterkte van de wisselwerking tussen twee gastatomen als functie van de afstand.
- Als legeringen met gelijke concentraties worden vergeleken, blijkt dat de magnetische ordening van Pd-Mn in het geheel niet uitzonderlijk is. Er moet echter wel worden opgemerkt dat voor het geval dat $c > 3$ at.% Pd-Mn een "spin glass" wordt.
- Toevoeging van Ag of Rh aan Pd legeringen met Co, Fe of Mn heeft een grote invloed op het gedrag ervan. Deze invloed wordt nog niet helemaal begrepen.

Op verzoek van de Faculteit der Wiskunde en Natuurwetenschappen volgt hier een overzicht van mijn studie.

Nadat ik in 1963 het diploma H.B.S.-B had behaald aan het Christelijk Lyceum te Leiden (tegenwoordig Dr. Visser 't Hooft scholengemeenschap) begon ik mijn studie aan de Rijksuniversiteit te Leiden. In 1966 legde ik het kandidaatsexamen d' af in de Natuur- en Wiskunde met als bijvak Scheikunde; in 1969 volgde het doctoraalexamen experimentele natuurkunde.

Sinds 1967 ben ik werkzaam in de werkgroep "F.O.M.-metalen Mt IV", waarvan tot 1 november 1973 Prof. Dr. C.J. Gorter de leiding had. De dagelijkse leiding van de groep berust bij Dr. G.J. van den Berg en bij Dr. B. Knook.

Oktober 1968 trad ik in dienst van de Stichting voor Fundamenteel Onderzoek der Materie (F.O.M.) als wetenschappelijk assistent; sinds oktober 1969 als wetenschappelijk medewerker.

Gedurende de cursus 1968/1969 ben ik verbonden geweest aan het praktikum voor eerste jaars studenten in de biologie. Vanaf 1969 ben ik verbonden aan het werkcollege klassieke mechanica behorende bij het college van Dr. J. de Nobel; sinds 1971 als hoofdassistent.

In maart 1969 ben ik op voorstel van Dr. C. van Baarle begonnen met een literatuur onderzoek betreffende en de opbouw van een opstelling voor het meten van Electronen Paramagnetische Resonantie in metaallegeringen. Vanwege de nalatigheid van leveranciers en vanwege het vertrek van de doctoren Van Baarle en Swanenburg heb ik maart 1970 de voorbereidingen voor dit onderzoek gestaakt en ben ik begonnen aan het onderzoek voor dit proefschrift. Deze overgang was mogelijk dank zij het feit dat Dr. B.M. Boerstoel mij op stimulerende wijze had ingewijd in de problemen van de Pd-legeringen met Co, Fe of Mn en mij had leren werken met zijn voortreffelijke opstelling voor het meten van de warmte capaciteit bij lage temperaturen.

Vele medewerkers van het Kamerlingh Onnes Laboratorium en van andere instituten hebben een bijdrage geleverd voor het tot stand komen van dit proefschrift. Het is niet mogelijk hen hier allemaal te noemen; van enkelen is de naam vermeld bij het onderdeel dat met hun bijzondere medewerking tot stand is gekomen. Daarnaast wil ik nog noemen Drs. H.D. Dokter en de heer C.J. de Pater. Hun kritische vragen en opmerkingen waren nuttig.

Dr. W.M. Star heeft mij continu op de hoogte gehouden van de resultaten van zijn experimenten op het Francis Bitter National Magnet Lab., M.I.T., Cambridge, U.S.A. Naast de waardevolle discussies die wij hebben gehad, was hij bereid het manuscript nauwgezet te lezen en van opmerkingen te voorzien.

De chemische analyse van de preparaten werd uitgevoerd door mevr. M.A. Otten-Scholten en mej. B. van den Ende. De tekeningen en de foto's werden door de heer W.F. Tegelaar op de van hem bekende vaardige wijze verzorgd. Mevr. J.C. Smit-van Otten en de heer en mevr. Werkhoven maakten de tekst gereed voor de drukker.

